

From the Institute of Molecular Medicine
of the University of Lübeck
Director: Prof. Dr. Georg Sczakiel

**Investigation of the effect of human Argonaute
proteins on the maturation
of short hairpin RNAs**

Dissertation
for Fulfillment of
Requirements
for the Doctoral Degree
of the University of Lübeck
from the Department of Natural Sciences

Submitted by
Maria Rosaria Innarella
from Nola (NA), Italy

Lübeck 2014

First referee: Prof. Dr. Georg Sczakiel

Second referee: PD Dr. Thomas Weimar

Date of oral examination: 20.11.2014

Approved for printing. Lübeck, 21.11.2014

Abbreviations

A ₂₆₀	absorbance at 260nm
A ₂₈₀	absorbance at 280nm
Amp	ampicillin
APS	ammonium peroxodisulphate
asON(s)	antisense oligonucleotide(s)
bp(s)	base pair(s)
BSA	bovine serum albumin
cDNA	complementary desoxyribonucleic acid
<i>C. elegans</i>	<i>Caenorhabditis elegans</i>
C-terminus	carboxy-terminus
Ci	Curie
CPM	counts per minute
D	aspartate
DGCR8	DiGeorge syndrome chromosomal region gene 8
DMEM	Dulbecco's modified eagle medium
DMSO	dimethylsulphoxide
dNTP	deoxynucleoside triphosphate
ds	double-stranded
DTT	dithiothreitol
<i>E. coli</i>	<i>Escherichia coli</i>
E	glutamate
ECL	enhanced chemiluminescence
EDTA	ethylenediaminetetraacetic acid
EtBr	ethidium bromide
Exp5	Exportin-5
F	Fischer
FCS	fetal calf serum
Fwd	forward
G	glycine
h	hour
H	histidin
hAgo(s)	human Argonaute protein(s)
K _d	dissociation constant
LB	Luria-Bertani
M	molarity
min	minutes
miRNA(s)	microRNA(s)

miPDC	miRNA precursor deposit complex
mRNA	messenger RNA
N-terminus	amino-terminus
nt	nucleotide(s)
OD ₆₀₀	optical density at 600nm
OH	hydroxyl
ORF	open reading frame
p-bodies	processing bodies
PAA	Polyacrylamide
PAGE	polyacrylamide gel electrophoresis
PAZ	PIWI Argonaute Zwillie
PBS	phosphate buffered saline
PIWI	P-element induced wimpy testis
Pre-miRNA(s)	precursor microRNA(s)
Pri-miRNA(s)	primary microRNA(s)
PS	phosphorothioate
PTGS	posttranscriptional gene silencing mechanism
PVDF	polyvinyl difluoride
q-PCR	quantitative polymerase chain reaction
R	arginine
RIIID	RNase III domains
Rev	reverse
RLC	RISC loading complex
RISC	RNA-induced silencing complex
RITZ	RNA-induced initiation of transcriptional gene silencing
RNAi	RNA interference
RNase	ribonuclease
RT	reverse transcriptase
SDS	sodium dodecylsulphate
siRNA(s)	small interfering RNA(s)
ss	single-stranded
SSC	saline-sodium citrate
T	thymidine
TAE	triethanolamine
<i>Taq</i>	<i>Thermophilus aquaticus</i>
TBE	tris-borate-EDTA
TBS	tris-buffered saline buffer
TCA	trichloroacetic acid
TEMED	N,N,N,N,-tetramethylethylendiamin

Tris	trihydroxymethylaminomethane
tRNA	transfer RNA
u	unit, enzymatic activity
UTR	untranslated region
UV	ultraviolet
v/v	volume/volume
W	tryptophan
Wt	wild type
w/v	weight/volume
ϵ	molar extinction coefficient

Contents

1 Summary	1
2 Zusammenfassung	3
3 Introduction	5
3.1 RNAi: from the discovery to date	5
3.2 The RNAi mechanism	7
3.2.1 The siRNA-mediated RNAi pathway	7
3.2.2 short hairpin RNA (shRNA)-derived siRNA	11
3.2.3 miRNA	11
3.2.3.1 The biogenesis of miRNAs	11
3.2.3.2 Loading of mature miRNAs by Ago proteins and miRNA functions	14
3.3 RNase III proteins	15
3.3.1 Drosha	15
3.3.2 Dicer	16
3.4 The Argonaute family	17
3.4.1 Classification	17
3.4.2 The protein structure of human Argonautes	18
3.4.3 Functions	20
3.5 Aim of the study	21
4 Materials	23
4.1 Chemicals	23
4.2 Consumables	24
4.3 Devices	25
4.4 Buffers and solutions	26
4.5 Cell culture	28
4.5.1 Cell lines	28
4.5.2 Cell culture reagents	28
4.6 Bacterial culture	29

4.6.1	Bacterial strain	29
4.6.2	Bacterial culture media and plates	29
4.7	Nucleic acids	29
4.7.1	Plasmids/Vectors	29
4.7.2	Oligonucleotides	29
4.7.2.1	Deoxyribonucleotides "DNA oligonucleotides"	30
4.7.2.2	Ribooligonucleotides "RNA oligonucleotides"	33
4.7.3	Primers	34
4.8	Kits	34
4.9	Antibodies	35
4.10	Enzymes and molecular weight markers	35
4.11	Programs	36
5	Methods	37
5.1	Methods for nucleic acids	37
5.1.1	Determination of the concentration of nucleic acids	37
5.1.2	Agarose gel electrophoresis	37
5.1.3	Polyacrylamide gel electrophoresis (PAGE)	38
5.1.4	Detection of nucleic acids upon PAGE	40
5.1.5	Purification of total cellular RNA	40
5.1.6	RNA precipitation	40
5.1.7	Radiolabeling of the 5'-end of nucleic acids	41
5.1.8	Northern Analysis	42
5.2	Methods in molecular biology	44
5.2.1	Cloning of DNA fragments into a vector and DNA oligonucleotides design	44
5.2.1.1	Hybridization of complementary DNA oligonucleotides	45
5.2.1.2	Ligation of the dsDNA fragments into the pSilencer TM 2.1 neo-vector	45
5.2.2	Preparation of electrocompetent cells	46
5.2.2.1	Trasformation of <i>E.coli</i> JM110 cells by electroporation	46
5.2.2.2	Bacterial propagation	46
5.2.3	Preparation of bacterial glycerol stocks	47
5.2.4	Low- and high-copy plasmid DNA isolation	47
5.2.5	Enzymatic restriction analysis for the selection of positive clones	47
5.2.6	Nucleotide-Sequencing	47
5.2.7	Reverse transcription (RT) - cDNA synthesis	48
5.2.8	Quantitative polymerase chain reaction (q-PCR)	48
5.3	Biology methods	49

5.3.1	Culturing of human cells	49
5.3.2	Cell cryopreservation	50
5.3.3	Trypan blue staining	50
5.3.4	Transfection methods	50
5.3.4.1	Lipofectamine 2000-mediated transfection of human cells .	50
5.3.4.2	Lipofectamine TM LTX-mediated transfection of human cells	51
5.3.4.3	Turbofect-mediated transfection of human cells	51
5.4	Methods for handling proteins	52
5.4.1	Non-interfering TM protein assay for the determination of protein concentration	52
5.4.2	SDS-PAGE	52
5.4.3	Western blotting analysis	53
6	Results	55
6.1	Establishment of a system to study the roles of hAgo proteins	55
6.1.1	Tools for the downregulation of endogenous Ago1 and Ago2 in hu- man HeLa and ECV304 cell lines	55
6.1.1.1	Comparison and combinations of siRNA and asON-based approaches for hAgo1 downregulation	57
6.1.1.2	Knock-down of hAgo2 via siRNA and/or asON-based meth- ods	59
6.1.2	Establishment of a shRNA-based Ago knockdown system in HeLa cells	61
6.1.2.1	Evaluation of the shRNA effect on hAgo1 and hAgo2 at the protein and transcript levels in HeLa cells	64
6.1.2.2	Expression and maturation of shRNAs used in this study .	68
6.2	Study of the effect of hAgo proteins on the maturation of shRNAs in HeLa cells	73
6.2.1	Survey of the maturation of shRNA 2672 upon recombinant hAgos over-expression	73
6.2.2	Investigation of the effect of hAgos on structurally different shRNAs	75
6.2.2.1	Study of Ago effect on shRNA with different 3'-end length .	77
6.2.2.2	shRNA 4nt 3'-overhang with inverted strands	82
6.3	Analysis of the maturation of endogenous miRNAs in HeLa cells upon over-expression of recombinant hAgos	85
6.3.1	Identification of the most abundant miRNAs in HeLa cells	85
6.3.2	Investigation of hAgo effect on the maturation of endogenous miRNA	85
7	Discussion	89
7.1	A system to study the cellular role of hAgos	89

7.1.0.1	Downregulation of endogenous Ago proteins	90
7.2	Ago2 and Ago2 ^{Mut} over-expression leads to an increased amount of shRNA-derived mature siRNA	91
7.2.1	Human Ago1-4 proteins increase the quantity of shRNA 2672-derived siRNA to a different extent	93
7.3	Human Agos show differential effects on the maturation of shRNAs carrying different 3' termini	93
7.3.1	Human Ago1 protein shows two different effects on the maturation of shRNA with different termini	95
7.3.2	Ago2 has an enhancing effect on the siRNA derived from shRNA with 2 or 4 nt overhang at the 3'-end	96
7.3.3	Over-expression of hAgo3 inhibits the maturation of shRNAs	96
7.3.4	Ago4 leads to an increased amount of shRNA-derived siRNA having 4 nt overhang at the 3'-end	96
7.4	The Ago-enhancing effect is dependent on the 3'-terminus of shRNA while Ago3 inhibitory effect is influenced by the shRNA sequence	97
7.5	Nuclear export of shRNA with blunt end or with 5'-overhang	98
7.6	Endogenous miRNAs are not affected by hAgo up-regulation	98
8	Conclusions and Perspectives	101
9	References	103
10	Acknowledgements	121

1. Summary

The aim of this study was the establishment of a system allowing the functional analysis of the four human Argonaute proteins (hAgo1 to 4) with respect to their role in the maturation of small hairpin RNAs (shRNAs) and endogenous precursor microRNAs (pre-miRNAs).

Human Ago proteins are involved in RNA interference (RNAi), a cellular pathway by which gene expression is regulated at the post-transcriptional level. Human Ago proteins are essential for the survival of the cell as, so far, efforts to knock-out their genes in human cells were not successful. Therefore, it was attempted here to downregulate hAgo expression to a level that did not interfere with cell viability that allowed the functional analysis of individually overexpressed hAgo.

First, small interfering RNAs (siRNAs) and antisense oligonucleotides (asONs) were used to suppress hAgo1 and hAgo2 in human endothelial ECV304 cells and epithelial HeLa cells. Time course experiments revealed that maximum suppression at the protein level was achieved after 48 hours at maximal suppression of 40% in ECV304 and 50% in HeLa for hAgo1 and 60% in ECV304 and 80% in HeLa for hAgo2. This level of down-regulation for both proteins was regarded as being insufficient to exclude background activity of endogenous proteins during the functional analyses of individually overexpressed hAgo. Therefore, shRNAs were tested in HeLa cells. Western analyses as well as quantitative PCR (q-PCR) revealed that neither the protein level nor the amount of messenger RNA was reduced. Northern analyses unexpectedly revealed that the amount of the shRNA-derived siRNA was increased upon over-expression of hAgo2. The same observation was made upon over-expression of a variant of hAgo2 which was mutated in its active site involved in the cleavage of target RNA. Therefore, it appeared that a novel so far unknown activity might exist within hAgo2. Additionally, Northern analyses revealed that none of the hAgos is involved in the maturation of endogenous miRNAs.

In the light of this, it was investigated whether hAgo effect could be influenced by the overhang at the 3'-end of the shRNA structure.

More detailed *in vitro* analyses with all four hAgos and shRNAs with different overhangs at the 3'-terminus revealed that hAgo3 inhibited the formation of siRNA depending on the sequence of the shRNA. On the contrary, hAgo1, hAgo2, and hAgo4 all promoted the formation of siRNA. Moreover, hAgo1 showed to possess a trimming effect, which was

independent from the length, and sequence of the overhang at the 3'-end and resulted in the formation of three differently shRNA-derived siRNA sequences.

Further, the obtained data shed light on the different behaviours among the four hAgos on the maturation of shRNAs. The established system allowed the discovery of novel functions of hAgo proteins and, thus is a valid approach for the *in vitro* analysis of unknown hAgo functions and characteristics.

2. Zusammenfassung

Ziel der vorliegenden Arbeit war es, ein System zur funktionellen Charakterisierung der vier bekannten humanen Argonaut-Proteine (hAgo1 bis -4) zu etablieren, um ihre Rolle bei der Reifung von shRNA (engl. small hairpin RNA) sowie endogener Vorläufer-MikroRNA (engl. precursor microRNA, pre-miRNA) zu untersuchen.

Humane Ago-Proteine sind an dem RNA-Interferenz (RNAi) Prozess beteiligt, einem zellulären Vorgang, durch den die Gen-Expression auf der posttranskriptionalen Ebene reguliert wird. Bemühungen, die Argonauten-Gene vollständig zu inaktivieren, sind bislang fehlgeschlagen. Es wird daher vermutet, dass die Argonauten für das Überleben humaner Zellen essentiell sind. Um die Funktion einzelner hAgo-Proteine in der lebenden Zelle untersuchen zu können, war es deshalb notwendig, deren Expression soweit herunter zu regulieren, dass das Überleben der Zelle zwar gewährleistet war, jedoch ihre Hintergrundaktivität nicht die Funktionsanalyse nach Überexpression jeweils einer der vier rekombinanten hAgo-Proteine zu stark beeinträchtigte.

Dazu wurden zunächst siRNA (engl. small interfering RNA) bzw Antisense-Oligonukleotide (asON) gegen hAgo1 und hAgo2 verwendet.

Dabei wurde in humanen ECV304- und auch HeLa-Zellen eine maximale Suppression nach 48 Stunden auf Proteinebene beobachtet (für hAgo1 40% in ECV304- und 50% in HeLa-Zellen, für hAgo2-Protein 60% in ECV304- und 80% in HeLa-Zellen). Dies schien unzureichend, um Hintergrundeffekte durch die endogen exprimierten Ago-Proteine auszuschließen. Deshalb wurde die Wirkung von shRNA in HeLa-Zellen untersucht. Sowohl quantitative PCR (q-PCR) als auch Western Analysen ergaben, dass auch in diesem Ansatz weder die Menge der vorhandenen Boten-RNA noch des vorhandenen Proteins verringert werden konnte. Um auszuschließen, dass eine unzureichende Aktivierung des RNAi-Mechanismus hierfür verantwortlich war, wurde untersucht, ob genügend der shRNA-abgeleiteten siRNA-Moleküle entstanden waren. Northern Analysen ergaben, dass die Menge der gereiften siRNA während der Überexpression von hAgo2 zunahm. Die gleiche Beobachtung wurde für eine Mutante von hAgo2 (hAgo2^{Mut}), deren katalytisches Zentrum inaktiviert wurde, gemacht. Somit scheint es sich um eine bislang unbekannt zweite Aktivität des hAgo2 zu handeln. Hingegen konnte durch Northern Analysen eine Beteiligung der hAgo an der Reifung von miRNA ausgeschlossen werden. Aus diesem Grund wurde im weiteren Verlauf untersucht, ob bei Überexpression der

hAgo1, 3 und 4 ebenfalls ein solcher Effekt zu beobachten ist und welche strukturellen Eigenschaften der RNA die Spaltung beeinflussen, insbesondere des 3'-Überhangs, dessen Bedeutung für die Reifung von RNA in der Literatur beschrieben wurde.

Es konnte gezeigt werden, dass alle hAgo die Bildung von siRNA beeinflussen. Während hAgo1, 2 und 4 die Prozessierung von shRNA verstärkten, übte hAgo3 abhängig von der RNA-Sequenz eine hemmende Wirkung aus. Des Weiteren konnte für hAgo1 ein Trimmen der shRNA nachgewiesen werden, welches zur Bildung von drei reifen siRNA-Sequenzen führte. Diese Aktivität war unabhängig von Länge und Sequenz der getesteten 3'-Überhänge der shRNA.

Das etablierte System ermöglichte die Entdeckung neuer Funktionen der hAgo-Proteine und stellt demnach einen validen Ansatz zur *in-vitro*-Analyse unbekannter Funktionen und Eigenschaften der hAgo-Proteine dar.

3. Introduction

3.1 RNAi: from the discovery to date

The regulation of the gene expression has been for a longtime object of investigation, because it is a good strategy for carrying out experiments to study gene/protein functions or, alternatively, it is used in the therapeutic field to contrast the over-expression of dys-regulated genes [1]. In former times, the inhibition of gene functions was realized, for

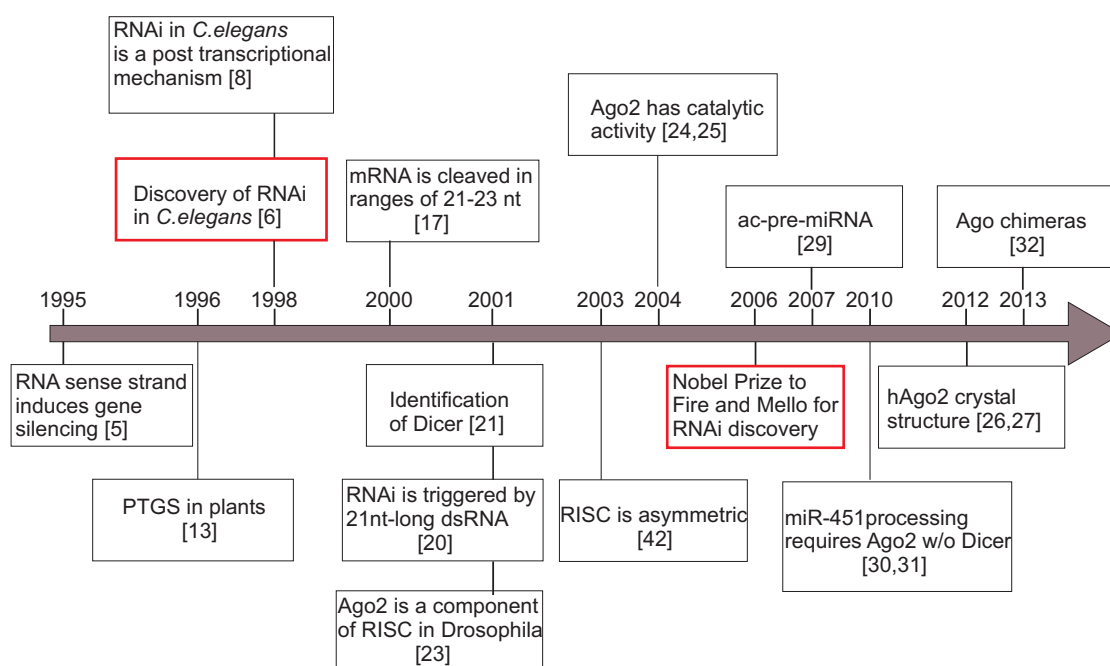


Figure 3.1: RNAi timeline

example, in *Caenorhabditis elegans* (*C. elegans*) [2], by using an antisense-based approach based on a single-stranded (ss) RNA that recognized messenger RNA (mRNA) target via Watson-Crick base pairing leading to translation suppression [3, 4]. In 1995 new surprising findings came out: in fact, Guo *et al.* [5], intended to suppress genes in *C. elegans* by using the antisense-based strategy, but realized that also the sense strand was able to induce gene silencing. This astonishing observation rose intriguing ques-

tions that required deeper insights. These were given by Andrew Fire and Craig Mello, whose lab groups, based on the previous scientific evidences, investigated whether gene silencing in *C. elegans* could be induced by double-stranded RNA (dsRNA) molecules as well. It came out that the effectiveness of dsRNA in mediating gene interference was even higher when compared to ssRNA [6]. Fire and Mello were awarded the Nobel Prize in 2006 for the discovery of this phenomenon in *C. elegans*, known as RNA interference (RNAi). Further experimental evidences in worms showed that the dsRNAs interfere with gene function by acting on a target transcript and consequently by inhibiting its translation [7]. Therefore, it was called posttranscriptional gene silencing mechanism (PTGS) [8]. The RNAi mechanism is primed in many organisms when they get in contact with a non-endogenous molecule that they consider a personal threat, representing on one hand, a defence mechanism, and on the other hand, a system to control gene expression [9–11]. Unlike *C. elegans*, RNAi in plants can be carried out at the transcriptional and post-transcriptional levels [12, 13]. Actually, the inhibition of the transcription was, for a long time, considered a consequence of DNA-methylation in the nucleus, which was mediated by DNA-DNA interactions [14]. However, it came out that the promoter methylation can also be an RNA-mediated gene silencing mechanism in higher plants [12, 15]. Moreover, *in vitro* studies suggested that, for the post transcriptional silencing, the recognition of the mRNA target is sequence-specific and that the minimum number of nucleotides (nt) required for triggering RNAi [16] is a 21-23-nt long guide strand derived from dsRNA [17–19]. Similarly, in mammalian cells RNAi is triggered by a 21-nt long dsRNA [20]. Since then, many in-depth studies have been carried out and have brought to light other surprising findings: Berstein *et al.* [21] identified an enzyme, Dicer, which belongs to RNase III family and that is conserved among flies, plants and mammals and that processes dsRNA, generating guide strands. The small dsRNA derived from the processing of long dsRNA were called siRNAs. Further, endogenous dsRNA molecules having hairpin bulged structure revealed to undergo to Dicer processing and they were called microRNAs (miRNAs) [22]. The protein complex involved in RNAi and called RNA-inducing silencing complex (RISC) contains a member of Argonaute family, Ago2 [23] whose catalytic activity was ascertained in 2004 [24, 25]. Its crystal structure was published only 8 years later [26, 27] and docking studies indicated that Ago2 binds the upper part of Dicer leading to the formation of a complex with three angles [28]. Evidences confirmed the involvement of Ago2 in the processing of miRNA precursors, leading to the formation of Ago2-cleaved precursor (ac-pre-miRNA) [29], or in the case of miR-451 processing to a mature miRNA which does not require Dicer activity [30, 31]. The study of Ago chimeras activity in 2012 shed light on the functions of each domain constituting Ago proteins [32]. In the last decade, many important steps forward have been made for understanding the mechanism underlying the RNAi pathway which are summarized in Figure 3.1.

3.2 The RNAi mechanism

In mammalian cells, RNAi can be triggered by two classes of dsRNA molecules: siRNAs as well as miRNAs [33]. The first are perfectly complementary RNA strands of 21-22 nt in length with 2nt overhang, while the second class has mismatches in its structure [34]. In accordance to whether a siRNA or a miRNA induces RNAi mechanism, it is possible to distinguish between siRNA- or miRNA-RNAi mediated pathway, respectively.

3.2.1 The siRNA-mediated RNAi pathway

The siRNA-mediated RNAi pathway can be triggered by siRNAs which are derived from hairpin RNA precursors encoded by a plasmid or from long dsRNA [35]. These molecules directly undergoes to Dicer processing leading to the formation of siRNAs, which is consequentially loaded into the RISC. RISC has a catalytic and cleavage activity due to the presence of the Dicer and Ago2 enzymes, respectively [36,37], while biochemical studies also revealed the presence of Ago1 [38] and other cofactors as the cytoplasmic transactivation response RNA binding protein (TRBP) that is responsible for the recruiting of Ago2 to Dicer complex [39]. Recently, it was also shown that TRBP is involved in regulating nuclear receptor activity [40]. It was suggested that RISC encounters siRNA as duplex, which afterwards is unwound [41]. Of the two strands only one, called antisense, is incorporated into the RISC while the other, named sense, undergoes to degradation [42] that facilitates the strand removal [43] (Figure 3.2). Schwarz *et al.* [42] suggested that the stability of the base pairs (bps) at the 5'-end of both strands constituting the siRNA duplex is responsible of the choice of the strand that must be loaded into the RISC. Typically, the less stable 5'-end containing strand is the one that is loaded [44]. Therefore, the two strands do not have the same possibility to be loaded; this gives rise to asymmetric feature of RISC [42]. The 5'-end of siRNA showed to have a key role since its chemical modifications suppress RISC activity. The loading of the antisense strand is considered to be irreversible, therefore no other RNA can be exchanged [38]. The antisense strand recognizes the mRNA by a perfect base pairing, inducing its cleavage [41]. In human cells, mRNA cleavage occurs by hydrolytic way by leading to the formation of 3'-hydroxyl (OH) and 5'-phosphate fragments [45]. Scientific evidences show that mRNA cleavage is not a necessary step for RISC assembly [43]. Since the RISC loading complex (RLC) *in vitro* does not require any cofactors or any inductive conditions to be assembled and active as the endogenous one [46]. The formation of the RISC does not depend on the dicing activity and it can load RNA molecules in an ATP-dependent manner. The Ago proteins that constitute the RISC do not show differential preferences toward different structured dsRNA molecules [47].

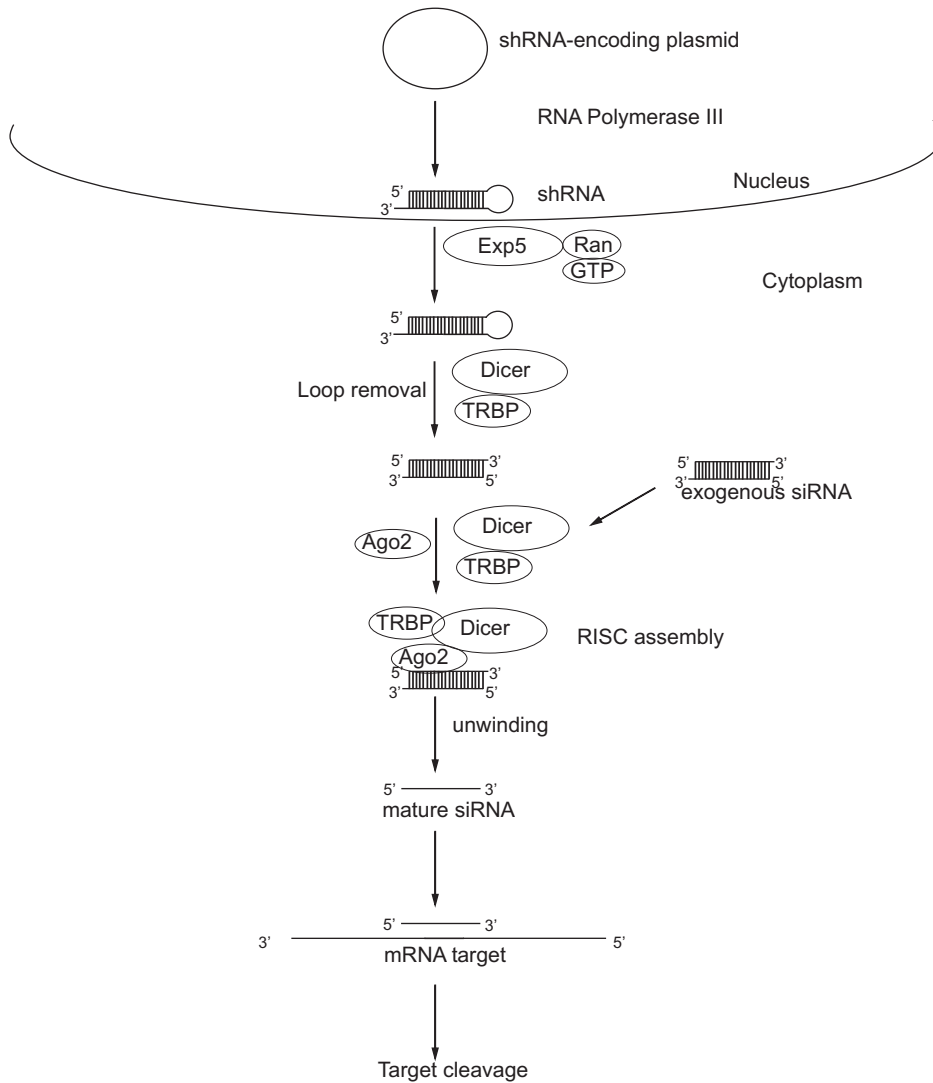


Figure 3.2: Exogenous siRNA or shRNA-derived siRNA pathways. shRNA are transcribed by the RNA polymerase III and exported into the cytoplasm by Exportin-5 (Exp5) which is a RanGTP-dependent protein [48]. Therefore, it mediates the transfer of molecules from the nucleus into the cytoplasm by using the energy derived from the conversion of the guanosine triphosphate (GTP) to guanosine diphosphate (GDP) that the protein Ran binds. In the cytoplasm the loop is removed by the Dicer/TRBP complex and the resulting siRNA or exogenous siRNA are loaded into Ago which removes the passenger strand. The remaining guide strand is used to target the corresponding mRNA transcript inducing its cleavage and degradation. Modified from de Fougères *et al.* [49].

In *Drosophila melanogaster*, Dicer was deemed responsible for processing dsRNA [21] and the biochemical purification of RISC indicated Ago2 as its component [23]. The four stages of RNAi pathway in *Drosophila* were identified [50] as described in Figure 3.3. However between human and fly, some differences are present: in the siRNA pathway in *Drosophila*, three proteins-containing complexes were found and called R1, R2 and R3. They require the involvement of Dicer, which interacts with siRNA leading to Ago loading [51]. Specifically, Dicer-2 and a protein called R2D2, so-called because it contains two dsRNA-binding domains (R2) and Dicer-2 (D2) [52], determines which of the two strands interact with Ago2-containing RISC [53]. Unlike human cells, in *Drosophila*, two different RISCs are constituted: Ago1- and Ago2-containing RISC. The first is formed in case the guide strand does not perfectly match with the mRNA target. On the contrary, Ago2-RISC loads the full complementary RNA strand [54,55]. RISC in *Drosophila* exerts the endonuclease function in Mg^{2+} -dependent manner [56] and kinetic analysis showed that the 5'-terminus of the siRNA is involved in determining the energy for binding RNA transcript, while the duplex region and 3'-terminus are responsible of catalysis [57]. In order to design functional siRNAs, many studies have been carried out to determine of the criteria that guarantee the siRNA activity. For example, the GC content that must be low (in a range between 36%-52%), internal repeat sequences must be avoided [58], the thermodynamic stability of the 3'-end of the sense strand plays also an important role since an unstable 3'-end allows the unwinding of the two strands [59]. In other words, the free energy value of the termini determines which strand is loaded by RISC [42,44]. The thermodynamic stability is another parameter to consider since it influences siRNA function, strand dissociation and strand loading into RISC [60]. Chemical modification at the 5'-end of the antisense siRNA affects silencing activity. Specifically, phosphorylation leads to a more efficient gene suppression [50] since it influences stability and also because it is recognized by Ago2 as a sort of fixed point to determine the cleavage position [61]. If the tyrosin located in the 5'-binding region of Ago is mutated with a negatively charged group, it creates repulsion for allocating the phosphorilated 5'-end of the siRNA leading to inhibition of gene silencing activity [62]. siRNAs are also used as a therapeutic tools to contrast the over-expression of genes in many diseases. However, side effects related to their administration were found: levels of p53 and p21 were affected [63], and the Jak-stat pathway was activated by up-regulation of interferone gene expression [64].

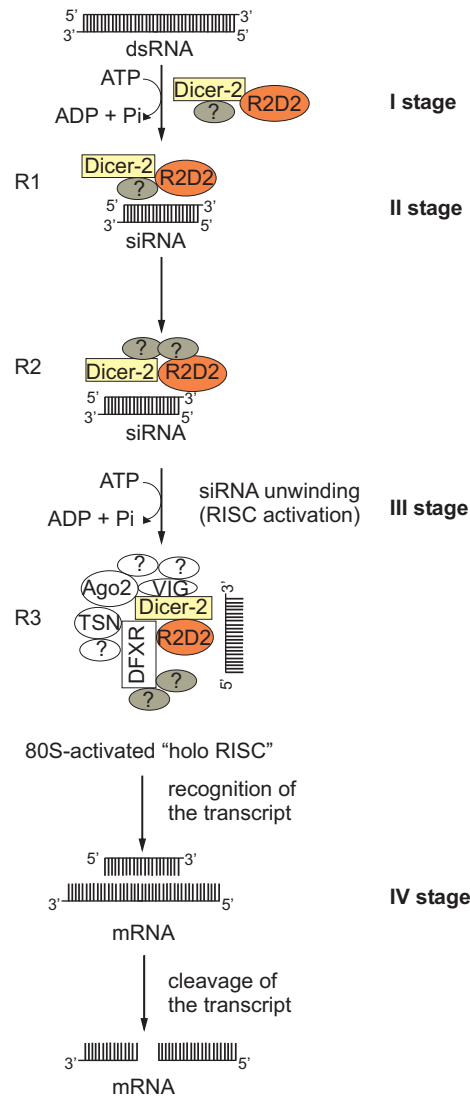


Figure 3.3: Proposed model for the siRNA pathway in *Drosophila*. Four stages were identified: (I) cleavage of dsRNA to give rise to siRNA in ATP-dependent manner; (II) loading of siRNA in a protein complex; (III) unwinding of the two strands of the siRNA by ATP; (IV) sequence-specific recognition of the target transcript followed by its cleavage. Dicer and dsRNA or siRNA lead to the formation of the so-called R1 complex which gives rise to R2 and R3 complexes. In this latter, unwinding of siRNA occurs. ? indicates unknown proteins. Modified from Nykänen *et al.* [50] and Pham *et al.* [51].

3.2.2 short hairpin RNA (shRNA)-derived siRNA

RNAi in mammalian cells can be also triggered by shRNAs that are encoded by plasmids and transcribed starting from the RNA polymerase II or III promoter. Since the discovery that endogenously produced small temporal RNAs (stRNAs), *let-7* and *lin-4*, take part in the RNAi mechanism [22, 65] and since evidence showed that stRNAs are derived from hairpin structured precursors, Paddison *et al.* [35] used their sequences as template to create mimic molecules able to trigger RNAi and to target the gene of interest. Initially, they performed those experiments in *Drosophila* and found that shRNAs were functional in gene silencing. Furthermore, they found out that shRNAs were able to induce gene suppression in mammalian cells as well. They were also tested in *Drosophila* where they are loaded into every Ago protein and the complex activation was favoured with the increase of the thermodynamic instability of the shRNA [66]. This can be explained by the fact that instable dsRNA leads to release the passenger strand from the slicing incompetent Ago proteins. On the contrary, Ago2-containing complex activation does not depend on the thermodynamic stability of the duplex RNA [66]. The human U6 small nuclear RNA (snRNA) promoter is efficient in producing siRNA [67], therefore U6 snRNA promoter cassettes proved to be a good strategy for expressing siRNA [68]. The goal of many studies is to design efficient shRNAs [69]. Even if all the criteria have been fulfilled, Dicer processing could be feckless [70]. For example, shRNAs bearing ≤ 19 bp cannot be processed by Dicer because they are too short. This opened the issue concerning their processing and in 2012, Dallas *et al.* [71] shed light on this issue. First of all they distinguished these small shRNAs (sshRNAs) in right (R) and left (L) depending on the position of the loop at the 5'- or 3'-end of the guide strand, respectively. They suggested that the R shRNA required the loop cleavage and subsequently removed the passenger strand. On the contrary, L shRNAs are processed without losing the loop, but with the removal of a small fragment from the passenger strand. Therefore, a ds portion is still present in the Dicer product that needs to be unwound giving rise to a long molecule [71]. shRNAs proved to be more efficient than siRNAs since shRNA, unlike siRNA, are transcribed in the nucleus allowing a constitutive expression of those molecules [72].

3.2.3 miRNA

3.2.3.1 The biogenesis of miRNAs

The miRNAs belong to a class of non-coding RNAs of 21-22 nt in length and are cellularly produced molecules [73]. They arise from gene transcription performed by the RNA Polymerase II or III that leads to the formation of primary miRNA (pri-miRNA) [74]. Pri-miRNAs undergo to the processing by the nuclear RNase Drosha III enzyme and become the precursors miRNAs (pre-miRNAs) which are characterized by a long stem loop (Figure 1.3) [75]. Drosha works in complex with DiGeorge syndrome chromosomal

region gene 8 (DGCR8) inducing the cleavage of hairpin precursor which leads to the formation of the pre-miRNA [76]. A model for pri-miRNA processing was proposed, which consists of two steps [77]. The first step requires that DGCR8 anchors the pri-miRNA. The second step is represented by the pri-miRNA processing by Drosha into precursor miRNA (pre-miRNA) [78], which is exported by Exp5 into the cytosol where it undergoes to further processing which leads to until the formation of mature miRNA. Concerning the latter step, it is important to distinguish different possible pathway and the main three are described below:

Dicer-dependent mechanism (canonical)

In the canonical mechanism, the pre-miRNA serves as a Dicer substrate that is responsible for loop removal, inducing the formation of the ds miRNAs (Figure 3.4). Dicer, TRBP, Ago, together with other cofactors, constitute the RISC where the miRNA is loaded and the two strands are separated [79]. Only one strand, the guide strand, remains bound to the RISC, while the passenger strand is degraded. The guide strand recognizes the 3'-untranslated region (3'-UTR) of mRNA target in a sequence-specific manner, forming bulges in the duplex guide/target and inhibiting its translation without inducing its cleavage. Nevertheless, some experiments gave rise to contrasting observations suggesting that both strands are present in the same amount in the cell [80]. These data were also supported by other studies that showed that also the so-called passenger strand can be loaded into RISC [81]. This knowledge brought up the intriguing question of whether the loop as well, after Dicer-mediated cleavage, could give rise to an active RNA sequence. Experiments performed by Diederichs's group [82] showed that loop sequences, called Loop-miRs, can mediate gene silencing.

Ago2-dependent mechanisms (non-canonical)

Cleavage of pre-miRNA by Ago2 leads to Ago2-cleaved precursor (ac-pre-miRNA)

Diederick and Haber [29] found that the catalytic active Ago2 is capable of performing a cleavage of the passenger strand at 11 or 12 nt from the 3'-end of the precursor miRNA. The outcoming molecule is called Ago2-cleaved precursor miRNA (ac-pre-miRNA) and it goes to Dicer processing, giving rise to a mature miRNA (Figure 3.4).

Ago2 alone is responsible for the maturation of pre-miR451

It was discovered that the miR-451 behaves in a different way from other miRNAs: in fact, in mice lacking catalytic Ago2 and expressing a mutated Ago2 that was slicing deficient, the expression level of mature miR-451 was highly reduced, while the amount of the its precursor did not change [30, 83]. This observation suggested that the presence of Ago2, capable of nuclease activity, was strongly involved in the maturation process of this miRNA.

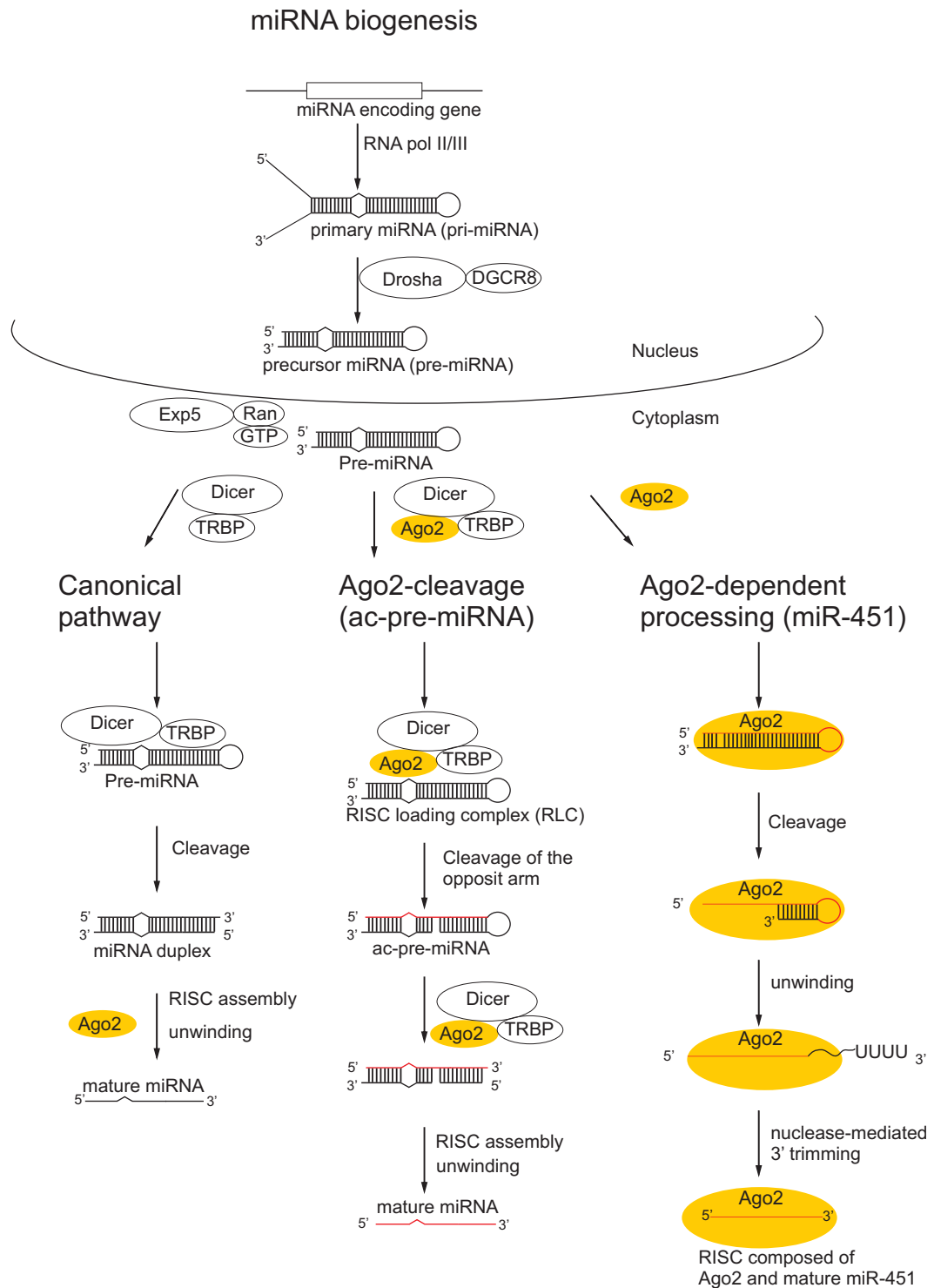


Figure 3.4: Biogenesis of miRNA. The three main pathways for the biogenesis of miRNAs are shown, which include a canonical pathway involving Dicer and two Ago2-mediated pathways: one involves Dicer in the formation of the RISC loading complex followed by the formation of the Ago2-cleaved pre-miRNA (ac-pre-miRNA); the other do not require Dicer neither during the loading nor in the processing of the pre-miRNA (miR-451). Modified from Winter *et al.* [84] and Yang *et al.* [85]

Moreover, the pre-miR451 is too short to be a Dicer substrate further supporting the concept that miR-451 could be processed without Dicer [83]. However, further investigation was needed to test this hypothesis. Cheloufi *et al.* [30] investigated the expression of miR-451 in mouse embryonic stem cells lacking Dicer and they found no evident alteration of the amount of mature miRNA confirming the previous hypothesis. Additionally, *in vitro* experiments gave rise to concordant results since Dicer could not process the pre-miR451 [30,31,83]. In conclusion, miR-451 is an example of miRNA processed in a Dicer-independent manner, outlining a non-canonical pathway (Figure 3.4). Since then, the rational design of RNA molecules which is based on the structural requirements of miR-451 was performed leading to products that are capable of gene silencing [86]. It came out that the presence of U at the 5'-end of pre-miRNA or the unpairing at the position +35 lead to an increased miRNA activity, while the processing efficiency is increased by reducing the content of GC in the distal hairpin region or by the unpairing of the pre-miRNA sequence [86].

Other examples of miRNAs processed in a non canonical way

Among the miRNAs that are originated via the so-called non-canonical pathway, it is possible to distinguish miRNA that do not require Dicer involvement such as miR-451 [30,87] and miRNA that are processed by Dicer [29]. An example are the mirtrons which derive from a pre-miRNA that, upon splicing, is processed in humans by debranching enzyme DBR1. The resulting pre-miRNAs have the structural requirements to be recognized by Exp5 which mediates their transfer into the cytoplasm. There, the pre-miRNAs are Dicer-substrates and give rise to a mature miRNAs [88,89]. Moreover, some miRNAs that resemble mirtrons, but whose origin occurs independently from the splicing mechanism, were discovered and called simtrons [90]. Both simtrons and mirtrons can mediate suppression of gene expression via association with all the members of Argonaute family [90].

3.2.3.2 Loading of mature miRNAs by Ago proteins and miRNA functions

Unlike the *Drosophila* system, in which the miRNAs are loaded into Ago1, while the siRNAs are loaded into Ago2 [54,55,91], experiments in human cells do not provide evidence for any selective loading of miRNAs among the four Ago proteins. However, the different effect of hAgo proteins is evident in determining the size of some miRNAs [92].

In *Drosophila*, it was demonstrated that the RISC loading process is ATP-dependent while the strand dissociation step does not require ATP or the cleavage competent Ago1 [93]. It was suggested that this observation concerning Ago1 *Drosophila* may also justify why also mammalian Ago proteins which are incapable of cleavage can unwind dsRNA [93]. The main genes that are silenced by miRNAs encode molecules within a wide range of functions, mostly with work in the regulation of transcription [94]. It was found that

in yeast, the decapping of mRNA and its degradation takes place in processing bodies (p-bodies) [95]. miRNA complementarity has also been an object of investigation since it was suggested that not only it is necessary for the formation of the duplex miRNA/mRNA, but it may also have regulatory role on non-mRNA targets [96]. *In vitro* experiments carried out in mammalian cell lysates showed that the miRNA precursor deposit complex (miPDC) constituted by precursor miRNA bound to Ago, TRBP and Hsp, in presence or absence of Dicer, represents the first important and necessary step prior to miRNA processing [97]. Transfection of human cells with pre-let-7a showed that the passenger strand, which usually is rapidly degraded, becomes more stable upon over-expression of human Ago proteins [98]. A systematic study was performed in order to identify sites in the miRNA sequence that are responsible for the interaction with mRNA target [99]. Two groups of target sites were identified: one requires base pairing at 5'- and 3'-end or only at the 5'-end of the miRNA; the other involves only the 3'-end of the miRNA in the target recognition [99]. It was demonstrated that the involvement of the 5'-region of the miRNA in leading to translation inhibition is due to the free energy that characterizes the first 8 nt of the sequence. However, the pairing at the 3'-end of the miRNA can also be important in some cases [100]. For example, if the interaction between the mRNA and the 5'-end of the miRNA is weak, then the miRNA 3'-end would play a crucial role in determining the base pairing with the transcript [100]. Several target sites on miRNA sequences can induce synergism in miRNA activity studies [99,100] leading to the so-called cooperativity effect that increments miRNA functions [101]. Human cancer cells showed to be characterized by variations in miRNA sequences [102]. Based on these evidences, Diederichs and Haber [102] performed studies aimed to understand the consequences of these changes. They found that these alterations induce modifications of predicted secondary pri-miRNA structure, hence they had no effect on their processing. Therefore, no functional alterations were derived from those modifications [102].

3.3 RNase III proteins

It is possible to classify RNase III proteins in three main classes. To the first class belong proteins which are found in yeast and bacteria, while in animal cells, RNase III proteins of the second class (such as Drosha) and of the third class (such as Dicer) can be found [76]. Proteins belonging to the class II and III are described in detail below.

3.3.1 Drosha

Drosha (130-160 kDa) presents two RNase III domains (RIIID), one domain responsible for binding dsRNA and a quite wide amino (N)-terminal domain [76]. The two RIIID in Drosha can be distinguished in a and b that are responsible for the cleavage at the 3'-end or 5'-end, respectively [76]. In the maturation of miRNA, the just transcribed stem loop

of structured RNA, called primary miRNA (pri-miRNA), is processed by Drosha into a molecule that is about 70 nt in length called precursor miRNA (pre-miRNA) that has 2nt at the 3'-overhang end [76]. Drosha was found in a complex of 650 kDa in size, which suggests that it is bound with other proteins in the cell [78]. In fact, in support of this idea, it was found that a protein capable of a nonspecific RNA-binding called DGCR8 [103] in mammalian cells interacts with Drosha [78, 104, 105]. Interestingly, experiments performed by testing recombinant human Drosha revealed its non-specific cleavage activity, while it was restored in presence of DGCR8 [106, 107]. The question about how Drosha can choose substrate hairpin RNA among many other similar RNAs prompted many studies that culminated in the observation which states that Drosha needs some structural requirements in its the substrate such as a large loop (≥ 10 nt) on the stem structured RNA [108] or ssRNA sequences flanking the pri-miRNA [109]. In fact, Zeng *et al.* [109] tested pri-miRNA having 8nt- flanking sequences and they observed that even a higher number of nt was required to achieve a high yield of the corresponding mature miRNA: for instance, 51 flanking nt were needed for the natural miR-31 to be highly expressed in the cell.

3.3.2 Dicer

Dicer belongs to the third class and showed to be more complex than the first two classes since it carries one dsRNA-binding domain, two RIIID (a and b), a substantial N-terminal with RNA helicase activity, a DUF283 domain whose function is not yet clear, and a PAZ domain [76]. MacRae *et al.* [110] determined the crystal structure of *Giardia* Dicer, in which a long helix links the PAZ domain to the RIIID a and it is surrounded by the N-terminal domain. RIIIDa is connected to RIIIDb domains via a large helix-shaped domain. Like Ago proteins, the PAZ domain in Dicer recognizes the 3'-overhang of the RNA molecule.

Human Dicer is about 200 kDa in size and it was shown that the RIIIDa domain mediates the cleavage of the hydroxyl group (OH) at the 5'-end while the domain b cuts the phosphate at the 5'-end of the RNA substrate [111]. Dicer is essential for many biological processes such as in the processing of pre-miRNAs [79], stem cell differentiation [112, 113] and in the development [114]. Betancur *et al.* [115] showed that Dicer is not necessarily involved in the formation of RISC. They proposed a possible explanation which suggested that Ago proteins can alone recognize the different thermodynamic stability of the two strands of the dsRNA. Unlike flies which possess two different Dicer: Dicer-1 and Dicer-2 which are responsible of processing the pre-miRNA and long dsRNA-derived siRNA [116, 117]. In mammalian cells only one Dicer is required for the processing [118]. In fact, recombinant Dicer showed to be able to cleave dsRNA into products of 22-23 nt in length and pre-let7 into mature miRNA [119, 120]. However, Dicer alone is not able to distinguish between those two kinds of substrates; this discrimination occurs only with

the help of other co-factors [118]. The cooperation between Dicer and other proteins influences the cleavage, which leads to the formation of different products: more 22 nt-long fragments than 20 nt-long products in comparison to Dicer alone [121]. Among the proteins that help Dicer in its function are Ago, TRBP, PACT [122]. It was shown that those proteins ensure a better synchronization of the cleavage by Dicer resulting in a specific and efficient product formation [122]. Dicer recognizes its substrate in three main sites. The 3'-end of the RNA interacts with PIWI Argonaute Zwiille (PAZ) domain of Dicer, the dsRNA portion with its dsRNA binding domain and the loop via interaction with the helicase domain [123]. The specific length of Dicer product is due to both PAZ domain and RNaseIII domains [123]. Until 2011 the prevalent Dicer cleaving model was based on Dicer 3'-end counting rule, that means that the cleavage by Dicer takes place after 22 nt from the 3'-end of the dsRNA [124]. Surprisingly, Park *et al.* [70] demonstrated that Dicer works as a ruler and can count from the 3'-end or from the phosphorylated 5'-end, indicating that the site of cleavage is determined also via the 5'-end counting rule. Moreover, a double anchoring model in which the 3'-end and 5'-end of dsRNA anchor Dicer in so called 3'- and 5'-pockets, respectively [70]. Additionally, a dsRNA substrate bearing 2 nt 3'-end-overhang (canonical substrate) is processed by Dicer more efficiently than a RNA molecule with blunt ends or than any other dsRNA with different termini [70]. The non canonical substrates, when undergoing Dicer processing, cannot ensure a fixed cleavage position making Dicer cleavage unpredictable and leading to the formation of several products. On the contrary, Dicer in *Giardia* does not follow the rules outlined for the human counterpart, showing to preferentially cleave substrates with blunt ends [70]. In addition to the 3'-end and 5'-end counting rule, also Dicer loop counting rule was proposed in order to identify the exact cleavage position on the substrate [125]. Moreover, it was suggested that Dicer is able to distinguish the siRNA to load on the base of their similarity with Dicer products (19 bp + 2 nt 3'-end-overhang) that, in the opinion of Sakurai *et al.* [126], was an indication that the siRNAs are active.

3.4 The Argonaute family

3.4.1 Classification

Ago proteins have been found in bacteria, archaea and eukaryote domains [127]. In eukaryotes, Ago proteins are divided in three different subfamilies: Ago, Piwi and worm-specific WAGO [128]. Each subfamily is able to bind a different class of RNA. The subfamily Ago binds siRNAs and miRNAs which trigger RNAi [129]. The P-element induced wimpy testis (PIWI) subfamily binds PIWI-interacting RNA which functions in germlines cells [24, 130] and worm-specific WAGO proteins that bind secondary siRNA which are produced by RNA polymerase directed by RNA (RdRPs) [131, 132]. In humans, the Ago

subfamily is composed of four members, called Ago1-4 and they are crucial proteins in the RNAi process [133]. Among these Agos only the gene encoding Ago2 is located on chromosome 8, while the other three proteins are encoded by a cluster of genes on chromosome 1 [134]. Unlike human, in *Drosophila* there are only two Ago proteins named Dm-Ago1 and Dm-Ago2 [135].

3.4.2 The protein structure of human Argonautes

The four human Agos are called Eukaryotic Translation Initiation Factors 2C (EIF2C1-4) [136]. Each Ago proteins is composed of four domains: N-terminal, PAZ, MID and PIWI domains [137]. Each domain is described below detail.

Initial evidence suggested that N-terminal domain of hAgo2 might be involved in the initial steps of unwinding of dsRNA [138]. Additionally, N-terminal domain of hAgo2 is required for cleaving the passenger strand and it may also play a role in the recognition of transcripts [138]. PAZ and the MID domains are responsible for the binding of 3'-end and 5'-end phosphate of the miRNA, respectively [139, 140]. It was found that PAZ domain is dispensable for the formation of slicing RISC, while it is required by non-cleaving Ago proteins to form an active RISC [141]. The crystal structure of *Drosophila* Ago2 PAZ domain revealed that this domain is necessary for the binding to siRNA and that the interaction between PAZ and siRNA occurs at the 2 nt 3'-end-overhang of the siRNA [142]. However, it was found that also PAZ domain of hAgo1 is able to bind to RNA [143] and that 2 nt at the 3'-end-overhang of the duplex RNA are required [144], similarly to *Drosophila*. MID domain was shown to be responsible for the interaction with the phosphorylated 5'-end of the RNA [140]. Afterwards, the crystal structure of the hAGO2 MID domain allowed to shed light on this interaction. In fact, it was proved a certain preference of MID domain in binding RNA in which the 5'-base is represented by A or U [145]. PIWI domain contains the catalytic tetrad: aspartate597/glutamate637/aspartate669/histidin807 (D597/E637/D669/H807) present in hAgo2 or hAgo3 PIWI domain, but only hAgo2 is able of RNase H activity [146]. In hAgo1 the tetrad contains an arginin (R) instead of the H (DEDR), while in hAgo4 tetrad there is only one D in comparison to hAgo1 [146]. Additionally, Faehnle *et al.* [146] demonstrated that the replacement of the hAgo2 tetrad in hAgo1 does not make it cleavage competent. This suggested that other features of the protein must be involved. Moreover, the substitution of the D in position 669 with an alanine leads to the loss of slicing activity [25]. Hauptmann *et al.* [32] carried out experiments that aimed to transform Ago1, Ago3, Ago4 into slicer competent proteins by exchanging some domains with the ones of Ago2, thus leading to the formation of so-called chimera molecules. Ago3 becomes slicer competent after exchange of its N-terminal domain with the one from Ago2. In other words, the N-terminal domain of hAgo3 suppresses ribonuclease activity. However, the complete N-terminal domain is not necessary for the slicing activity; only two sequences located on it are responsible for the cleavage [32]. This is in

agreement with other studies that proved that the slicing competence of PIWI domain of hAgo3 can be achieved by introducing 2 motifs (motif I is constituted by Ago2 residues 44-48 while motif II ranges between Ago2 residue 134 and residue 166) of the N-terminal domain of the active hAgo2 in the hAgo3 sequence [147]. Therefore, in order to have slicer Agos, the catalytic sequence and the combination of near and distant protein regions are required. In fact, to create a cleavage competent Ago1, the catalytic sequence with mutated loop that is located close to the active side and the N-terminal domain of Ago2 are needed [146]. Moreover, Ago1 can be turned into a catalytic active protein by changing PIWI and N-terminal domain [32].

Crystal structure of hAgo2

Currently, two crystal structures of hAgo2 are available: one in complex with a mixture of 10-20 nt-long RNAs [26] and an other one in complex with miR-20a [27]. The two structures showed high resemblances. The miRNA anchors, the MID and PAZ domains leading to an higher stable conformation of the protein which, otherwise, would be very flexible. The crystal structure of hAgo2 in complex with miR-20a resembles a duck in

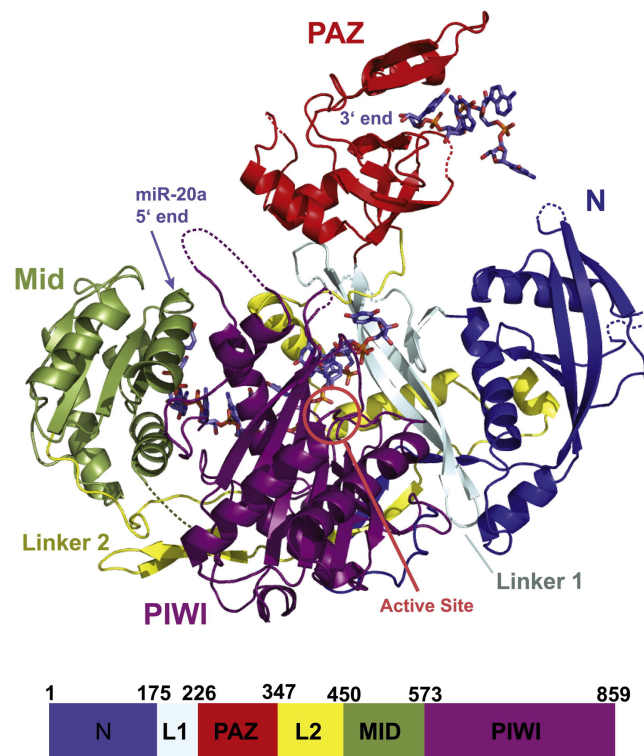


Figure 3.5: Depiction of the crystal structure of hAgo2 in complex with miR-20a and representation of hAgo2 domains: N, PAZ, MID and PIWI color-coded in blue, red, green and purple, respectively. The red circle indicates the active site while the binding position between 5'-end of miR-20a and hAgo2 MID domain is indicated by an arrow. Taken from Elkayam *et al.* [27].

which PAZ domain is representing the head containing the 3'-end of miRNA, while the

body is constituted by the PIWI domain and the MID domain, that interacts with the 5'-end of the miR-20a [27]. The N-terminal domain can be considered as wing covering the miRNA sequence as shown in Figure 3.5. The interaction between the 5'-end phosphate and the MID domain is very strong and determines the right accommodation of the mature miRNA in order to allow a precise transcript cleavage [27]. The seed region of the miRNA is blocked in a slot in which there are interactions between each phosphate of the backbone with the protein [27]. Schirle's and Macrae's [26] showed that the domain structure is conserved in prokaryotics and eukaryotics, while they differ for the global organization.

3.4.3 Functions

Ago proteins play an essential role at the both transcriptional [148] and post-transcriptional gene silencing [25, 135]. In fact, it was shown that Ago1 is present in the complex which is formed during the RNA-induced initiation of transcriptional gene silencing (RITS) [148] being necessary for the assembly of the heterochromatin domain and required for silencing the gene located in it [149, 150]. Instead, in the post-transcriptional gene silencing Ago load a RNA fragment leading to the formation of the RISC in RNAi pathway [18, 151]. Concerning the role of each hAgo proteins in RNAi, only hAgo2 is cleavage competent [24, 25]. Moreover, it is the only responsible of the maturation of pre-miR451 by giving rise to an Ago2-dependent pathway [30] as described in detail in 3.2.3 and in Figure 3.4. On the contrary, in *Drosophila* both Ago1 and Ago2 are slicing competent [91, 152]. Other studies shed light on an other feature of hAgo2 that makes it still quite different from the Ago1-3-4. In fact, Ago2 works alone, while Ago1-3-4 act in cooperation [153]. It was suggested that Ago2 different behaviour is due to its conformation which might prevent the interaction with other Agos or may be it is surrounded by other proteins [153]. The restoring of each Ago expression in mouse Embryonic stem cells deficient for Ago1-4 induces the recovery of gene silencing pathways which are triggered by endogenous miRNA [154]. This observation revealed that all Ago are implicated in RNAi pathway and it was suggested that they have overlapping functions [154]. Studies of binding and cleavage activity revealed that hAgo2 binds more strongly a ssRNA in comparison to a dsRNA [155]. Moreover, its activity is enhanced in presence of Mn^{2+} which specifically improve the cleavage of the antisense strand having OH group at the 5'-end, while the antisense with phosphate at 5'-end is cleaved by Ago2 more efficiently anyway [155]. Additionally, the PIWI domain of Ago2 showed to interact with TRBP and this interaction does not occur via RNA [155]. Although Ago2 is the only Ago to hold catalytic ability [25], all four Ago proteins can associate with miRNAs [24] and play a role in determining the size of mature miRNA [156] and also in regulating mature miRNA levels. Actually, higher Ago levels induce a higher amount of mature miRNA derived from transfected precursors [29, 157]. The binding between Ago2 and miRNA induces firmness of the protein

that, otherwise, would be too flexible and unstable [158, 159]. The complex Ago-guide strand loses stability when it encounters a target RNA that is highly complementary to the guide [160]. This leads to a faster removal of the guide from the entire complex [160]. The association between Ago3 and siRNA instead gives rise to a complex totally incapable of cleavage [161]. This observation rised the idea that hAgo3 can contrast gene silencing mediated by Ago2 or that the complex siRNA/Ago3 needs other requirements for the unwinding of siRNA [161]. It was suggested that Ago proteins in order to enter the RNAi pathway are transported from cytoplasm into the nucleus with a mechanism that involves TNRC6A, that is a human paralog of a protein called GW182 because of its size (182-kDa) and of multiple glycine(G)-tryptophan(W) repeats. In the light of it, it was suggested that proteins that belong to GW family can play a role in mediating gene silencing in the nucleus and in the cytoplasm [162, 163]. Little is known about nuclear RNAi, but the discovery of the existence of complex between Ago2 and pre-miRNA in the nucleus reinforces the belief in a nuclear gene silencing but this remains unclear [164].

3.5 Aim of the study

This study aimed to establish a cell culture-based system to study the role of hAgos and to investigate the effect of those proteins on the maturation of shRNAs and endogenous pre-miRNAs. To investigate the functions of the four hAgos first, the knock-down of the endogenous hAgo proteins and second, the expression of recombinant hAgos were considered necessary conditions in order to carry out an accurate analysis of the distinct proteins. Therefore, the most suited cell-based system for hAgo1 or hAgo2 knock-down need to be identified. Hence, silencing tools like asONs, siRNAs or their combinations should be tested in two human cell lines, ECV304 and HeLa. Subsequently, cloning and validation of plasmid-based constructs need to be performed in order to downregulate hAgo1 or hAgo2. Then a quantitative detection system for shRNA-derived siRNAs should be established, while finally the effects of over-expressed recombinant hAgos on the amount of siRNA derived from shRNA should be analyzed.

4. Materials

4.1 Chemicals

Name	Supplier
Acetic acid	Roth, Karlsruhe
Acetone	Roth, Karlsruhe
Agar	Sigma-Aldrich, Deisenhofen
Agarose	Biozym, Hessisch Oldendorf
Ammonium peroxodisulphate (APS)	Fluka, Buchs (Switzerland)
Ammonium sulphate $[(\text{NH}_4)_2\text{SO}_4]$	Gerbu Biochemicals, Gaiberg
Ampicillin (Amp)	Sigma-Aldrich, Deisenhofen
Boric acid	Roth, Karlsruhe
Bromophenol blue	Sigma-Aldrich, Deisenhofen
Calcium chloride (CaCl_2)	Roth, Karlsruhe
Chloroform/isoamyl alcohol (24:1,v/v)	Merck, Darmstadt
Coomassie brilliant blue R-250	Sigma-Aldrich, Deisenhofen
Dimethyl sulphoxide (DMSO)	Roth, Karlsruhe
Dithiothreitol (DTT)	Sigma-Aldrich, Deisenhofen
Ethanol	Fisher Scientific, Schwerte
Ethidium bromide (EtBr)	Serva, Heidelberg
Ethylenediaminetetraacetic acid (EDTA)	Merck, Darmstadt
Glycerol	Merck, Darmstadt
Glycine	Roth, Karlsruhe
Isopropanol	Merck, Darmstadt
Magnesium chloride (MgCl_2)	Sigma-Aldrich, Deisenhofen
Magnesium sulphate (MgSO_4)	Sigma-Aldrich, Deisenhofen
Methanol	Roth, Karlsruhe
N,N,N',N',-tetramethylethyldiamin (TEMED)	Roth, Karlsruhe
NP-40	LKB, Bromma (Sweden)
Phenol/chloroform/3-Methyl-1-butanol	Roth, Karlsruhe
Potassium chloride (KCl)	Roth, Karlsruhe

Potassium dihydrogen phosphate (KH ₂ PO ₄)	Roth, Karlsruhe
Potassium hexacyanoferrate (III) [K ₃ Fe(CN) ₆]	Sigma-Aldrich, Deisenhofen
Potassium hexacyanoferrate (II) trihydrate [K ₄ Fe(CN) ₆ · 3H ₂ O]	Sigma-Aldrich, Deisenhofen
Rotiphorese gel 40 (acrylamide/bisacrylamide; 19/1)	Roth, Karlsruhe
Rotiphorese gel 30 (acrylamide/bisacrylamide; 37.5/1)	Roth, Karlsruhe
Skim milk	Roth, Karlsruhe
Sodium acetate (NaC ₂ H ₃ O ₂ · 3H ₂ O)	Merck, Darmstadt
Sodium chloride (NaCl)	Roth, Karlsruhe
Sodium dodecylsulphate (SDS)	Roth, Karlsruhe
Sodium phosphate dibasic (Na ₂ HPO ₄)	Merck, Darmstadt
Stains-All	Sigma-Aldrich, Deisenhofen
SYBR gold	Invitrogen, Carlsbad, CA (USA)
Trihydroxymethylaminomethane (Tris)	Roth, Karlsruhe
Trichloroacetic acid (TCA)	Sigma-Aldrich, Deisenhofen
Triton-X 100	Sigma-Aldrich, Deisenhofen
Tween-20	Roth, Karlsruhe
Urea	Roth, Karlsruhe
Xylene cyanol	Roth, Karlsruhe
[γ - ³² P]ATP (6000 Curie (Ci)/mmol)	Hartmann Analytic, Braunschweig

4.2 Consumables

Name	Supplier
3 MM paper	Whatman, Brentford (UK)
Cell culture flasks (25, 75 and 162 cm ²)	Sarstedt, Nümbrecht
Cell culture plates (24-, 12-, 6-wells)	Sarstedt, Nümbrecht
Centrifuge tubes (15 or 50 ml)	Greiner, Frickenhausen
Gel filtration micro columns (NICK, G-50)	GE-Healthcare, München
Hybond-N+ nylon membrane	GE-Healthcare, München
Immobilon-P membrane	
Polyvinyl difluoride (PVDF)	Millipore, Schwalbach
Membrane filters (0.45 μ m)	Whatman, Brentford (UK)
Pipette (10 μ l-1000 μ l)	Eppendorf, Hamburg
Pipetten set (2 μ l-100 μ l-200 μ l)	Gilson, Middleton, WI (USA)
Scalpels	Feather, Köln
Syringes	Bec. Dic., Franklin Lak., NJ (USA)

4.3 Devices

Name	Supplier
Biotrap Gel chamber	Hofer, San Francisco, CA, (USA)
Blotting device	Hofer, San Francisco, CA, (USA)
CO ₂ incubator	Forma Scientific, Marietta, OH, (USA)
Centrifuge Beckman	Beckman, Fullerton, CA (USA)
DNA Thermal Cycler	Biometra, Göttingen
Electroporation apparatus	Bio-Rad, München
Electroporation cuvette (2 mm)	Fisher Scientific, Schwerte
Electrophoresis Power Supply-EPS 3500	Pharmacia biotech, Dsseldorf
Fluorescence microscope	Zeiss, Jena
Freezer -20 °C	Liebherr, Ochsenhausen
Freezer -80 °C	Forma Scientific
Fridge +4 °C	Liebherr, Ochsenhausen
Gel chamber for agarose gels (Mini-Sub4 Cell GT)	Bio-Rad, München
Gel chamber for Polyacrylamid gel (Maxigel: 17 x 18 cm)	Biometra, Göttingen
Gel chamber for Polyacrylamid gel (Minigel: 13 x 15 cm)	Biometra, Göttingen
Gel chamber for SDS-Gel (10 x 10.5 cm)	Hofer, San Francisco, CA (USA)
Incubator (bacteria)	Heraeus, Hanau
Incubator for Northern blotting (Herahydrid 12)	Heraeus, Hanau
NanoDrop spectrophotometer ND-1000	Peqlab, Erlangen
pH meter	Schott, Darmstadt
PhosphorImager screen	GE-Healthcare, München
PhosphorImager Typhoon TM 8600	Amersham biosciences, Freiburg
Precision balance	Kern & Sohn GmbH, Balingen-Frommern
Rotors JLA-10.500	Beckman Coulter, Krefeld
Scintillation counter (liquid) Wallac 1409	Perkin Elmer, Boston, MA (USA)
Spectrophotometer Beckman DU-640 or 600	Beckman Coulter, Krefeld
Speed Vac SC 110-A	Faust, Bochum
Storage Phosphor Screen	Amersham biosciences, Freiburg
Table centrifuge	IKA Labortechnik, Staufen
Thermoblock	Eppendorf, Hamburg

Vacuum pump	Werner Hassa GmbH, Lübeck
Vortex Vibrofix VF1	IKA Labortechnik, Staufen
Water bath W22	Sörk-Tronik, Medingen
Water Purification System	Millipore, Schwalbach

4.4 Buffers and solutions

Name	Components
Coomassie blue staining solution (for PVDF membrane)	40% (v/v) Methanol 10% (v/v) Acetic acid 0.01% (w/v) Coomassie brilliant blue R-250
2x Denaturing loading buffer (PAGE)	7.0 M Urea 0.1% (w/v) Bromophenol blue 0.1% (w/v) Xylene cyanol in 1x TBE buffer pH 8.0
Destaining solution for Coomassie (for PVDF membrane)	40% (v/v) Methanol 1.0% (v/v) Acetic acid
2x HEPES-buffered saline (HBS) (pH 7.1)	50 mM HEPES 280 mM NaCl 1.5 mM Na ₂ HPO ₄
6x Non-denaturing loading buffer	0.25% (w/v) Bromophenol blue 0.25% (w/v) Xylene cyanol 25% (w/v) Ficoll 400 in 1x TAE buffer pH 7.4
10x Phosphate buffered saline (PBS) (pH 7.4)	1.37 M NaCl 0.027 M KCl 0.081 M Na ₂ HPO ₄ 0.0147 M KH ₂ PO ₄
10x Running buffer (SDS-PAGE)	0.25 M Tris-HCl pH 8.3 2.50 M Glycine 10% (w/v) SDS
20x Saline-sodium citrate buffer (SSC) pH 7.0	2.9 M NaCl 0.3 M Na citrate
2x Sample buffer (SDS-PAGE)	0.10 M Tris-HCl pH 6.8 0.02 M DTT 4% (w/v) SDS 20% (v/v) Glycerol 0.2% (w/v) Bromophenol blue

1x Stains-All-Solution	15 mM	Tris-HCl pH 8.8
	0.005% (w/v)	Stains-All
	5% (v/v)	Formamid
	25% (v/v)	Isopropanol
10x Tris-buffered saline buffer (TBS) (pH 7.6)	1.37 M	NaCl
	0.20 M	Tris-HCl
	3.8% (v/v)	HCl
1x TBS-T buffer	1x	TBS buffer
	0.1% (v/v)	Tween-20
1x Transfer buffer (for Western blotting)	0.025 M	Tris-HCl pH 8.3
	0.190 M	Glycine
	20% (v/v)	Methanol
10x Tris-borate-EDTA buffer (TBE)(pH 8.0)	0.89 M	Tris
	0.02 M	EDTA
	0.89 M	Boric acid
10x Triethanolamine buffer (TAE) (pH 8.5)	0.40 M	Tris
	0.01 M	EDTA
	0.20 M	Acetic acid
Washing solution I (for Northern blotting)	2x	SSC
	0.05%	SDS
Washing solution II (for Northern blotting)	0.1x	SSC
	0.1%	SDS

4.5 Cell culture

The cell lines used in this study derived from the cervical carcinoma of Henrietta Lacks (HeLa) [165], or from human bladder carcinoma (ECV304) [166].

4.5.1 Cell lines

In the table below are listed the cell lines used in this study and the relative medium used for their maintenance in culture.

Cell line	Culture Medium
HeLa	DMEM 10% (v/v) fetal calf serum (FCS)
ECV304	Medium 199 10% (v/v) FCS

Table 4.5: Cell lines and relative media used in this study

4.5.2 Cell culture reagents

Name	Supplier
Dulbeccos modified eagle medium (DMEM)	Biochrom, Berlin
FCS (superior)	Biochrom, Berlin
Lipofectamine 2000	Invitrogen, Carlsbad CA (USA)
Lipofectamine TM LTX and Plus TM Reagent	Invitrogen, Carlsbad CA (USA)
Medium 199	Lonza, Köln
opti-MEM	Gibco, Karlsruhe
Trypan Blue	Sigma-Aldrich, Deisenhof
Trypsin/EDTA (10x)	PAA, Pasching (Austria)
Turbofect	Thermo scientific, Schwerte

4.6 Bacterial culture

4.6.1 Bacterial strain

Strain	Supplier	Genotype
<i>Escherichia coli</i>	Stratagene	<i>rpsL</i> (Str ^r) <i>thr leu thi-1 lacY galk galT ara tonA tsx</i>
(<i>E. coli</i>) JM110	Waldbronn	<i>dam dcm supE44 Δ(lac-proAB)[F' traD36 proAB lacI^qZΔM15]</i>

4.6.2 Bacterial culture media and plates

Name	Components
Luria-Bertani (LB)-Medium (1x, pH 7.4)	0.5% (w/v) yeast extract 1.0% (w/v) tryptone 1.0% (w/v) NaCl 100 μg/ml Amp
Agar plates	LB medium 18 g/l agarose 100 μg/ml Amp

4.7 Nucleic acids

4.7.1 Plasmids/Vectors

Name	Supplier
CLIP-tagged hAgo-encoding plasmids	A. Mescalchin, Institute of molecular medicine, Lübeck
pEGFP-C1	R. Kretschmer-Kazemi Far, Institute of molecular medicine, Lübeck
pSilencer U6 neo vector	Ambion-Life Technologies TM , Darmstadt
SNAP/CLIP Vector	New England Biolabs, Ipswich, MA (USA)

4.7.2 Oligonucleotides

AsONs, siRNAs and RNA markers were provided by the Institute of Molecular Medicine of Lübeck; DNA oligonucleotides for cloning and DNA probes used for Northern were purchased by Biomers, Ulm.

4.7.2.1 Deoxyribonucleotides "DNA oligonucleotides"

DNA oligonucleotides used for cloning

The strand with GATCC sequence at the 5'-end is named TOP and it has 5'→3' orientation, while the complementary strand (3'→5' orientation) is called Bottom.

Name	Strand	Sequence (5' → 3')							
shRNA 2792	Top	GAT	CCA	GAA	CGC	TGT	TAC	CTC	ACT
		ACT	CGA	GAA	GTG	AGG	TAA	CAG	CGT
		TCT	GCT	TTT	TTG	GAA	A		
	Bottom	AGC	TTT	TCC	AAA	AAA	GCA	GAA	CGC
		TGT	TAC	CTC	ACT	TCT	CGA	GTA	GTG
		AGG	TAA	CAG	CGT	TCT	G		
shRNA 2798	Top	GAT	CCG	TGT	TAC	CTC	ACT	GGA	TAG
		AAC	TCG	AGA	TCT	ATC	CAG	TGA	GGT
		AAC	AGC	TTT	TTT	GGA	AA		
	Bottom	AGC	TTT	TCC	AAA	AAA	GCT	GTT	ACC
		TCA	CTG	GAT	AGA	TCT	CGA	GTT	CTA
		TCC	AGT	GAG	GTA	ACA	CG		
shRNA 2672	Top	GAT	CCG	TAC	ACT	CAG	ACC	AAC	AGA
		TAC	TCG	AGA	ATC	TGT	TGG	TCT	GAG
		TGT	AGC	TTT	TTT	GGA	AA		
	Bottom	AGC	TTT	TCC	AAA	AAA	GCT	ACA	CTC
		AGA	CCA	ACA	GAT	TCT	CGA	GTA	TCT
		GTT	GGT	CTG	AGT	GTA	CG		
shRNA 3024	Top	GAT	CCG	AGA	GTG	AAA	GCA	ACA	CAA
		ACT	CGA	GAT	TGT	GTT	GCT	TTC	ACT
		CTC	AGT	TTT	TTG	GAA	A		
	Bottom	AGC	TTT	TCC	AAA	AAA	CTG	AGA	GTG
		AAA	GCA	ACA	CAA	TCT	CGA	GTT	TGT
		GTT	GCT	TTC	ACT	CTC	G		
shRNA Ambion	Top	GAT	CCG	AGA	GTG	AAA	GCA	ACA	CAA
		TTC	AAG	AGA	TTG	TGT	TGC	TTT	CAC
		TCT	CAG	TTT	TTT	GGA	AA		
	Bottom	AGC	TTT	TCC	AAA	AAA	CTG	AGA	GTG
		AAA	GCA	ACA	CAA	TCT	CTT	GAA	TTG
		TGT	TGC	TTT	CAC	TCT	CG		
shRNA Grimm	Top	GAT	CCG	AGA	GTG	AAA	GCA	ACA	CAA
		TCA	AGA	GTT	GTG	TTG	CTT	TCA	CTC
		TCA	GTT	TTT	TGG	AAA			

shRNA 2nt-3'-end- overhang	Bottom	AGC	TTT	TCC	AAA	AAA	CTG	AGA	GTG
		AAA	GCA	ACA	CAA	CTC	TTG	ATT	GTG
		TTG	CTT	TCA	CTC	TCG			
	Top	GAT	CCG	GAA	CGC	TGT	TAC	CTC	ACT
		ACT	CGA	GAA	GTG	AGG	TAA	CAG	CGT
		TCC	TTT	TTT	GGA	AA			
shRNA 10nt-3'-end- overhang	Bottom	AGC	TTT	TCC	AAA	AAA	GGA	ACG	CTG
		TTA	CCT	CAC	TTC	TCG	AGT	AGT	GAG
		GTA	ACA	GCG	TTC	CG			
	Top	GAT	CCA	GAA	CGC	TGT	TAC	CTC	ACT
		ACT	CGA	GAA	GTG	AGG	TAA	CAG	CGT
		TCT	GCT	CTC	TCT	TTT	TTG	GAA	A
shRNA with inverted strands	Bottom	AGC	TTT	TCC	AAA	AAA	GAG	AGA	GCA
		GAA	CGC	TGT	TAC	CTC	ACT	TCT	CGA
		GTA	GTG	AGG	TAA	CAG	CGT	TCT	G
	Top	GAT	CCA	GTG	AGG	TAA	CAG	CGT	TCT
		ACT	CGA	GAA	GAA	CGC	TGT	TAC	CTC
		ACT	GCT	TTT	TTG	GAA	A		
shRNA NC	Bottom	AGC	TTT	TCC	AAA	AAA	GCA	GTG	AGG
		TAA	CAG	CGT	TCT	TCT	CGA	GTA	GAA
		CGC	TGT	TAC	CTC	ACT	G		
	Top	GAT	CCA	CTC	GAG	ATT	TTT	TGG	AAA
		AGC	TTT	TCC	AAA	AAA	TCT	CGA	GTG

DNA probes used for Northern blot analysis

Targeted shRNA	Detected strand	Sequence of the probe (5' → 3')							
shRNA 2792 ^{1,2}	antisense	GCA	GAA	CGC	TGT	TAC	CTC	ACT	
shRNA 2792	sense	AGT	GAG	GTA	ACA	GCG	TTC	T	
shRNA 2798	antisense	GCT	GTT	ACC	TCA	CTG	GAT	AGA	
shRNA 2798	sense	TCT	ATC	CAG	TGA	GGT	AAC	A	
shRNA 2672	antisense	GCT	ACA	CTC	AGA	CCA	ACA	GAT	
shRNA 2672	sense	ATC	TGT	TGG	TCT	GAG	TGT	A	
shRNA 3024 ³	antisense	CTG	AGA	GTG	AAA	GCA	ACA	CAA	
shRNA 3024	sense	TTG	TGT	TGC	TTT	CAC	TCT	C	

¹ DNA probes, used for shRNA 2792, were also employed for the detection of shRNA 2nt or 10nt 3'-end-overhang because they differ only at the 3'-end length.

² The probe used to detect the antisense strand of shRNA 2792 was used to detect the sense strand of shRNA 4nt 3'-end-overhang with inverted strands.

³ DNA probes, used for shRNA 3024, were also employed for the detection of shRNA Ambion or shRNA Grimm since they differ only in the loop region.

Targeted miRNA	Detected strand	Sequence of the probe (5' → 3')							
miR-16	guide	CGC	CAA	TAT	TTA	CGT	GCT	GCT	A
miR-16	passenger	TCA	GCA	GCA	CAG	TTA	ATA	CTG	G
miR-21	guide	TCA	ACA	TCA	GTC	TGA	TAA	GCT	A
miR-21	passenger	ACA	GCC	CAT	CGA	CTG	GTG	TTG	
miR-30a	guide	CTT	CCA	GTC	GAG	GAT	GTT	TAC	A
miR-30a	passenger	GCT	GCA	AAC	ATC	CGA	CTG	AAA	G
<i>let-7b</i>	guide	AAC	CAC	ACA	ACC	TAC	TAC	CTC	A
<i>let-7b</i>	passenger	GGG	AAG	GCA	GTA	GGT	TGT	ATA	G

asONs

asONs were described by Mescalchin *et al.* [167] and are fully phosphorothioate (PS)-modified.

Name	Target mRNA	Sequence (5' → 3')							
asON1-3'-UTR-A ¹	human Ago1	AGA	GTT	GAC	CTT	ACC	AAG	CT	
asON1-3'-UTR-B ²	human Ago1	TGT	GCT	ACG	TTT	TGT	GAG	TT	
asON2 ³	human Ago2	GTG	TTT	TGT	GTT	GCT	TTC	ACT	
		CTC							
asT1-inv-control	-	TAC	CGC	TCT	TTT	GAC	TTT	TA	

¹asON3124/20 ²asON4879/20 ³as3024/24

4.7.2.2 Ribooligonucleotides "RNA oligonucleotides"

siRNA sequences were designed by Meister *et al.* [24], they are 21-nt long and the anti-sense strand had 5' phosphorylated end.

siRNA targeting hAgo1

Name	Sequence (5' → 3')							
siAgo1 (antisense)	GAG	AAG	AGG	UGC	UCA	AGA	AUU	
siAgo1 (sense)	UUC	UUG	AGC	ACC	UCU	UCU	CUU	

siRNA targeting hAgo2

Name	Sequence (5' → 3')							
siAgo2 (antisense)	GCA	CGG	AAG	UCC	AUC	UGA	AUU	
siAgo2 (sense)	UUC	AGA	UGG	ACU	UCC	GUG	CUU	

siRNA without endogenous target which served as control: siRNA scramble (siscr3)*

Name	Sequence (5' → 3')							
siscr3 (strand1)	CGA	ACU	CAC	UGG	UCU	GAC	CdTdT	
siscr3 (strand2)	GGU	CAG	ACC	AGU	GAG	UUC	GdTdT	

* siscr3 sequence was described by R. Kretschmer-Kazemi Far *et al.* [168].

RNA markers

Name	Length (nt)	Sequence (5' → 3')							
as miR-1	21	UGG	AAU	GUA	AAG	AAG	UAU	GUA	
as let7-P	22	UGA	GGU	AGU	AGG	UUG	UAU	AGU	U
mlet7as	23	UGC	GUU	AGU	AGG	UUG	UAU	AGU	UU

4.7.3 Primers

All the primers used for the quantitative polymerase chain reaction (q-PCR) listed here were described by Mescalchin *et al.* [167].

Name	Sequence (5' → 3')								
Forward (Fwd) pSilencer	CAC	CAC	GTG	ACG	GAG	CGT	GAC		
Common Fwd CLIP/SNAP	GCT	CGC	CGT	GAA	AGA	GTG	GCT	G	
Rev Middle domain hybrids	TGT	CTC	CCA	CGC	GCT	TGA	CCT		
Fwd mRNA hAgo1	GAC	CTC	CGC	ACG	GGT	ATA	TG		
Rev mRNA hAgo1	GGT	TTC	CCC	ACA	GTG	CCA	AT		
Fwd mRNA hAgo2	TGG	TTT	GGC	TTC	CAT	CAG	TCC		
Rev mRNA hAgo2	CCT	TGT	AAA	ACG	CTG	TTG	CTG	AC	
Fwd mRNA Glucuronidase	TTT	GGA	ATT	TTG	CCG	ATT	TCA	T	
Rev mRNA Glucuronidase	GCC	GAG	TGA	AGA	TCC	CTT	T		

4.8 Kits

Name	Supplier
Bio-Rad protein assay	Bio-Rad, München
Enhanced chemiluminescence (ECL) TM	Pierce, Rockford, IL (USA)
GenElute plasmid miniprep kit	Sigma-Aldrich, Deisenhofen
Miniprep kit	Sigma-Aldrich, Deisenhofen
pSilencer TM neo Kit	Ambion, Darmstadt
Decade TM Marker System	Ambion, Darmstadt

4.9 Antibodies

The antibodies were diluted in 3% milk in TBS-T except for Polyclonal goat anti-rabbit that was diluted in 5% milk in TBS-T. Sodium Azide was added to reach the final concentration of 0.02% (w/v).

Name	Dilution (v/v)	Supplier
Monoclonal rat anti-hAgo1 (4B8)	1:50	Ascenion, München
Monoclonal rat anti-hAgo2 (11A9)	1:50	Ascenion, München
Polyclonal mouse anti-CLIP/SNAP (anti-human MGMT)	1:400	Millipore, Schwalbach
Polyclonal rabbit anti-human -actin	1:5000	Abcam, Cambridge (UK)
Polyclonal goat anti-mouse IgG HRP*-conjugated	1:1000	Dako, Hamburg
Polyclonal goat anti-rabbit IgG HRP-conjugated	1:2000	Dako, Hamburg
Polyclonal goat anti-rat IgG HRP-conjugated	1:2000	Jackson Immuno-Research, Suffolk (UK)

* Horseradish Peroxidase-Conjugated Antibodies (HRP)

4.10 Enzymes and molecular weight markers

Name	Supplier
BamHI	Fermentas, St. Leon-Rot
Gene Ruler TM DNA Ladder Mix	Fermentas, St. Leon-Rot
PageRuler TM Prestained Protein Ladder	Fermentas, St. Leon-Rot
NotI	Fermentas, St. Leon-Rot
T4 DNA Ligase (1u/μl)	Fermentas, St. Leon-Rot
T4 Polynucleotide Kinase (10u/μl)	Fermentas, St. Leon-Rot
Taq DNA Polymerase (5u/μl)	Fermentas, St. Leon-Rot
XhoI	Fermentas, St. Leon-Rot

4.11 Programs

Name	Source
Fusion 15.09	Vilber Lourmat, Eberhardzell
GeneAmp 5700 SDS	Perkin-Elmer Biosystems, Waltham, MA (USA)
Image Quant 5.2	Molecular Dynamics, Sunnyvale, CA (USA)
Mfold	http://mfold.rit.albany.edu/?q=mfold/
Multalinan	http://npsa-pbil.ibcp.fr
OligoAnalyzer 3.1	http://eu.idtdna.com/analyzer/Applications/OligoAnalyzer/
ExPASy	http://web.expasy.org/
Sfold	http://sfold.wadsworth.org/cgi-bin/index.pl

5. Methods

5.1 Methods for nucleic acids

5.1.1 Determination of the concentration of nucleic acids

Nucleic acids were quantified by measuring the absorbance at 260 nm (A_{260}) using a BECKMAN DU640 spectrophotometer that requires quartz cuvette ($d = 1$ cm) or a NanoDrop spectrophotometer that allows the analysis of only $1 \mu\text{l}$ of sample. It is possible to determine the concentration of nucleic acids applying the Lambert-Beer's law as described below:

$$A_{260} = \epsilon \cdot c \cdot d \iff c = \frac{A_{260}}{\epsilon \cdot d} \quad (5.1)$$

In this formula, A represents the absorbance, ϵ the molar extinction coefficient, c the concentration and d the optical path of the cuvette. Therefore, for nucleic acids with known sequence and accordingly with known molar extinction coefficient the concentration was calculated by using the derived equation. Conversely, the following approximate conversions were used:

1 A_{260} Unit = 50 $\mu\text{g/ml}$ dsDNA

1 A_{260} Unit = 33 $\mu\text{g/ml}$ ssDNA

1 A_{260} Unit = 40 $\mu\text{g/ml}$ ssRNA

Moreover, the purity of DNA or RNA solutions was evaluated by considering the ratio A_{260}/A_{280} that must be ≥ 1.8 or ≥ 2.0 , respectively. A value below the threshold indicates the presence of contaminating proteins or chemicals used for the DNA or RNA purification.

5.1.2 Agarose gel electrophoresis

To analyze plasmids, or to test RNA integrity, agarose gel electrophoretic technique under non-denaturing conditions was used.

Specifically, DNA or RNA samples were diluted in DNA loading buffer or RNA loading dye, respectively. They were loaded onto agarose gel that was previously assembled by

dissolving the required amount of agarose in 1x TAE buffer and by heating it for about 5 min at 800 W in a microwave oven. The amount of agarose and the relative volume of buffer were determined depending on the percentage of agarose gel required for the size separation of dsDNA fragments to perform, as described in Table 5.1, while the RNA integrity was checked on 1% (w/v) agarose gel.

Agarose (% w/v)	dsDNA fragment sizes (bp)
0.5	1,000 - 30,000
0.7	800 - 12,000
1.0	500 - 10,000
1.2	400 - 7,000
1.5	200 - 3,000
2.0	50 - 2,000

Table 5.1: Agarose concentration and relative size range of nucleic acids in non-denaturing electrophoresis

The agarose solution was poured into a gel casting chamber containing 0.004% (w/v) EtBr that is required for bands detection, since it intercalates into the double helix of DNA or binds to RNA secondary structures. The solution was then left for about 30 min at room temperature to solidify. The gel was run horizontally in 1x TAE buffer at 10V/cm for 20-60 min depending on the gel size. The nucleic acid bands on non-denaturing agarose gel electrophoresis were visualized under ultraviolet (UV) light irradiation (312 nm) since EtBr under these conditions fluoresces.

5.1.3 Polyacrylamide gel electrophoresis (PAGE)

In order to allow a fine-resolution separation of nucleic acids PAGE technique was used. The solution for the polyacrylamide gel was filtered by using 0.2 μ m filter under vacuum and stored at 4°C or immediately used after the addition of APS for polymerization and TEMED as catalyst. The solution was quickly poured into a vertical gel chamber (18 x 16 cm or 15 x 13 cm) which was previously assembled by using two glass plates separated by a 1 mm spacer. The gel was left at RT for 45 min to polymerize.

Denaturing PAGE

The analysis of ss oligonucleotides was carried out by using denaturing PAGE. To prepare the small denaturing gel (13 x 15 cm), a volume of 20 ml solution was required and it was made by mixing 2 ml 10x TBE and 10 g of Urea to reach 8 M of final concentration and an appropriate volume of acrylamide/bisacrylamide (ratio: 19/1) to achieve the concentration

suited for separating fragments of specific length, as described in Table 5.2. To prepare the big denaturing gel (17 x 18 cm), a volume of 35 ml solution was required. The solution was mixed and APS and TEMED were added to a concentration of 0,05% (w/v) and 0,1% (v/v), respectively. The gel was pre-run at 180-200 V (small gel) or 300 V (big gel) at RT for 30 min to reach a temperature of 55°C which allows the denaturation of the oligonucleotides. As running buffer 1x TBE was routinely used, except for gels for Northern analysis in which 0.5x TBE was needed. Samples were dissolved in Milli-Q water or TE buffer, diluted in denaturing loading buffer and heated at 95°C for 5 min prior to the loading onto the gel that was run at 200-250 V (small gel) or 350 V (big gel) for 2h at RT.

Acrylamide (%)	Nucleic acid fragment length (nt)
4	100 - 500
5	70 - 300
6	45 - 70
8	35 - 45
10	25 - 35
20	8 - 25

Table 5.2: Concentration of acrylamide used for denaturing PAGE and relative nucleic acid fragment length

Non-denaturing PAGE

In order to analyze the annealing of DNA oligonucleotides which were required for cloning shRNA sequences into plasmids, initially, a non-denaturing PAGE was used. The solution (20 ml) for gel preparation was composed of 2 ml 10x TBE buffer, acrylamide/bisacrylamide (ratio: 19/1) in a concentration that was proper to the size of the nucleic acid fragments (Table 5.3). Milli-Q water was added to a final volume of 20 ml. Annealed strand (400 pmol/well) and single strands (200 pmol/well) which served as control were dissolved in water and non-denaturing loading buffer. The samples were loaded on the gel at 4°C and its running occurred at 200 V for about 2h.

Acrylamide (%)	Nucleic acid fragment sizes (bp)
3.5	100 - 2,000
5.0	75 - 500
8.0	50 - 400
12.0	35 - 250
15.0	20 - 150
20.0	5 - 100

Table 5.3: Acrylamide concentration used for non-denaturing PAGE and corresponding sizes of nucleic acids

However, using the non-denaturing PAGE for the analysis of long oligonucleotides made the analysis difficult since ss oligonucleotides having a size of about 65 nt folded into secondary structures and their run on the gel was similar to the annealed strands. Therefore, in these specific cases a semi-denaturing PAGE was used as described below.

Semi-denaturing PAGE

The solution for semidenaturing gel differed from a denaturing gel solution only for the final UREA concentration which was 4 M instead of 7 M. Ss oligonucleotides (500 pmol/well) were dissolved in Milli-Q water and diluted in an appropriate volume of annealing buffer and denaturing loading buffer while 400 pmol/well of annealed oligonucleotides were mixed with non-denaturing loading dye and loaded on the gel that was run using 1x TBE as running buffer at 200V for about 2h at 4°C .

5.1.4 Detection of nucleic acids upon PAGE

The detection of nucleic acids upon PAGE was obtained by staining the gel in the Stains-All solution (1h at RT under shaking and in the dark). For the detection of nucleic acid, a minimum amount of 250 pmol/well of samples was needed. Radiolabelled oligonucleotides were instead visualized by exposing the gel on a PhosphorImager screen for about 1 h followed by scanning of the screen using the Typhoon 8600 scanner.

5.1.5 Purification of total cellular RNA

To purify the total cellular RNA, HeLa cells were harvested and pelleted by centrifugation (5 min, 1,000xg). The pellet was stored at -80°C or directly resuspended in 400 μ l of 1x PBS containing 1% (v/v) of NP-40 detergent. An equal volume of Roti®-Aqua-P/C/I pH 4.5 -5 was added to separate nucleic acids from proteins. The extraction of RNA was carried out by shaking the samples for 3 min at RT followed by centrifugation for 5 min at 20,000xg at 4°C to allow the separation of the organic phase from the aqueous phase. The upper phase (aqueous) was recovered and then transferred into a new vial. To remove the residues of the organic phase, the aqueous phase was mixed with an equal volume of Chloroform/Isoamylalcohol ratio (24/1; v/v) followed by shaking of the the samples for 5 min at RT and by centrifugation for 5 min at 20,000xg at 4°C. The washing of the RNA with the Chloroform/Isoamylalcohol solution was performed twice prior to the precipitation of RNA.

5.1.6 RNA precipitation

The aqueous phase containing the total cellular RNA was collected, then transferred in a new tube and mixed with an appropriate volume of sodium acetate pH 5.2 to reach a final concentration of 0.3 M. Then 2.5 volumes of 100% (v/v) cold ethanol were added.

The samples were mixed and incubated at -80°C for 30 min or -20°C overnight. The precipitate was collected by centrifugation at $20,000\times g$ for 20 min at 4°C . In order to wash the RNA pellet, a volume of $500\ \mu\text{l}$ of cold 100% (v/v) EtOH was added to each sample followed by centrifugation at $20,000\times g$ for 10 min at 4°C . The supernatant was discarded and the RNA pellet was lyophilized by using Speed Vac SC 110-A. The RNA was then dissolved in an appropriate volume of RNase free water (usually $30\ \mu\text{l}$). In order to obtain the amount of RNA which was required for Northern analysis ($30\ \mu\text{g}$ RNA/well) (see 5.1.8), the experiments were performed in triplicate and the wells were combined before RNA extraction.

5.1.7 Radiolabeling of the 5'-end of nucleic acids

DNA labeling

Probes used for Northern blot analysis were ss DNA oligonucleotides having a free OH group and they were 5'-end labeled by using T4 polynucleotide kinase (T4 PNK) that catalyzes the transfer of $[\gamma\text{-}^{32}\text{P}]$ from $[\gamma\text{-}^{32}\text{P}]\text{dATP}$ to the 5'-OH group. This is called forward reaction, and for this reaction a buffer called A (500 mM Tris-HCl pH 7.6, 100 mM MgCl_2 , 50 mM DTT, 1 mM spermidine) was required. The labeling solution was prepared as described in Table 5.4 followed by incubation of the reaction solution at 37°C for 30 min. The reaction was stopped by incubation at 95°C for 2 min which led to enzyme inactivation. The labelled oligonucleotide was purified by using a Nick column (G-50), which was previously equilibrated with nuclease-free water following manufacturer's instructions. The incorporation of $[\gamma\text{-}^{32}\text{P}]$ into DNA sequence was checked by analysis of the counts per minute (CPM) by using a scintillation counter. Labelled DNA (300,000 CPM/well) was diluted in formamide buffer and analyzed by 20% denaturing PAGE (see 5.1.3). Free $[\gamma\text{-}^{32}\text{P}]\text{ATP}$ was loaded as well on the gel and served as control. The gel was exposed to a PhosphorImager screen for 1h at RT in an autoradiography cassette. The screen was then scanned on the Typhoon 8600 scanner.

Components	DNA labeling	RNA labeling
oligonucleotide	$0.9\ \mu\text{M}$	$1\ \mu\text{M}$
10x T4 PNK buffer	1 x	1 x
T4 PNK	40 u	0.5 u
$[\gamma\text{-}^{32}\text{P}]\text{ATP}$	$100\ \mu\text{Ci}$	$60\ \mu\text{Ci}$
Final Volume	$80\ \mu\text{l}$	$10\ \mu\text{l}$

Table 5.4: Components and relative final concentration for labeling ss DNA or RNA oligonucleotide

RNA markers labeling

RNA markers used for Northern analysis were 5'-end labeled by using T4 Polynucleotide Kinase that catalyzed the transfer of [γ - 32 P] from [γ - 32 P]dATP to the free 5'-end-OH group of asmiR-1 and mlet7as (forward reaction) or it exchanged the phosphate group at the 5'-end of aslet7-P with [γ - 32 P] from [γ - 32 P]dATP (exchange reaction). The forward and exchange reactions were performing by using buffer A or buffer B (500 mM imidazole-HCl pH 6.4, 180 mM MgCl₂, 50 mM DTT, 1 mM spermidine and 1 mM ADP), respectively. Both reactions were performed at 37°C for 30 min followed by heating at 95°C for 2 min to inactivate the PNK enzyme. Then, 90 μ l of nuclease-free water was added to each sample and mixed with 100 μ l of Chloroform for purifying the labeled RNA from the reaction mixture and centrifuged briefly at maximum speed at 4°C. The supernatant was transferred into a new tube then diluted using an equal volume of 2x RNA Loading dye and finally heated at 95°C for 5 min before performing PAGE (see 3.1.3).

RNA DecadeTM marker labeling

Ambion DecadeTM marker system was used to assign the length of RNA sequences upon Northern analysis. It consists of one RNA molecule of 150 nt in length that upon cleavage gave rise to markers whose lengths are in a range of 10-150 nt. The reaction solution is described in Table 5.5.

Components	Final concentration
Decade Marker RNA	100 ng
Kinase reaction buffer	1 x
[γ - 32 P]ATP	10 μ Ci
T4 PNK	10 u
Final volume	10 μ l

Table 5.5: Components and relative final concentration of the mixture for labeling RNA DecadeTM Marker

An incubation at 37°C for 1h was required to activate the kinase and it was followed by cleavage of the RNA molecule by adding 2 μ l of 10x Cleavage reagent and 8 μ l of nuclease-free water. The cleavage reaction occurred at RT for 5 min. The resulting solution was diluted using an equal volume of Gel Loading Buffer II and heated at 95°C for 5 min prior to sample separation by 12% denaturing gel or prior to storage at -20°C.

5.1.8 Northern Analysis

To detect siRNA or miRNA or their precursor High Resolution Northern analysis was used. It consists of three steps: separation of samples by PAGE, blotting of the nucleic

acid on the membrane and hybridization of the RNA by using a radiolabeled DNA probe.

PAGE

To avoid RNA degradation by RNases all the solutions that were used for Northern analysis were RNase free and all the required material was pre-treated in H₂O₂ for 20 min. RNA samples (typically 30 µg/well) or RNA markers were diluted in water and an equal volume of 2x RNA loading dye followed by denaturation of the RNA at 95°C for 5 min. Samples were loaded on the 12% (v/v) denaturing gel (see 5.1.3), which was previously pre-run at 350 V for gel with a size of 17 x 18 cm, 250 V for gel with size of 13 x 15 cm for 30 min at RT using 0.5x TBE as running buffer. The pre-run was required so that the gel could achieve a temperature of 55°C which allowed denaturation of nucleic acids. Separation of the samples occurred at constant voltage (450 V for gel of size 17 x 18 cm, 350 V for gel of size 13 x 15 cm) for 60-90 min at RT. The gel cast was disassembled and then gel was blotted on a positive charged nylon membrane.

Blotting

Hybond-N+ (positively charged nylon membrane) was soaked in 0.5x TBE for at least 10 min. The blotting unit was assembled in the following order: 3 pieces of 3MM paper of appropriate size were soaked in 0.5x TBE buffer and positioned in the blotting apparatus. The membrane was positioned on them, the gel was placed on the membrane and covered by 3 pieces of 3MM paper of the same size soaked in 0.5x TBE. The transfer occurred at 250 mA for 1h at RT, followed by crosslink of RNA on the membrane via UV irradiation at 312 nm for 3 min.

The membrane was wrapped between two dried pieces of 3MM paper and heated at 80°C for 30 min then stored at 4°C until use.

Hybridization

For hybridizing the RNA with the radiolabeled probe (in the range $8 \cdot 10^6$ - $16 \cdot 10^6$ total CPM), Express Hybridization Solution was used. It was heated at 68°C to dissolve the precipitate then it was equilibrated at 37°C for 30 min. The membrane was placed into RNase-free tubes, and a volume of 10 ml Hybridization Solution was added followed by incubation at 37°C for 30 min under rotation. The radiolabeled DNA probe (see 5.1.7) was then added and the hybridization was performed at 37°C under rotation for 1h. The membrane was then washed, at 37°C twice by using a low stringency washing solution I (2x SSC, 0.05% SDS) for 5 min and once by using a high stringency washing solution II (0.1x SSC, 0.1% SDS) for 5 min. The membrane was removed from the tube by using forceps, then wrapped in a plastic foil and exposed to a PhosphorImager screen in an autoradiography cassette at -20°C for 3-4 days. The screen was scanned on the Typhoon 8600 scanner.

5.2 Methods in molecular biology

5.2.1 Cloning of DNA fragments into a vector and DNA oligonucleotides design

In order to produce shRNA encoding plasmids, the Ambion pSilencerTM 2.1 U6 neo was chosen as vector. It is characterized by U6 RNA pol III promoter which is a strong promoter and it allows robust shRNA expression. Moreover, it carries Neomycin and Amp resistance genes for antibiotic selection in eukaryotic or procaryotic cells, respectively. The

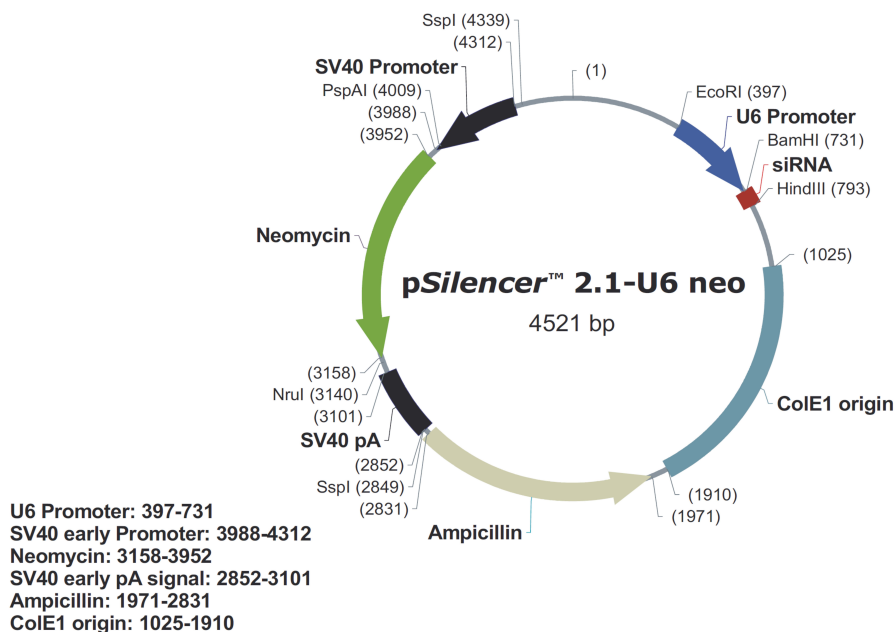


Figure 5.1: pSilencer neo vector map taken from Ambion data sheet

pSilencerTM 2.1 U6 neo was supplied from the manufacturer as the linear vector and carried sticky-ends generated by using BamH I and Hind III enzymes. As inserts, complementary oligonucleotides (called top and bottom strands) having 5'-end-overhangs that encode for 19-21 bp long shRNA sequences were designed to have BamH I and Hind III restriction sites at the 5' and at the 3'-end, respectively. Downstream of the BamH I recognition site, a G or an A were inserted since the RNA pol III gives rise to a more efficient transcription if the first base is a purine. A poly (T) tail at the 3'-end of the top strand was instead required as signal for RNA pol III to end the transcription. Additionally, the sequence encoding the loop was designed to contain XhoI recognition site in order to allow the selection of positive clones also by restriction analysis. Exceptions are represented by shRNA Ambion and shRNA Grimm, so named because the loop sequence that was designed by using the Ambion online tool [169] or by Grimm *et al.* [170]. Moreover, a DNA fragment carrying only the XhoI loop sequence without flanking regions was cloned

into a plasmid that served as negative control (shRNA NC).

shRNA	Loop sequence (5' → 3')	Tot bp number
shRNA 2792	ACUCGAGA	19
shRNA 2798	ACUCGAGA	19
shRNA 2672	ACUCGAGA	19
shRNA 3024	ACUCGAGA	19
shRNA Ambion	CAAGA	21
shRNA Grimm	CAAGA	20
shRNA 10nt-3'-overhang	ACUCGAGA	19
shRNA 2nt-3'-overhang	ACUCGAGA	19
shRNA with inverted-strands	ACUCGAGA	19

Table 5.6: Loop sequences and total bp number of the central region of the shRNAs used in this study

5.2.1.1 Hybridization of complementary DNA oligonucleotides

After testing their purity via 20% (w/v) denaturing PAGE (see 5.1.3), the DNA complementary strands were annealed by mixing 1,000 pmol of each oligonucleotide in 1x annealing buffer. Heating at 95°C for 5 min was performed to achieve strand denaturation, followed by incubation at 37°C for 1h or alternately, by cooling down to RT. The annealing of the two strands was checked by PAGE as described in 5.1.3 and the gel was stained in StainsAll as described in 5.1.4. The percentage of dsDNA was determined by using Image Quant 5.2.

5.2.1.2 Ligation of the dsDNA fragments into the pSilencerTM 2.1 neo-vector

The annealed siRNA templates or the annealed sequences for shRNA NC were ligated into the pSilencerTM 2.1 neo-vector by using T4 DNA ligase. Reaction components are listed in Table 5.7.

Components	With insert	Without insert
annealed siRNA template	11 ng	–
DNA annealing solution	1 x	1 x
T4 DNA Ligase buffer	1x	1 x
pSilencer TM 2.1 U6 neo vector	1 u	1 u
T4 DNA Ligase	5 u	5 u
Final Volume	10 μ l	10 μ l

Table 5.7: Reaction components for the ligation of siRNA template inserts into the pSilencerTM 2.1 U6 neo vector

In order to control whether the vector alone can re-ligate, a reaction mixture without insert was also performed (see Table 5.7). Incubation at 22 °C for 1 h was performed, followed by enzyme inactivation at 70 °C for 5 min. The samples were stored at -20 °C or immediately used to transform *E. coli* JM110 cells as described below.

5.2.2 Preparation of electrocompetent cells

E. coli JM110 cells were plated on a LB-agar plate containing 100 µg/ml of Amp and incubated at 37 °C for 8 h and used to inoculate 7.5 ml of LB medium that was left at 37 °C overnight under shaking. When the bacterial culture reached an optical density at 600 nm (OD₆₀₀) of 0.01, it was then diluted in 500 ml of LB medium and incubated at 37 °C under shaking until the OD₆₀₀ reached a value of 0.6. All the flasks were then put on ice for 15 min and centrifuged for 20 min at 5,200 RPM (Beckman centrifuge + JLA-10.500 rotor) at 2 °C. The pellet was resuspended in 500 ml of cold autoclaved water. Bacterial cells were centrifuged again at 5,200 RPM (Beckman centrifuge + JLA-10.500 rotor) for 20 min at 2 °C and washed in 500 ml of cold autoclaved water. After a further centrifugation at 5,200 RPM (Beckman centrifuge + JLA-10.500 rotor) for 20 min at 2 °C, the bacterial pellet was resuspended in 40 ml of 10% (v/v) glycerol followed by centrifugation at 5,200 RPM (Beckman centrifuge + JLA-10.500 rotor) for 15 min at 2 °C. The electrocompetent cells were finally resuspended in 3 ml cold 10% (v/v) glycerol and stored at -80 °C.

5.2.2.1 Transformation of *E. coli* JM110 cells by electroporation

For the transformation of *E. coli* JM110 cells with the ligated vector, 40 µl of electrocompetent cells (see 5.2.2) were mixed with 2-4 µl of the ligation solution (see 5.2.1.2). The mixture DNA-cells was placed into a pre-chilled electroporation cuvette (0.2 cm thickness) which was positioned in the electroporation chamber and pulsed once for about 5 msec at the following fixed parameters: voltage at 1.5 kV, resistance at 200 Ω and capacitance at 25 µF. A volume of 500 µl of LB pre-warmed at 37 °C was quickly added and the cell suspension was transferred into a new tube followed by incubation at 37 °C for 30 min. Transformed cells carried the gene encoding for Amp resistance, therefore LB agar plates containing 100 µg/ml of Amp were used to plate 300 µl of transformed cell suspension. Bacteria were then incubated at 37 °C over night to allow the formation of colonies.

5.2.2.2 Bacterial propagation

For the screening of positive colonies some colonies were picked by using a sterile toothpick and spreaded onto a fresh agar plate containing 100 µg/ml of Amp. The plate was incubated at 37 °C for 8 h to let bacteria grow. The day after each colony was transferred into tubes containing LB medium (5 ml/tube) supplemented with 100 µg/ml of Amp and

incubated at 37°C over night under shaking. Bacteria were then collected by centrifugation as described in 5.2.4 and bacterial pellet were used to isolate plasmid DNA via low-copy plasmid purification

5.2.3 Preparation of bacterial glycerol stocks

Bacteria cultures having an OD₆₀₀ of 0.7 were mixed with glycerol [final concentration 50% (v/v)] and stored at -80°C until use.

5.2.4 Low- and high-copy plasmid DNA isolation

For the purification of about 20 µg of plasmid DNA, 5 ml of LB medium containing 100 µg/ml Amp were inoculated with bacteria from the bacterial glycerol stock (see 5.2.3) and incubated at 37°C overnight under shaking. The GeneEluate Plasmid Miniprep Kit was used to isolate the plasmid DNA according to manufacturer's instructions. Alternatively, 5 ml bacterial culture (after 8h of incubation at 37°C under shaking) was diluted in 500 ml of LB medium which contained 100 µg/ml Amp and further shaken at 37°C overnight. Bacteria were then collected by centrifugation (at 4°C 6,000xg for 10 min) and plasmid DNA was purified by using Nucleobond Xtra Maxi prep Kit following instructions described in the supplied manual. This kit allows the purification of about 500 µg of plasmid DNA.

5.2.5 Enzymatic restriction analysis for the selection of positive clones

ShRNA encoding plasmids were digested by the XhoI restriction enzyme since they had XhoI restriction site in their loop sequence. Plasmids encoding CLIP-tagged hAgos were digested by using BamHI and/or NotI enzymes and pEGFP-C1 was digested by using BamHI. Typically, 200 ng of plasmid were mixed with 1x Green fast digest buffer and 1 unit of each restriction enzyme in a total volume of 20 µl. All restriction enzymes used in this study were purchased by Fermentas and they required an incubation at 37°C for 30 min to cleave their substrate and heating at 80°C for 5 min for their inactivation. Upon enzyme inactivation, reaction solutions were loaded onto 1% (w/v) agarose gel (see 5.1.2) and visualized under UV light at 312 nm.

5.2.6 Nucleotide-Sequencing

The sequencing of DNA plasmids was performed by the company Eurofins MWG operon (Ebersberg) using Fwd pSilencer primer for shRNA encoding plasmids, and Common Fwd CLIP/SNAP and Rev Middle domain hybrids primers for sequencing of plasmid encoding CLIP-tagged hAgos (see 4.7.3).

5.2.7 Reverse transcription (RT) - cDNA synthesis

Upon assessing the integrity of total cellular RNA extracted from HeLa cells (see 5.1.5), it was reverse transcribed into a complementary DNA (cDNA) by using RevertAid First Strand cDNA Synthesis Kit and further used for q-PCR (see 5.2.7 and 5.2.8). For the cDNA synthesis, initially, 800 ng of RNA were mixed with random hexameric primers in a final volume of 12 μ l and heated at 70°C for 5 min. Subsequently, the other components of the reaction were added as described in Table 5.8 .

Components	Final concentration
Total RNA	800 ng
random hexamer primers	5mM
5x reaction buffer	1x
deoxynucleoside triphosphate (dNTP) mix	1mM
<i>RibolockTM</i>	20 u
RevertAid M-Mul V RT	200 u
Final Volume	20 μ l

Table 5.8: Reaction mixture for cDNA synthesis

The mixture was incubated at 25°C for 10 min, followed by activation of the enzyme at 42°C for 60 min and its inactivation at 75°C for 10 min. The cDNA was chilled on ice, diluted with water to a final volume of 200 μ l and stored at -20°C until use.

5.2.8 Quantitative polymerase chain reaction (q-PCR)

To evaluate downregulation by shRNAs of hAgo1 or hAgo2 at the mRNA level, q-PCR was performed in a 96-well plate and by using cDNA prepared as described in 5.2.7 and by employing hAgo1 or hAgo2 specific primers. In order to detect amplification products, Platinum SYBR Green q-PCR SuperMix was used as a sequence-independent detection method according to manufacturer's instructions. The reaction mixture was prepared as described in Table 5.9.

Components	Final concentration or Volume
cDNA	5 μ l
2x SYBR Green Mix	1x
Fwd and Rev primers	375 nM *
Final Volume	20 μ l

Table 5.9: Reaction mixture for q-PCR. * concentration of each primer

Moreover, a mix solution containing primers for a housekeeping gene like β -glucuronidase was prepared as well and served for normalization of the data. Additionally, RNA and RNase free water were used as non RT control and water control, respectively. The reaction cycle of real-time q-PCR is composed of 3 steps:

1. Initial denaturation (95°C for 10 min)
 2. Annealing and elongation (60°C for 60 sec)
 3. Denaturation (95°C for 15 sec)
-] x 40

The data were analyzed by GeneAmp 5700 SDS programm and CT (cycle threshold) values were considered as number of cycles required for crossing the threshold. To calculate the copy number after n cycles the following equation was used:

$$C_n = C_i \cdot (1 + E)^n \quad (5.2)$$

in which n is number of cycles, C_i is initial copy number, C_n is the copy number at cycle n and E is the efficiency of target amplification. When efficiency is maximum (=1) the equation is

$$C_n = C_i \cdot 2^n \quad (5.3)$$

that means that the increase will be 2-fold at each cycle. The data analysis was based on the assumption that the control constituted by water required the maximum number of cycles ($CT_{H_2O}=40$) and the values were normalized to β -glucuronidase as follow:

$$Relative\ quantification = \frac{2^{(40-CT\ sample)}}{2^{(40-CT\ \beta glucuronidase)}} \quad (5.4)$$

5.3 Biology methods

5.3.1 Culturing of human cells

Human cells were grown at 37°C and 5% CO₂ and 95% humidity in a CO₂-incubator. They were harvested by removing the culture medium, followed by a wash with 1x PBS and addition of 1x Trypsin/EDTA. Cells were incubated at 37°C for about 3 min to allow cell detachment. Medium containing 10% FCS (complete medium) was added to inactivate the enzyme Trypsin and the cells were centrifuged at 1,000xg for 3 min. The supernatant was discarded then the cell pellet was resuspended in complete medium and a proper amount of cells was spread into a new flask. Cell viability was evaluated by using Trypan blue staining as described in 5.3.3 and cell counting was performed by using a Neubauer Chamber.

5.3.2 Cell cryopreservation

Cell lines and relative medium used for the cryopreservation are listed in Table 5.10.

Cell line	Freezing Medium
HeLa	DMEM
	20% FCS
	10% DMSO
ECV 304	Medium 199
	20% FCS
	10% DMSO

Table 5.10: Cell lines and relative freezing medium

Human cells were harvested as described in 5.3.1 and the cell pellet was resuspended in the relative freezing medium. About 10^6 cells *per* vial were stored in a box containing isopropanol at -80°C for three days before being transferred into liquid nitrogen for long term storage.

5.3.3 Trypan blue staining

Trypan blue staining was performed to discern viable and non-viable cells due to the intact cell membrane of the first ones which, therefore, do not absorb the dye. On the contrary, the stain goes through the membrane of non-viable cells giving rise to blue colored cells. A volume of $10\ \mu\text{l}$ of diluted cell suspension (in PBS or complete medium) was mixed with trypan blue solution [0.4% (w/v) in 0.85% (w/v) NaCl] in a ratio 1/1 (v/v). The cells were counted within 5 min from the addition of the dye to avoid its absorption also by the living cells.

5.3.4 Transfection methods

In this study the experimental designs which were performed, required a transfection of cells with plasmids encoding CLIP-tagged hAgos and the day after by a transfection with shRNA-encoding plasmids or with downregulating tools. In the light of this, an appropriate confluence of cells for both transfections was required.

5.3.4.1 Lipofectamine 2000-mediated transfection of human cells

Lipofectamine 2000 is a lipid molecules-containing reagent that, in aqueous solution, is able to form cationic liposomes which bind negatively charged molecules as nucleic acids. To transfect cells by using Lipofectamine 2000, typically 350,000 cells *per* well were seeded in a 6-well plate to reach a confluence of 70% after 24h. Cells were transfected

with about 2 μg of plasmid/well and the ratio $\mu\text{g DNA}/\mu\text{l Lipofectamine 2000}$ suggested by the manufacturer was 0.4 therefore an appropriate volume of Lipofectamine was diluted in OptiMEM to a final volume of 400 μl and incubated for 5 min at RT. OptiMEM is a reduced serum medium that is suited for the formation of Lipofectamine 2000:DNA complexes. The Lipofectamine 2000/ OptiMEM solution was mixed with an equal volume of a OptiMEM containing the plasmid DNA and incubated for 30 min at RT to allow time for the complex formation. Cells were then washed twice with 1x PBS and the transfection solution was added to each well followed by incubation for 4 h at 37°C and 5% of CO₂. The transfection solution was then removed and complete medium was added to the cells which were further incubated at 37°C, 5% CO₂ overnight until a second transfection was performed. Cells were then collected two days after the second transfection in order to be assayed.

5.3.4.2 LipofectamineTM LTX-mediated transfection of human cells

The procedure by using LipofectamineTM LTX allowed a low cytotoxicity and required about 70% of cell confluence therefore 350,000 cells were seeded in a 6-well plate to be transfected after 24h. For this transfection method, the cells were transfected with about 2 μg of plasmid/well. Specifically, this method required the ratio $\mu\text{g DNA}/\mu\text{l Plus reagent}$ to be 1. A given volume of DNA was mixed with the relative volume of Plus reagent then OptiMEM was added to reach the final volume of 400 μl . The solution was incubated for 5 min at RT. Then 4-20 μl of LipofectamineTM LTX were diluted in OptiMEM up to 400 μl and incubated for 5 min at RT. The two solutions were mixed together and added to the cells which were previously washed twice with 1x PBS. Cells were then incubated at 37°C, 5% CO₂ with the transfection solution that was removed after 4h and replaced with complete medium. Cells were incubated at 37°C, 5% CO₂ overnight and then transfected again as described above. Cells were then harvested 2 days after the second transfection.

5.3.4.3 Turbofect-mediated transfection of human cells

Turbofect is a cationic polymer-based method which forms polymers in aqueous environment that bind to negatively charged nucleic acids. The Turbofect transfection method has a low cytotoxicity therefore it requires the seeding of 245,000 cells/well in a 6 well-plate to achieve about 70% of cell confluence at the second transfection. The cells were transfected with about 2 μg of plasmid/well and the recommended ratio $\mu\text{l Turbofect}/\mu\text{g DNA}$ was 2. The procedure consisted in diluting the corresponding volume of plasmid solution in serum-free DMEM in a ratio 1:10 (v/v). Incubation at 15-20 min at RT was required before applying the mixture solution drop wise to each well without removing the growth medium. The so-treated cells were incubated at 37°C, 5% CO₂ overnight. The day after, the second transfection was performed as described above. The cells were

harvested after 48h.

5.4 Methods for handling proteins

5.4.1 Non-interferingTM protein assay for the determination of protein concentration

Protein concentration was measured by non-interferingTM protein assay that is a colorimetric assay that employed a precipitating agent for immobilizing all the proteins contained in the sample upon centrifugation while the supernatant containing the precipitating agent is decanted. The assay is based on the use of a solution containing copper salt whose concentration is known. The copper ions bind the protein while only the unbound ions are measured therefore their concentration is inversely proportional to the protein amount. The assay was performed according to the manufacturer's instruction and the absorbency was measured at 480nm by BECKMAN DU640 spectrophotometer while an empty cuvette was used as blank. A standard curve was created by measuring known amount as bovine serum albumin (BSA) protein and the concentration of the sample was determined consequently.

5.4.2 SDS-PAGE

Proteins were analyzed by SDS-PAGE composed of 4% (v/v) stacking gel and a resolving gel whose percentage of acrylamide was chosen according to the size of the proteins to analyze (Table 5.11). In this study 10% (v/v) SDS PAGE was performed on vertical gel casting system in 0.75 mm thick gels. The cell pellet was resuspended in 1x PBS and 2x loading buffer in a ratio 1:1 (v/v).

	Stacking gel		Resolving gel	
	4% (w/v)	8% (w/v) (35-100 kDa)	10% (w/v) (15-70 kDa)	15% (w/v) (10-40 kDa)
Rotiphorese gel 30%	1.4 ml	1.3 ml	1.7 ml	2.5 ml
1.5 M Tris-HCl (pH 8.8)	-	1.3 ml	1.3 ml	1.3 ml
1.0 M Tris-HCl (pH 6.8)	250 μ l	-	-	-
10% (w/v) SDS	20 μ l	50 μ l	50 μ l	50 μ l
H ₂ O	1.4 ml	2.3 ml	1.9 ml	1.1 ml
TEMED	4 μ l	4 μ l	4 μ l	4 μ l
10% (w/v) APS	20 μ l	50 μ l	50 μ l	50 μ l

Table 5.11: Stacking and resolving gel composition for preparing SDS-PAGE

The samples were heated at 95 °C for 7 min for ensuring protein denaturation and loaded on the gel. The adequate size marker was loaded as well (see 4.10). The gel was initially run at a constant voltage of 100 V for 30 min to let the proteins reach the interface between the stacking and running gel and then at 150 V for 90 min at RT by using 1x running buffer (see 4.4).

5.4.3 Western blotting analysis

Proteins were transferred from the gel to a PVDF membrane by using a "semi-dry" method. First the hydration of the Immobilon-P membrane in methanol for 1 min was performed followed by its washing in millipore water for 5 min. Subsequently, the membrane and the gel were equilibrated in 1x transfer buffer then the blotting unit was assembled as follows:

(-) anode

3 pieces of 3MM paper

SDS-PAGE gel

Immobilon-P membrane

3 pieces of 3MM paper

(+) cathode

The blotting was performed at 0.8 mA/cm² for 90 min at RT. Prior to the detection of proteins, the membrane was incubated with 5% (w/v) milk in 1x T-TBS (see 4.4) for 1-2 h at RT to avoid unspecific binding by the antibodies to the PVDF membrane. The membrane was washed three times with 1x T-TBS to remove any residues of SDS and then incubated overnight with the specific primary antibody as listed in 4.9. Other three washes were required to remove unbound antibody and then the membrane was further incubated for 1h at RT under shaking with the corresponding Horseradish Peroxidase-Conjugated (HRP) secondary Antibody (see 4.9). An ECL system was used for the detection of the secondary antibody according to manufacturer's instructions. Moreover, β -actin was detected as well and served as loading control. The PVDF membrane was stained by addition of Coomassie blue staining solution (see 4.4) followed by incubation under shaking conditions for 1 h at RT. After removal of the staining solution, a destaining solution (see 4.4) was added to the membrane followed by incubation for 1h at RT.

6. Results

6.1 Establishment of a system to study the roles of hAgo proteins

In order to investigate the different cellular roles of the four hAgo proteins an experimental system needed to be established allowing, on one hand, the over-expression of recombinant hAgos to investigate their individual properties and on the other hand, to suppress endogenous hAgo proteins to avoid their interference. These were considered at the beginning necessary conditions, therefore a search of the possible suited strategies was required. The literature allowed to outline two possible methods: the first leads to deactivation of the genes encoding for Ago proteins in mouse cells [154] via an Ago knock-out-based approach. The mouse Ago knock-out system was developed by Su *et al.* [154] by using mouse embryonic stem (mES) cells in which Ago knock-out was inducible by 4-hydroxytamoxifen (4OH-T) treatment. The second approach is based on the downregulation of hAgos at the transcript and protein levels by using a gene knock-down system [24, 167].

In this study an approach was established and applied which allowed the over-expression of recombinant hAgo proteins in human cells upon downregulation of the endogenous Agos by using post-transcriptional gene silencing tools like siRNAs, asONs or shRNAs-encoding plasmids. Initially, a pilot study was performed in the use of siRNAs or asONs as tools for the downregulation of endogenous hAgo1 or hAgo2.

6.1.1 Tools for the downregulation of endogenous Ago1 and Ago2 in human HeLa and ECV304 cell lines

In previous studies, asONs and siRNAs were used as tools to induce gene silencing by targeting the mRNA of hAgos [171–173]. These approaches exploit different mechanisms: in fact, an siRNA, which is a double-stranded RNA of 21-22 bp, participates in the RNAi mechanism in which one strand (passenger) is degraded while the other strand (guide) is loaded onto Ago proteins and the complex recognizes a specific sequence on the target mRNA leading to mRNA cleavage [20]. However, the downregulation of hAgo proteins by siRNAs show a disadvantage since their target proteins are needed

for carrying out siRNA activity. This problem can be avoided by using an other class of molecules such as asONs, which are ss RNA or DNA molecules that do not require the RNAi pathway to exploit their action. They recognize their target RNA and act via RNase H-dependent mechanism leading to the cleavage and degradation of transcripts [174]. However, for both tools, the structure and the accessibility of the target influence their activity [168, 175]. In this study, asONs, siRNAs or their combinations were tested in HeLa or ECV304 cells in order to, on one hand, to test their efficiency in target downregulation, their possible additive or synergic effect and, on the other hand, to find the most suitable cell line to perform further experiments. Furthermore, cells were also transfected with recombinant hAgos in order to compensate for the loss of the endogenous proteins. The recombinant proteins were provided by A. Mescalchin and are codon optimized in order to increase the protein rate and to reach a comparable expression level of all four hAgos which was required in this study. HAgO1-3-4 were made codon optimized based on the

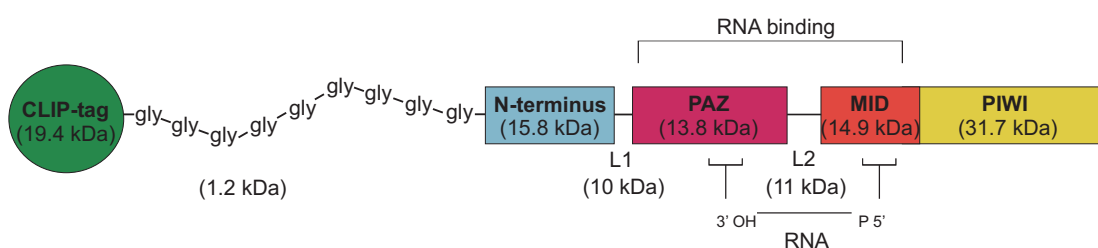


Figure 6.1: Schematic representation of CLIP-tagged hAgo used in this study. CLIP-tag is indicated in green and is linked, by a flexible linker constituted by 9 residues of glycine (gly), to the N-terminus of each hAgo protein. The four domains of hAgo are illustrated as well: N-terminus (blue) is connected to PAZ domain (purple) by a linker (L1), while a longer linker (L2) connects PAZ to MID domain (orange) which is closed to PIWI domain (yellow) at carboxy-terminus (C-terminus). PAZ and MID domains are responsible for the binding of the 3'-end and the 5'-end of RNA, respectively. PIWI domain contains the catalytic tetrad (D597/E637/D669/H807) which determines the cleavage activity only of hAgo2 although it is present also in the PIWI domain of hAgo3. The predicted molecular weight of each domain and linker is indicated in brackets. It was obtained by using the SIB Bioinformatics Resource Portal (ExPASy) and it refers to CLIP-hAgo2, whose total predicted molecular weight is 117.8 kDa. This depiction was modified from Ender and Meister-2010 [176].

wild type hAgo2 sequence which is the most abundant Ago in the cell. The technique of codon optimization has been widely and successfully employed in previous published studies [133]. In the present study CLIP-hAgo proteins were used. The CLIP-tag (New England Biolabs) is derived from the mutation of the protein O6-alkylguanine DNA alkyltransferase (hAGT) and its weight is ≈ 20 kDa. The CLIP tag was chosen for its ability to interact with benzylcytosine-structured molecules, allowing for one to perform labeling experiments. Moreover, their design was performed by considering also to create fourteen common restriction sites so that, these constructs could be used also for the development of chimera molecules via replacement of domains or portions of them. The Ago2^{Mut} is slicing incompetent as described in 6.1.2.1.

6.1.1.1 Comparison and combinations of siRNA and asON-based approaches for hAgo1 downregulation

The asONs used to downregulate hAgo1 were designed by Mescalchin *et al.* [167], and their development arose from a theoretical approach based on predicted secondary structures of RNA target and the search of the most suitable local sequences to target [175, 177].

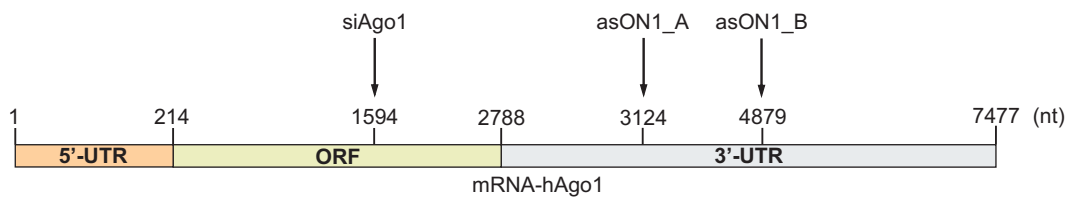


Figure 6.2: Schematic representation of the siRNAs and asONs targeting the mRNA of hAgo1. siAgo1 targets the ORF while asON1-A and asON1-B target the 3'-UTR. Each arrow indicates the first nt at the 5'-end of the target region. ORF: open reading frame.

The 20 nt-long asONs targeting hAgo1 called asON1-A and asON1-B were used to target the 3'-UTR of hAgo1 mRNA starting from nt 3124 or 4879 from the 5'-end, respectively (Figure 6.2). Both asONs were characterized by a fully modified PS-backbone in which a non-bringing oxygen is replaced by a sulfur atom to prevent nuclease degradation [174]. The siRNA used in this study to downregulate hAgo1 (siAgo1) was designed by Meister *et al.* [24]. It recognizes a region on the ORF of the hAgo1 mRNA (Figure 6.2), and its antisense strand had a phosphate group at the 5'-end. The siRNA and the asONs were tested alone or in their combinations. Additionally, an asON control and a siRNA scramble (siscr3) having no endogenous human target served as controls to analyze the extent of target suppression by the specific tools. Moreover, asON control and siscr3 were also used in combinations with the downregulating tools to achieve in each transfection an equal total amount of siRNA and asON in order to rule out any competitive effect. In order to identify the most suited human cell line for this kind of study, HeLa and ECV304 cells were used. Cells were seeded and after 24h they were transfected with siRNA and/or asONs directed against hAgo1. After 24h a second transfection with a plasmid encoding for a recombinant hAgo1 was performed to compensate the loss of the endogenous proteins. The recombinant proteins did not carry any binding site for the investigated asONs or siRNA. The western analysis was performed by using a rat anti-human hAgo1 antibody which led to the detection of both endogenous hAgo1 as approximately 100 kDa band and recombinant protein (130 kDa). To quantify the suppression of endogenous hAgo1 mediated by the investigated tools, the ratio between the band intensities of endogenous hAgo1 and β -actin, that served as the loading control, was determined. The control group (asON control and siscr3) was set 1 and used for the

normalization of the data. The results in ECV304 cells (Figure 6.3 A) showed that the expression level of endogenous hAgo1 upon asON1-A and siAgo1 transfection was reduced of 40%. On the contrary, asON1-B alone did not lead to Ago1 downregulation when compared to the control and in combination with asON1-A or siAgo1 or both of them, it revealed to have a competitive effect which led to only 20% of protein downregulation. These results in ECV304 cells suggest that asON1-B may compete with siAgo1 and asON1-A, for example, for the binding to cellular proteins involved in the downregulation of hAgo1 and thus leading to a reduction of the molecules available for the interaction with the other tools (Figure 6.3 A). The combination of siAgo1 and asON1-A instead led to the same effect than when they were applied separately indicating the absence of any additive effect (Figure 6.3 A). Surprisingly, in HeLa cells 48h after transfection, asON1-A or asON1-B showed to induce an up-regulation of the endogenous Ago1 protein (Figure 6.3 B) while siAgo1 alone had no effect on hAgo1 protein level in comparison to the control. However, the combination of siAgo1 with asON1-A or asON1-B or both of them led to up to 50% of protein suppression (Figure 6.3 B). These data in-

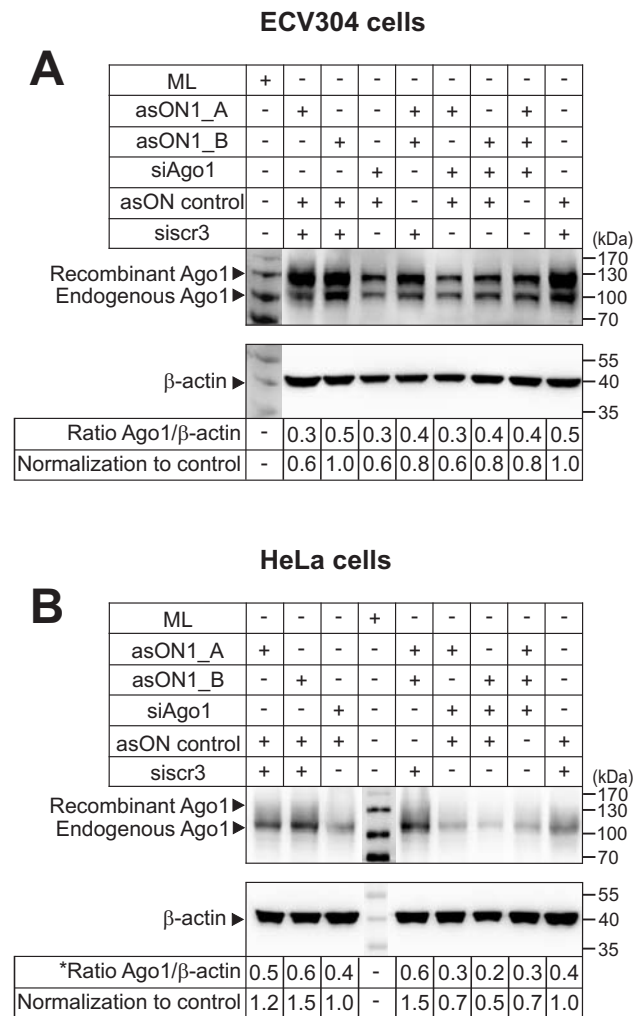


Figure 6.3: Western analysis showing the endogenous human Ago1 level in cells harvested 48h after the transfection with downregulating tools. Twenty-four h after cell seeding (50,000 cells/well in a 24-well plate), ECV304 cells (A) or HeLa cells (B) were transfected with 100nM siRNA or asON1-A or asON1-B or their combinations. An asON (asON control) and a siRNA (siscr3) whose sequences were unable to recognize any endogenous target in human were used as negative controls. Twenty-four h later, ECV304 or HeLa cells were transfected with a recombinant hAgo1 and harvested 48h after the first transfection. The Lipofectamine 2000-mediated transfection method was used for both transfections. A specific antibody, rat-anti human Ago1, was used. β -actin was detected as loading control to allow the calculation of the ratio hAgo1/ β -actin that was further normalized to the control group that was set 1. * Ratio values are expressed as 10^{-2} . PageRulerTM Prestained Protein Ladder as Mass Ladder (ML) was used. Here, composed figures are shown.

B or both of them led to up to 50% of protein suppression (Figure 6.3 B). These data in-

indicate that in HeLa cells, unlike ECV304 cells, the hAgo1 suppression was achieved only by combining siAgo1 with asONs directed against hAgo1. This phenomenon observed in HeLa cells could be consistent with the hypothesis that the protein suppression may be more efficient when the corresponding mRNA is targeted by the association of tools that hybridize on the transcript at two different sites distant from each other [178]. This could explain why the combination of siAgo1 and asON1-B led to a higher suppression of hAgo1 expression in comparison to the association of siAgo1 and asON1-A (Figure 6.2 and Figure 6.3 B). In HeLa cells the lack of competition among the different tools, which was observed in ECV304 cells (Figure 6.3 A), could be due to the number of cellular proteins available for the interaction with asONs and siRNAs that in HeLa cells was probably higher. Unexpectedly, the detection of the recombinant hAgo1 (CLIP-hAgo1) was highly different between the two tested cell lines. In fact, in ECV304 cells, the expression of CLIP-hAgo1 (130 kDa) was very abundant while in HeLa cells it was very low (Figure 6.3 B). This could be due to toxic effect of the double transfection by using Lipofectamine 2000 as transfectant. Therefore, for the experiments with shRNA-encoding plasmids (see 6.1.2) the less toxic Lipofectamine LTX or Turbofect were used. In conclusion, siAgo1, asON1-A and asON1-B revealed to be not enough effective for achieving the level of hAgo1 downregulation required in this study. In parallel to this study, the knock-down of hAgo2 by siRNA- and asON-based tools was also investigated and described below.

6.1.1.2 Knock-down of hAgo2 via siRNA and/or asON-based methods

To suppress hAgo2 expression level a specific siRNA (siAgo2) or asON (asON2), or their combination was tested. The siAgo2 was designed by Meister *et al.* [24] to target the ORF

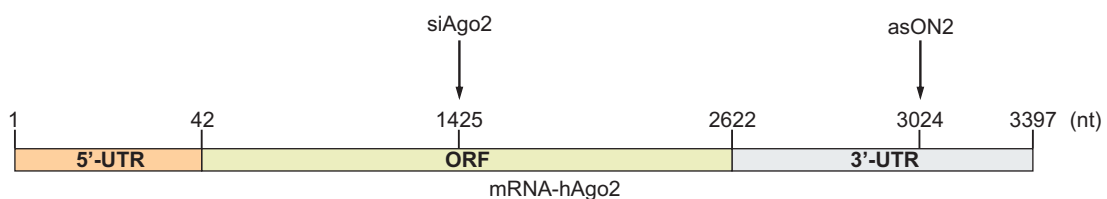


Figure 6.4: Schematic representation of siRNA and asON targeting mRNA of hAgo2. siAgo2 targets ORF while asON2 target the 3'-UTR. The position indicated by the arrows show the first nt from the 5'-end of the target region.

of hAgo2 mRNA while a 24nt-long asON, which was designed by Mescalchin *et al.* [167] targeted the 3'-UTR of hAgo2 transcript (Figure 6.4). Two cell lines, HeLa or ECV304 cells, were tested. The association of asON control and siscr3, which were unable to recognize any endogenous human target, served as negative control. Twenty-four h after the transfection with the tools directed against endogenous hAgo2, cells were transfected with recombinant hAgo2 in order to overcome the consequent drawbacks due to the low level of endogenous hAgo2 and to allow the cellular RNAi pathway. In the sequence of the

recombinant Ago2 there were no target regions for the investigated siAgo2 and asON2. Cells were harvested 48h after the first transfection and Western analysis was performed by using a specific antibody rat-anti human Ago2 that recognizes both endogenous and recombinant hAgo2. Endogenous Ago2 protein was detected as two bands that represent two different isoforms (~ 100 kDa) while the recombinant protein was detected as 130 kDa band (Figure 6.5). Actually, the predicted molecular weight for CLIP-hAgo2 was 117.8 kDa (see Figure 6.1). This difference between the theoretical and the real size could be due to mobility of the protein through the gel. β -actin was detected as loading control and the ratio hAgo2/ β -actin of the control group (asON control and siscr3) was set 1. In ECV304 cells the maximum hAgo2 knock-down achieved was of 60% and it was observed upon asON2 treatment (Figure 6.5 A). Interestingly, in ECV304 cells siAgo2 was not as efficient as siAgo1 leading to only 20% of endogenous hAgo2 suppression (Figure 6.5 A and Figure 6.3 A) and its combination with asON2 led to a decrease of asON2-mediated effect (Figure 6.5 A). These results suggested that Ago2 plays an essential role

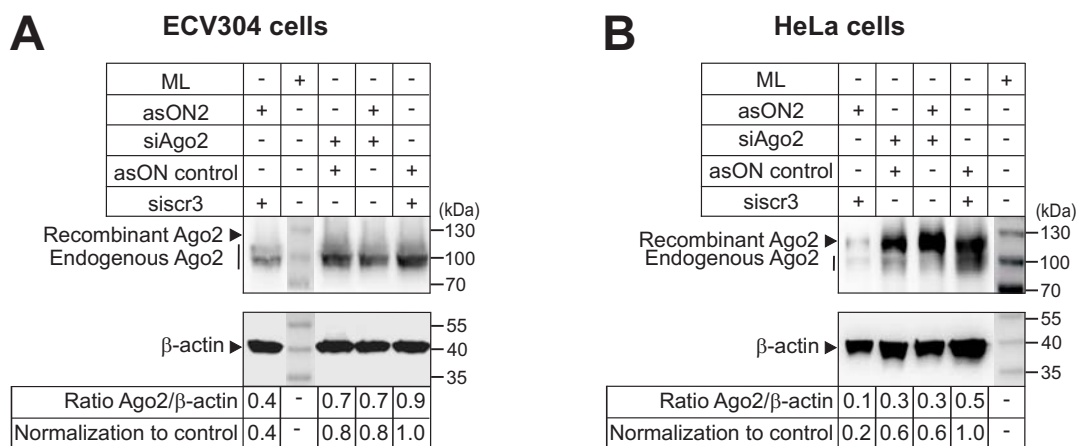


Figure 6.5: Composed figures showing Western analysis of endogenous Ago2. (A) ECV304 cells or (B) HeLa cells were transfected with 100nM siRNA or asON2 or their association. asON control and siscr3 were used as negative control. After 24h both cell lines were transfected with recombinant Ago2. The cells were collected 24h or 48h after the second transfection. Both transfections were performed by using Lipofectamine 2000-mediated transfection method. The specific antibody, rat-anti human Ago2, was used. Beta-actin was detected as loading control and the ratio hAgo2/act corresponding the combinations of the two controls was set 1. For ECV304 cells the quantification at 48h was not possible because of smeared actin bands. The Mass Ladder (ML) that was used was PageRulerTM Prestained Protein Ladder. The values were rounded.

in the RNAi process and its decreased amount could lead to a partial loss of RNAi and affect, consequently, the efficiency of the siRNA and in ECV304 cells, the expression of the recombinant hAgo2 was probably too low to compensate the loss of endogenous hAgo2 (Figure 6.5 A). On the contrary, in HeLa cells Ago2 knock-down by asON2 and siAgo2 (Figure 6.5 B) was higher than the one observed in ECV304 cells. Actually, asON2 confirmed to be the most efficient tool leading to 80% protein suppression in comparison to the control group (Figure 6.5 B). Surprisingly, the expression of the recombinant hAgo2

was also reduced upon asON2 treatment. However, the recombinant Ago2 is lacking the target site for the asON. This could be due to an autoregulatory function of hAgo2 which may lead to protein degradation, when the endogenous protein level reaches a certain threshold. The siAgo2 alone led to 40% protein suppression and its combination of the asON2 revealed to be less effective when compared to asON2 alone (Figure 6.5 B). In summary, in ECV304 cells the expression of recombinant hAgo2 was missing and only a limited downregulation of the endogenous hAgo2 was achieved. Therefore, ECV304 cells were considered not suited for performing further experiments in the use of recombinant hAgo2 or its mutant hAgo2^{Mut}. On the contrary, in HeLa cells the expression of CLIP-hAgo2 was sufficient for further investigations. Taken together, the results described here show that the investigated asON- and siAgo-based tools were not able to induce a complete depletion of the endogenous hAgo2, and this was probably due to their transient inhibitory effect. To solve this issue, a further approach was required, which allowed the constitutive expression of Ago-directed tools, such as shRNA-encoding plasmids.

6.1.2 Establishment of a shRNA-based Ago knockdown system in HeLa cells

In order to establish a system for the suppression of endogenous hAgos and the expression of the recombinant ones to study their roles, another approach was tested. The

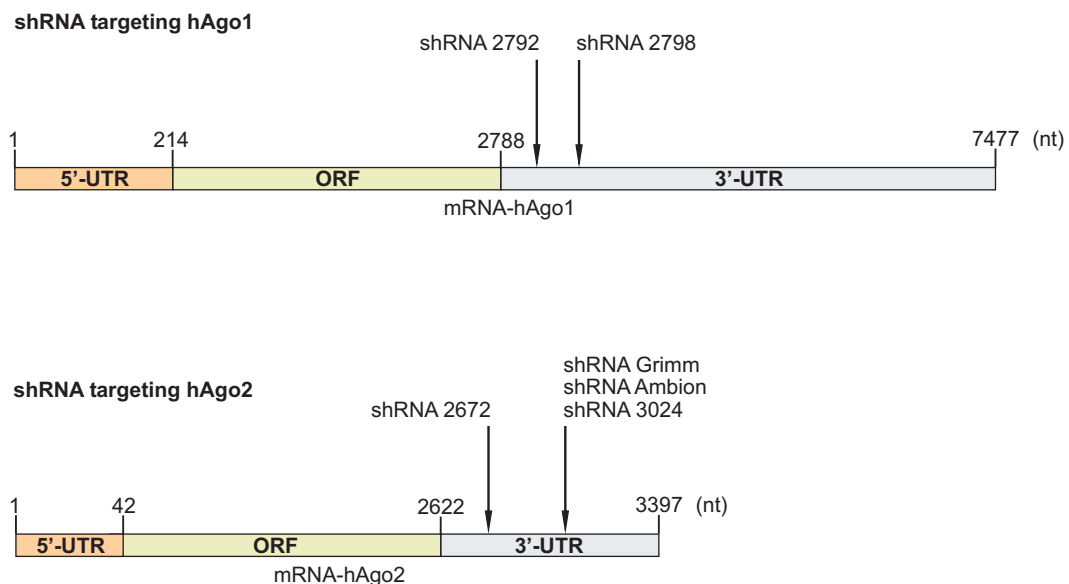


Figure 6.6: A schematic representation of hAgo1 and hAgo2 mRNAs targeted by shRNAs used in this study. Each arrow indicates the first nt at the 5'-end of the target region and it gives the name to the relative shRNA. 5'-UTR: 5' untranslated region; ORF: open reading frame, 3'-UTR: 3' untranslated region

method is based on the possibility to induce a long-term gene-silencing in human cells via expression of shRNAs from DNA constructs by employing the human U6 promoter [68]

and it was applied in many previous studies [35, 179, 180]. Usually canonical shRNAs are used for gene silencing [181–183]. They are dsRNA with 2 nt overhang at the 3'-end constituted by two perfect complementary strands and linked by a loop. They are called canonical since it was shown that Dicer preferentially cleaves shRNAs having 2 nt overhang at the 3'-end rather than blunt-end shRNAs [70]. Unlike transfected siRNAs, whose effect is only transient, the shRNA-based approach allows a long term gene silencing. In fact, shRNAs encoding plasmids are transcribed in the nucleus, the shRNAs are exported by Exp-5 to the cytosol where upon Dicer processing they are chopped into endogenously generated siRNAs. Recent studies described that shRNAs with a length

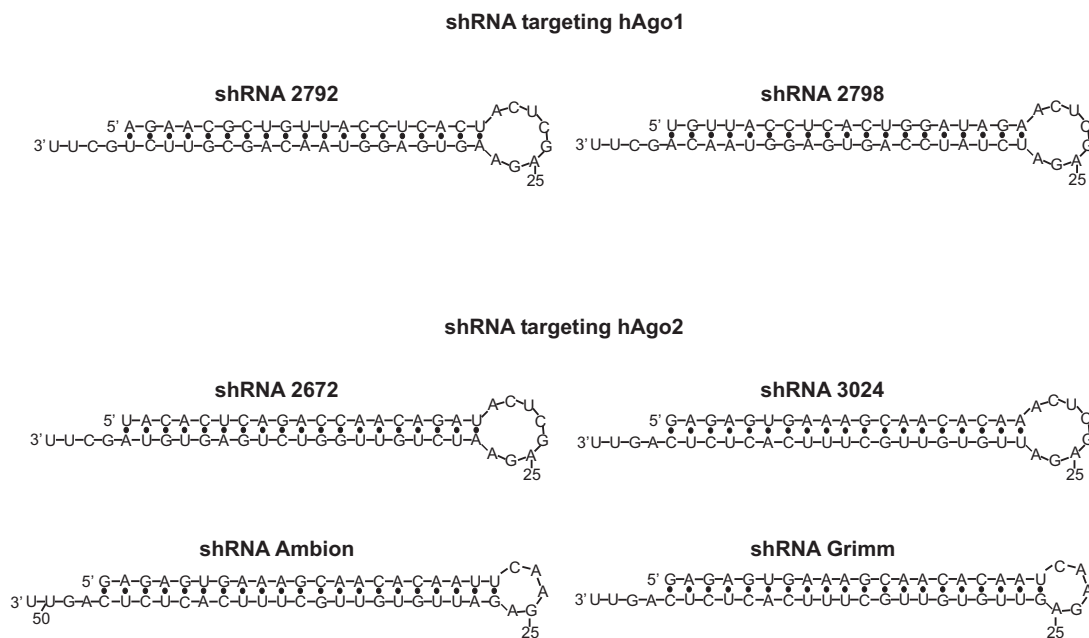


Figure 6.7: Sfold predicted structures of shRNA used in this study.

≤ 19 bp can be processed via an alternative pathway (Dicer-independent way) which involves hAgo2 [71]. The shRNAs used in this study were dsRNA consisting of 19-21 bp in which the two strands were perfectly complementary and connected by a loop. They were transcribed from vectors creating by ligating 63 to 65 nt-long DNA oligonucleotides and inserting them into a pSilencerTm neo expression vector carrying the human U6 promoter (see Figure 5.1). For this purpose, DNA oligonucleotides encoding for shRNA sequences were designed (see 5.2.1). Since the RNA polymerase III is responsible of the shRNA encoding plasmid transcription and recognizes a tract of poly(T) as terminal signal, the resulting shRNA was characterised by two uridine at 3'-end overhang in ac-

cordance with what described by Elbaschir *et al.* [20].

ShRNA were designed to target the 3'-UTR of hAgo1 or hAgo2 mRNA in order to avoid the downregulation of the recombinant hAgo proteins that were expressed as well and that carried a different 3'-UTR sequence. In Figure 6.6 a schematic representation of the mRNAs and target regions is shown. Each arrow represents the first nt at the 5'-end of the target region and gives the name to the relative shRNA. In details, shRNA targeting hAgo1 were called shRNA 2792 and shRNA 2798, while shRNA targeting hAgo2 were named shRNA 2672, shRNA 3024, shRNA Ambion and shRNA Grimm. The loop of each shRNA contained the restriction site for XhoI therefore called XhoI loop (ACUCGAGA). An exception was represented by shRNA Ambion and shRNA Grimm whose sequences were the same as shRNA 3024 but their loops were designed by using Ambion web site [169] (UUCAAGAGA) or by Grimm *et al.* [170] (UCAAGAG), respectively. Their secondary structures were predicted by using Sfold [184] and they are shown in Figure 6.7.

6.1.2.1 Evaluation of the shRNA effect on hAgo1 and hAgo2 at the protein and transcript levels in HeLa cells

In order to test the efficacy of the designed shRNAs in downregulating Ago1 or Ago2 proteins, HeLa cells were seeded and 24h later they were transfected with a plasmid encoding recombinant CLIP-hAgo2 to ensure the functioning of the RNAi pathway even upon the loss of endogenous hAgo2. Alternatively, HeLa cells were transfected with a plasmid encoding CLIP-hAgo2^{Mut} (slicing deficient) for comparison or with CLIP-tag encoding plasmid which served as negative control. The slicing incompetent CLIP-hAgo2^{Mut} was generated by introducing a mutation in the catalytic tetrad located in the PIWI domain. Actually, the catalytic tetrad of Wt-hAgo2 (D597/E637/D669/H807) was changed by replacing the D at the position 669 with Alanin [25]. The day after HeLa cells were transfected with shRNA 2792 or shRNA 2798 targeting hAgo1 mRNA or with shRNA Ambion or shRNA Grimm or shRNA 3024 or shRNA 2672 which are directed against hAgo2. Western analysis was performed in order to, on one hand, evaluate the level of endogenous hAgo1 or hAgo2 and, on the other hand, to check whether the expression of recombinant proteins occurred. For estimating the downregulation of hAgo1 or hAgo2, a

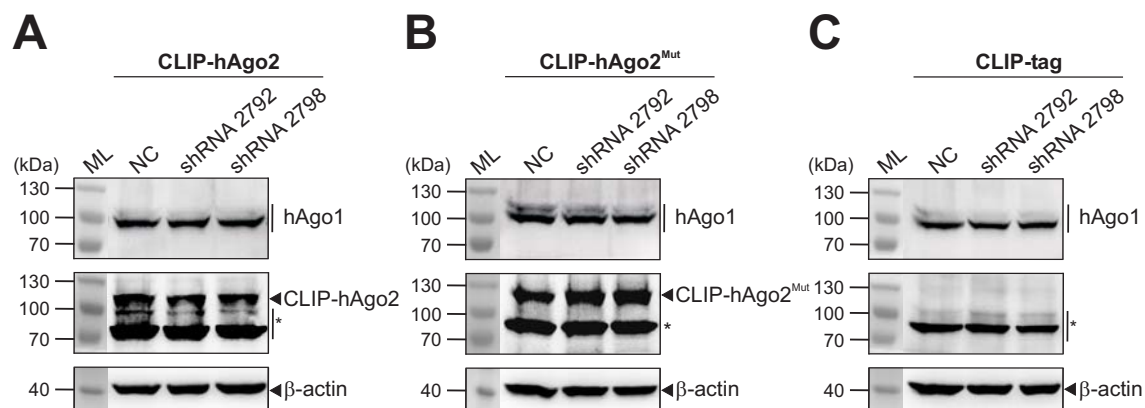


Figure 6.8: Detection of hAgo1 in HeLa cells by Western analysis to evaluate the effect of shRNA 2792 or shRNA 2798. Upon expression of recombinant CLIP-tagged hAgo2 (A) or the slicing deficient CLIP-hAgo2^{Mut} (B) or CLIP-tag (C) used as negative control, HeLa cells were transfected with a plasmid that did not encode for any shRNA (NC), or with shRNA 2792 or shRNA 2798 to target the mRNA of hAgo1. LipofectamineTM LTX-mediated transfection was used as transfection method. Ninety-six h after seeding, the cells were harvested to perform Western analysis. In the upper panels, the expression of endogenous hAgo1 is shown and it was detected as band of 100 kDa by using a monoclonal rat anti-hAgo1 antibody. In the middle panels, the expression of recombinant hAgo2 (A) or CLIP-hAgo2^{Mut} (B) is indicated and detected as 130 kDa band by using polyclonal mouse anti-CLIP/SNAP antibody. On the contrary, no band was detected as 130 kDa in the cells transfected with the plasmid encoding the CLIP-tag. β -actin, that was detected as well by using a polyclonal rabbit anti-human β -actin and used as loading control, is shown in the lower panels. * unspecific band. ML: Mass Ladder (PageRulerTM Prestained Protein Ladder). Here, composed figures are shown.

comparison with the normal endogenous level of the corresponding protein was required.

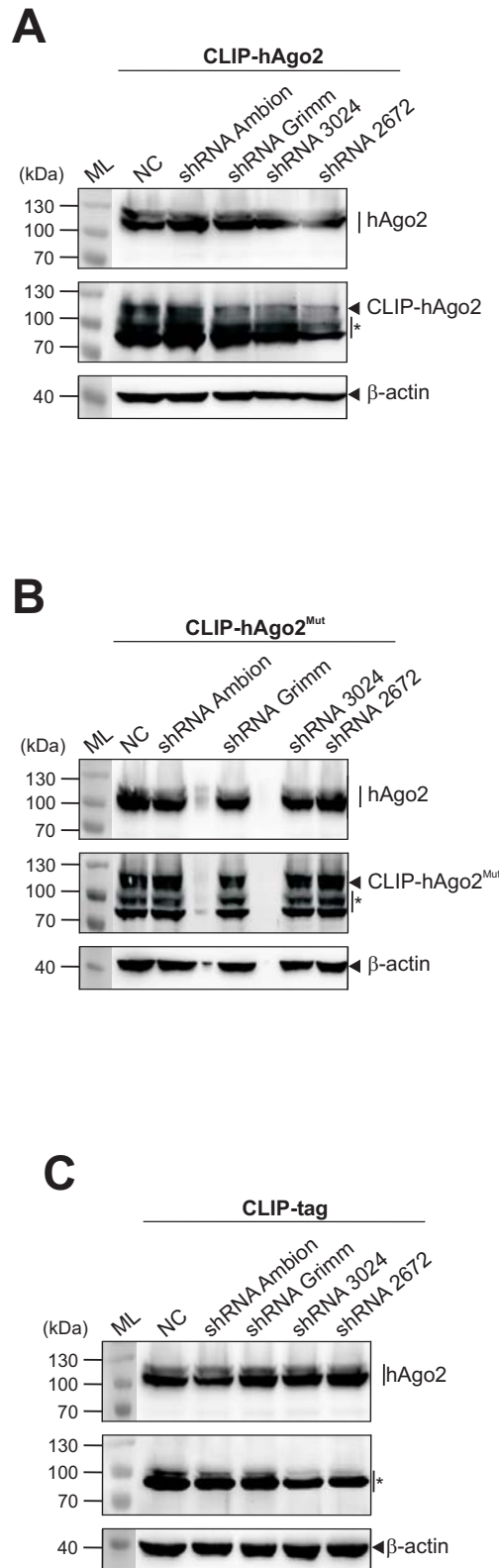


Figure 6.9: Detection of hAgo2 at the protein level in HeLa cells to investigate the effect of shRNA Ambion, shRNA Grimm, shRNA 3024 or shRNA 2672. HeLa cells were transfected with recombinant CLIP-tagged hAgo2 (A) or the cleavage incompetent CLIP-hAgo2^{Mut} (B) or CLIP-tag (C) used as negative control. After 24h they were transfected with NC plasmid, with shRNA Ambion, shRNA Grimm or shRNA 3024. The transfection was performed by using LipofectamineTM LTX. Ninety-six h after seeding, the cells were harvested to perform Western analysis. The upper panels show the endogenous protein level hAgo2. In the middle panels, the expression of the recombinant hAgo2 proteins is shown. As loading control β -actin was used and its detection is shown in the lower panels. * unspecific band. ML: Mass Ladder (PageRulerTM Prestained Protein Ladder). In all the panels composed figures are shown.

Therefore, cells were transfected with shRNA targeting hAgo1 or hAgo2 or with a plasmid (NC) that did not encode for any shRNA and consequentially, it was not able to recognize any endogenous target. The Figure 6.8 shows the level of endogenous hAgo1 upon transfection with shRNA 2792 or shRNA 2798. hAgo1 was detected as 100 kDa band by using rat-anti hAgo1. CLIP-hAgo2 (Figure 6.8 A) and CLIP-hAgo2^{Mut} (Figure 6.8 B) were detected as 130 kDa bands (Figure 6.8 middle panel). β -actin was detected as loading control.

In cells transfected with shRNA 2792 or shRNA 2798, the hAgo1 protein level

did not decrease when compared to the endogenous Ago1 level of the cells transfected with NC plasmid (Figure 6.8). The expression of CLIP-hAgo2 and CLIP-Ago2^{Mut} was the same in all tested groups. In Figure 6.9 are shown the Western analysis results of hAgo2 level upon transfection of shRNA Ambion, shRNA Grimm, shRNA 3024 or shRNA 2672 and upon cellular expression of recombinant Ago2 or Ago2^{Mut}. The detection of endogenous hAgo2 was performed by using the antibody rat-anti hAgo2 and it was revealed as two bands with an apparent mass of 100 kDa approximately that represent two isoforms of this protein [136] (Figure 6.9). Both CLIP-Ago2 and CLIP-Ago2^{Mut} showed a similar expression level in all treated groups (Figure 6.9). The amount of endogenous hAgo2 was not reduced by the specific shRNAs when compared to the endogenous Ago2 level of the cells transfected with NC plasmid. The survey of the downregulation of hAgo1 (Figure 6.10) or hAgo2 (Figure 6.11) at the transcript level by shRNA was carried out as well and it was performed via q-PCR using specific primers recognizing endogenous Ago1 or endogenous Ago2. In both cases, primers for β -glucuronidase were used and

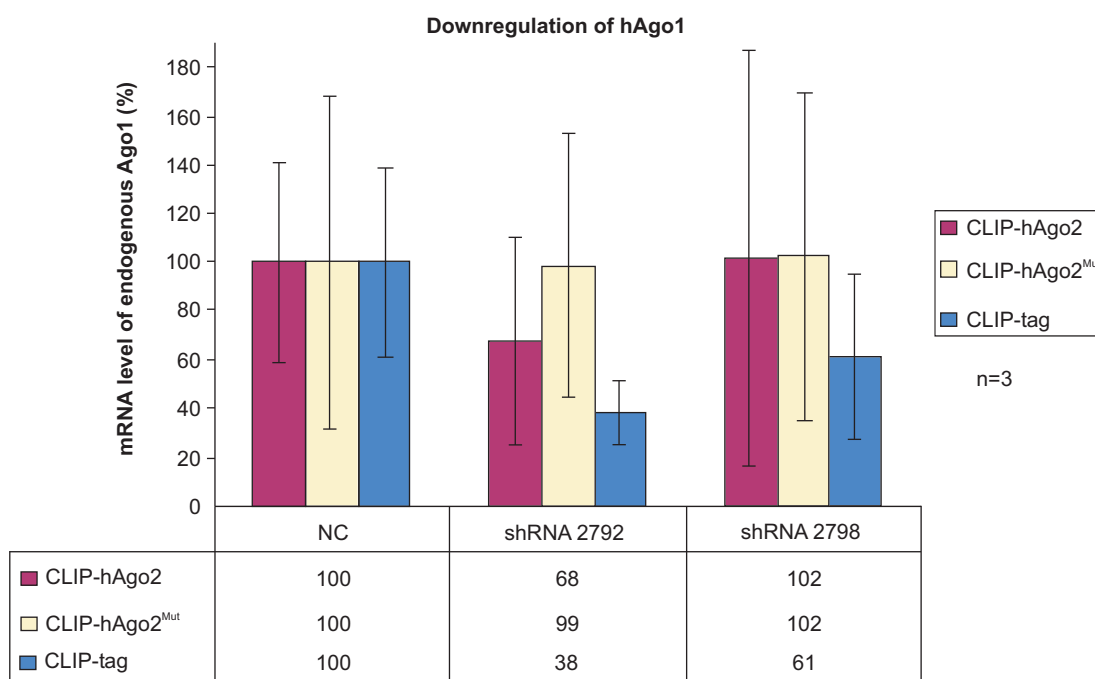


Figure 6.10: Rating of the effect of shRNA 2792 or shRNA 2798 on the expression of hAgo1 at the transcript level in HeLa cells upon expression of CLIP-hAgo2 or CLIP-hAgo2^{Mut} that was slicing inactive or CLIP-tag used as negative control. HeLa cells were transfected with recombinant hAgo and after 24h with NC plasmid or with shRNA 2792 or shRNA 2798 by using LipofectamineTM LTX. Forty-eight h after the second transfection cells were harvested, the total RNA was isolated and reverse transcribed. The cDNA was quantified by q-PCR. hAgo1 mRNA level of the cells transfected with the plasmid NC was set 100. Percentage of mRNA Ago1 expression is shown and the error bars indicate standard deviations. The graphic is a representation of three independent experiments.

the expression values of this housekeeping gene were used for normalization of the data. The mRNA of endogenous Ago1 or Ago2 of the samples transfected with NC plasmid

upon over-expression of each recombinant Ago was set 100. Percentage values and standard deviations were calculated consequently. Three independent experiments were

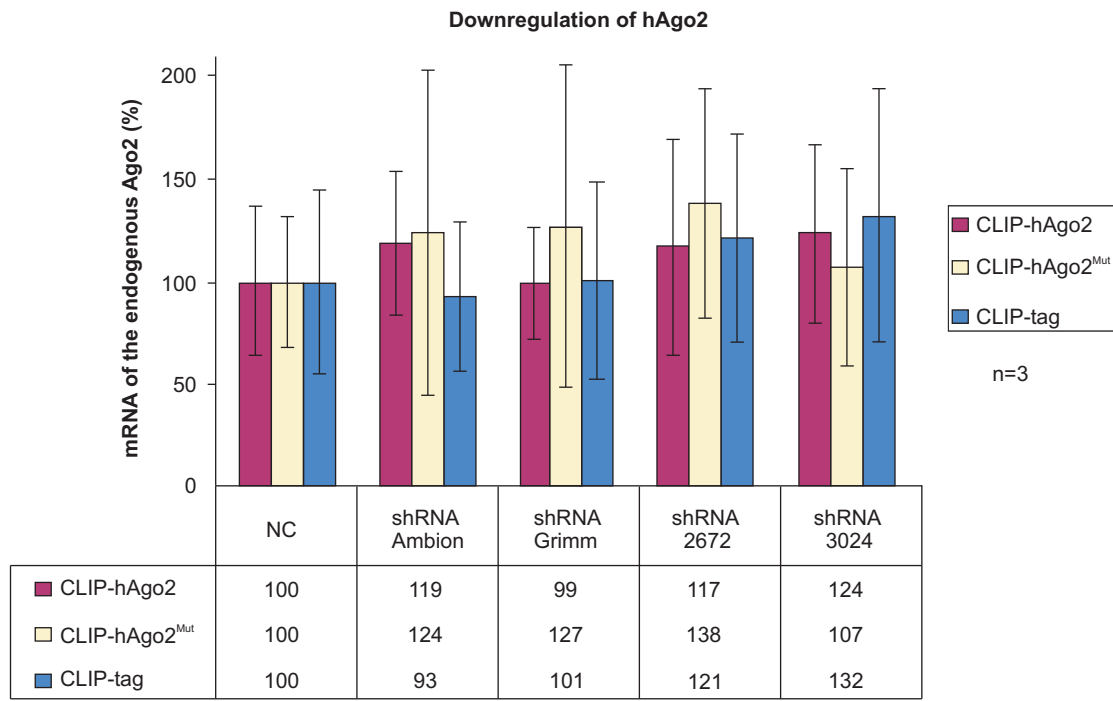


Figure 6.11: Estimation of the effect of shRNA Ambion, shRNA Grimm, shRNA 3024 or shRNA 2672 on the mRNA level of hAgo2. HeLa cells were transfected with CLIP-hAgo2 or with CLIP-hAgo2^{Mut} that lost the cleavage competence or with CLIP-tag as negative control. After 24h, the transfection with NC plasmid or with a plasmid encoding for shRNA Ambion or shRNA Grimm or shRNA 3024 or shRNA 2672 occurred. LipofectamineTM LTX-mediated transfection was used as transfection method. The harvest of the cells was performed 48h after the second transfection, the total cellular RNA was isolated and reverse transcribed. The cDNA was quantified by q-PCR. The mRNA level of hAgo2 relative to the cells transfected with shRNA NC was set 100 to allow to calculate the percentage of the expression of hAgo2 mRNA in order to determine whether any downregulation occurred. Moreover, standard deviations are indicated by error bars. The graphic represents an average of 3 experiments that were carried out independently.

performed, and the average was calculated to plot a single chart. A statistical analysis of the data in Figure 6.10 and Figure 6.11 was also performed in order to ascertain whether a significant difference existed among the calculated means. For each shRNA three averages were compared (CLIP-tag, CLIP-hAgo2, CLIP-hAgo2^{Mut}). Therefore, the Fischer's test (F-test) was applied as statistical test. The F values for the tested shRNA ranged between 0.2 and 2.7, while the critical value was 3.55 for all shRNAs except for shRNA Ambion which was 3.63 for a F distribution with $\alpha=0.05$ (probability of 95%). In light of these results, differences among the three means were not significant since F was lower than the critical value. Moreover, the F test was also applied to evaluate the significance of the values relative to the downregulation mediated by shRNAs against hAgo1 or hAgo2 upon the over-expression of CLIP-tag, CLIP-hAgo2 or CLIP-hAgo2^{Mut} compared to the values obtained from the transfection of shRNA NC. It confirmed that

the differences relative to the group of shRNA targeting hAgo1 or hAgo2 with the NC were not significant since the F were under the critical values (for $\alpha=0.05$). However, the calculation of the least significant difference (LSD) which is a *post-hoc* control performed between two specific means of the group, revealed that only the differences between the mean values of shRNA 2792 or shRNA 2798 with the shRNA NC upon CLIP-tag were significant ($t_{NC-shRNA2792}=3.65$ and $t_{NC-shRNA2798}=2.28$ while the critical value was 1.7341 with $\alpha=0.05$). These results suggested that the shRNA 2792 and shRNA 2798 were able to induce cleavage and degradation of hAgo1 mRNA only in absence of recombinant hAgos. However, the reduction of Ago1 at the transcript level (Figure 6.10) was not reflected by a reduction of the hAgo1 protein (Figure 6.8). In this section, in order to shed light on the results described, further experiments were performed to investigate the maturation and expression levels of the shRNA designed and tested here.

6.1.2.2 Expression and maturation of shRNAs used in this study

Therefore, it was wondered whether shRNAs maturation occurred in the cells to produce siRNAs that trigger RNAi pathway leading to gene silencing or whether the failed hAgo knock-down was due to the essential role that hAgos play in the cell. HeLa cells were seeded and, 24h later, transfected with plasmid encoding CLIP-hAgo2, CLIP-hAgo2^{Mut} (slicing incompetent) or CLIP-tag only used as negative control. After 24h shRNA-encoding plasmids transfection was performed. Alternatively, HeLa cells were transfected with NC plasmid that did not encode for any shRNA. The choice of transfecting cells 24h after the first transfection was due to the awareness, derived from preliminary experiments, that CLIP-tagged hAgos were already highly expressed at the protein level at this time point. Cells were harvested 48h after the second transfection to allow shRNA synthesis and the yield of siRNAs derived from shRNAs was then evaluated. For this purpose Northern analysis (see 5.1.8) appeared to be the most suited method allowing to determine the size and the abundance of shRNA-derived siRNAs and, eventually, the presence of shRNA intermediate products. The results concerning shRNAs targeting hAgo1 are shown in Figure 6.12. These data showed that shRNA 2792 (Figure 6.12 A) or shRNA 2798 (Figure 6.12 B) gave rise to siRNAs detected as band with about 20 nt in length. Moreover, from Northern analysis of shRNA 2792, it was possible to detect bands ranging between 30-40 nt in length that were called intermediate products since they were shorter than the shRNA designed as 50 nt-long sequence and longer than the derived siRNA (Figure 6.12 A). The intermediate products reminded the Ago2-cleaved-pre-miRNA (ac-pre-miRNA) that Diederick and Haber described for *pre-let-7a* [29]. They demonstrated that ac-pre-let-7a was the result of Ago2-mediated endonucleolytic cleavage of the passenger strand located at the 3'-end of pre-miRNA. In the light of this, it was hypothesized that the intermediate products observed in this study were derived from cleavage of the sense strand at the 5'-end of shRNA. Surprisingly, the over-expression of CLIP-hAgo2 or

tag only (Figure 6.12 A). The quantification of shRNA-derived siRNA (shown in (Figure 6.12 A as ratio siRNA/U6) was performed and the value upon CLIP-tag over-expression was set 1 and used for normalization of the data. It turned out that the expression of CLIP-hAgo2 or CLIP-Ago2^{Mut} increased the amount of siRNA derived from shRNA 2792 by 5- or 4-fold, respectively (Figure 6.12 A). In order to shed light on this phenomenon the quantification of the band intensities of the intermediate products was also performed (shown in Figure 6.12 A as ratio intermediate product/U6). The results showed that the amount of the intermediate products upon the over-expression of cleavage competent hAgo2 was similar to the corresponding amount upon CLIP-tag which was used as control (Figure 6.12 A). The over-expression of the CLIP-hAgo2^{Mut} instead led to an increased quantity of the intermediate product of 1.5-fold in comparison to the control. Taken together, these data indicated that the increment of the amount of siRNA derived from shRNA 2792 did not depend on the cleavage activity of hAgo2 and that the amount of intermediate product was not affected by the slicing active hAgo2. These results suggested that, in case of shRNA 2792, hAgo2 and its mutant might play a role on the maturation of shRNA by Dicer for example, by interacting with Dicer and thus leading to a better target positioning and to a higher cleavage efficiency. A previous study showed that the expression of Ago2 with functional binding domain (PAZ) led to an increased copiousness of mature miRNA derived from transfected pre-miRNA [29]. Therefore, it could also be that CLIP-hAgo2 or CLIP-hAgo2^{Mut} might form a complex with the shRNA making it more stable for Dicer binding. The intermediate products shown in Figure 6.12 A could be the results of a minor and not favoured function of the endogenous cleavage active hAgo2. However, they are too short to be further processed by Dicer [71] and this could explain why the amount of intermediate product did not change or changed only slightly while the amount of shRNA-derived siRNA resulted enhanced. In Figure 6.12 B the Northern analysis results for shRNA 2798 upon the over-expression of CLIP-hAgo2 or CLIP-hAgo2^{Mut} are shown. ShRNA 2798 upon expression of CLIP-tagged hAgos gave rise to a 2-fold increase in the amount of the derived siRNA when compared to the control group (CLIP-tag) (Figure 6.12 B). For shRNA 2798 no intermediate products were detected probably because their expression was under the detection limit (Figure 6.12 B). The Figure 6.13 A shows the results of the Northern analysis of shRNA 2672. The siRNA derived from shRNA 2672 was detected as a band at 20 nt, and several bands between 30 and 50 nt that were identified as intermediate products (Figure 6.13 A). Due to the high number of intermediate products and to the high background the quantification intermediate product/U6 not possible. The amount of siRNA derived from shRNA 2672, when compared to the amount yielded upon expression of CLIP-tag, showed to be increased by the expression of CLIP-hAgo2 or CLIP-hAgo2^{Mut} by 1.16-fold or 1.5-fold, respectively. In the Figure 6.13 B the Northern results of the maturation of shRNA 3024, shRNA Ambion or shRNA Grimm are shown.

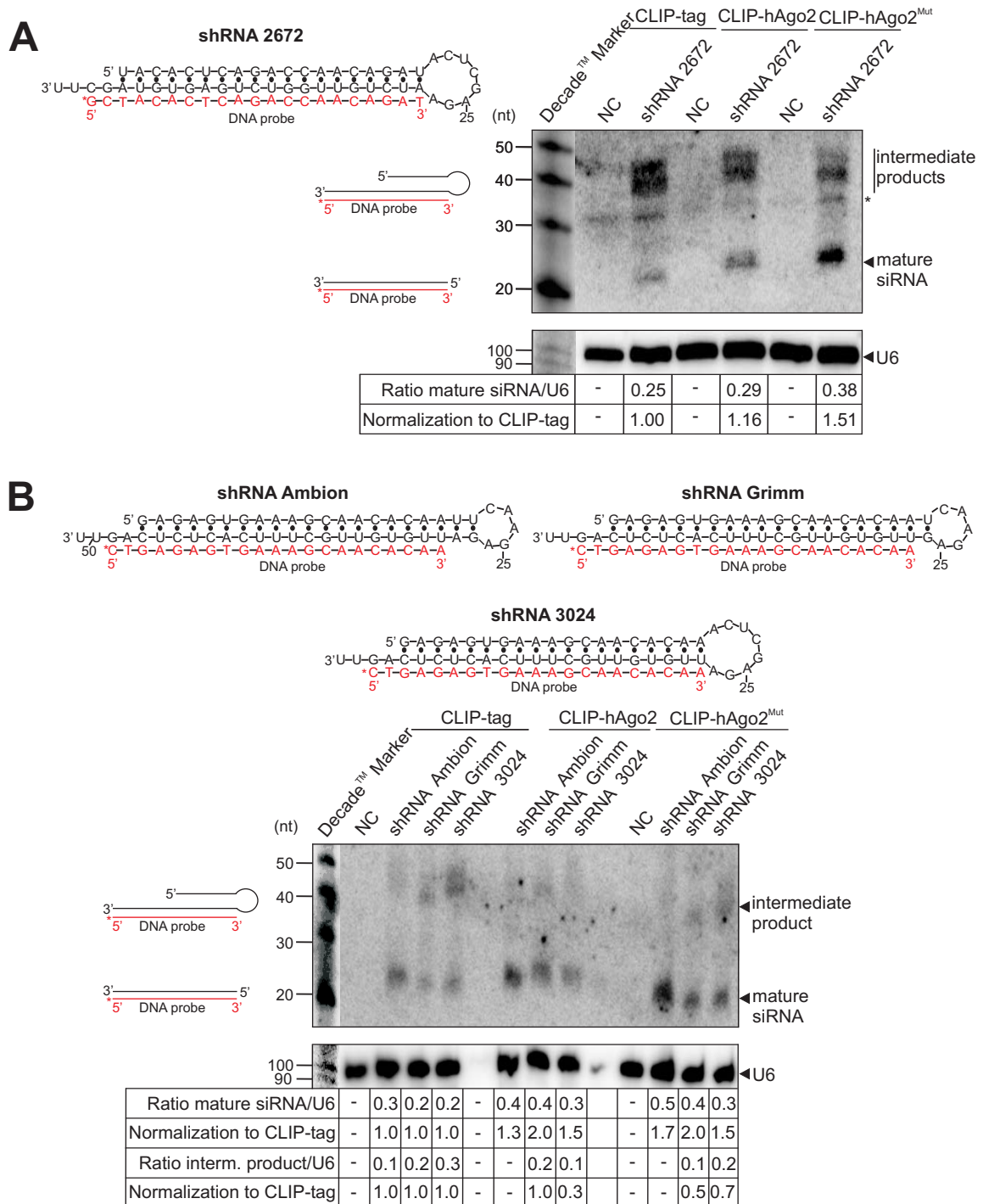


Figure 6.13: Evaluation of the maturation of shRNAs targeting hAgo2 in HeLa cells via Northern analysis. Maturation of shRNA 2672 (A), shRNA 3024, shRNA Ambion or shRNA Grimm (B) upon expression of CLIP-hAgo2 or CLIP-hAgo2^{Mut} that lacks of the cleavage activity or upon the expression of CLIP-tag used a control. The shRNA secondary structures that are shown were predicted by using Sfold. The DNA probe designed to detect complementary the antisense strand of shRNA 2672 or to detect the antisense strand of shRNA 3024, shRNA Ambion, as well as shRNA Grimm, is highlighted in red and the 5' radiolabeled end is indicated by *. Additionally, the cells were transfected with a plasmid called negative control (NC) since it did not encode for any shRNA. Those samples were used negative control (NC) to check the sequence-specificity of the probe used for the detection. LipofectamineTM LTX was used as transfecting reagent. DNA probe for U6 RNA detection was used to allow the calculation of the ratio siRNA/U6 upon CLIP-tag expression that was set 1. Consequently, the ratio siRNA/U6 upon expression of recombinant hAgo was determined. Radiolabeled Decade Marker System was used to identify the length of detected bands. * Unspecific band. In A and B composed figures are shown.

shRNA-derived siRNAs were detected as bands at 20 nt and their amount resulted increased upon over-expression of recombinant Ago2 or Ago2^{Mut}. The intermediate products were also detected and they ranged between 30 and 40 nt. The ratio intermediate product/U6 was calculated for shRNA Grimm and shRNA 3024 while for shRNA Ambion the quantification was not possible due to the low intensity band signal and also to the high background. Like shRNA 2792, also in case of shRNA Grimm CLIP-hAgo2 cleavage competent did not influence the amount of intermediate product when its ratio with U6 was normalized to the control that was set 1 (Figure 6.13 B). Instead, the hAgo2 over-expression led to a 2-fold increase in the amount siRNA derived from shRNA Grimm in comparison to CLIP-tag. Also in this case hAgo2 may participate and support the maturation process, for example, by interacting with Dicer and helping shRNA positioning. The slicing deficient hAgo2^{Mut} showed to increase the amount of shRNA Grimm-derived siRNA and to reduce the amount of intermediate product. This suggested that, because of its binding capability, the CLIP-hAgo2^{Mut} may compete with the endogenous hAgo2 for the binding to shRNA shifting the equilibrium toward the derived siRNAs rather than intermediate products. In the case of shRNA 3024, its intermediate product was reduced upon transfection with CLIP-hAgo2 or CLIP-hAgo2^{Mut} (ratio intermediate/U6 was 0.3 or 0.7, respectively) (Figure 6.13 B). However, also shRNA Ambion and shRNA 3024 showed to be influenced by up-regulation of hAgo2 or hAgo2^{Mut} resulting in the enhancement of the amount of shRNA-derived siRNA in comparison to the control. These results showed that shRNA directed against hAgo1 or hAgo2 were transcribed by transfected cells and underwent to the endogenous maturation pathway giving rise to siRNAs. Hence, it is possible that the designed shRNAs were not functional since the expected hAgo1 or hAgo2 knock-down was not achieved (see 6.1.2.1). However, this system highlighted another interesting phenomenon which is the increased amount of shRNA-derived siRNAs upon hAgo2 and hAgo2^{Mut} over-expression. Therefore, further investigations to shed light on the role of the four hAgos on the maturation of shRNA were performed.

6.2 Study of the effect of hAgo proteins on the maturation of shRNAs in HeLa cells

It was shown that hAgo proteins are involved in the formation of RISC [185] and that all four hAgos are able to load dsRNA [47, 186] (Figure 6.14) although only hAgo2 is slicing active [24, 25].

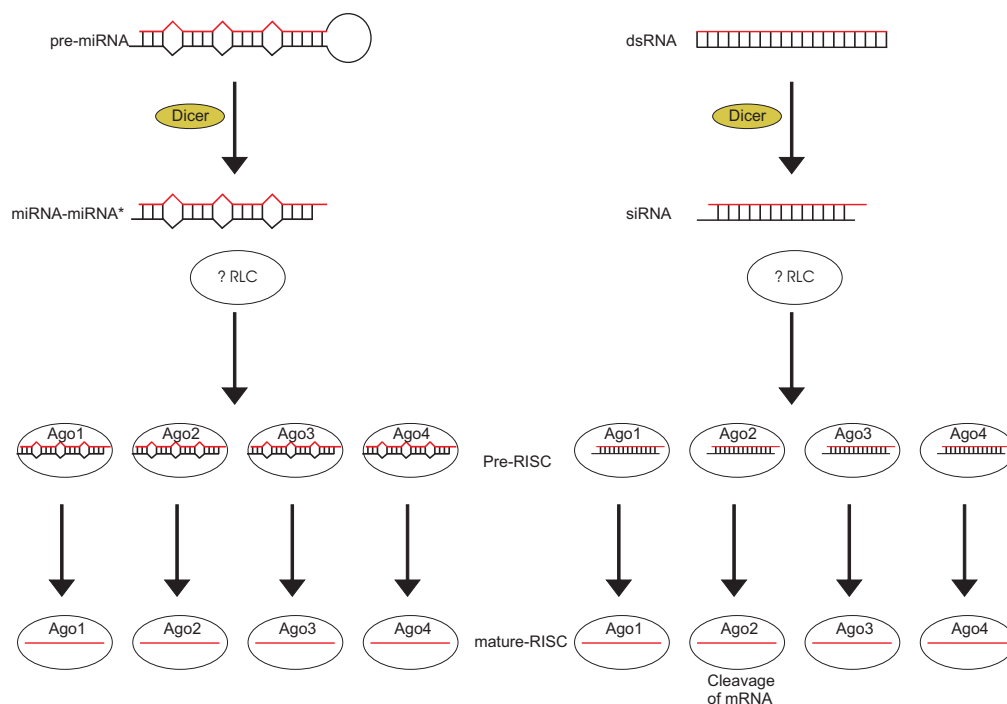


Figure 6.14: Schematic representation of the RISC loading process in human in which all hAgos are able of dsRNA loading, but only Ago2 has cleavage activity. On the left side a pre-miRNA is shown and the red bar indicates the guide strand. On the right side a perfect complementary dsRNA is depicted and the red bar indicates the antisense strand. Modified from Kawamata-2010 *et al.* [186].

However, only little is known about the exact involvement of each hAgo in RNAi mechanism. In the view of this, the system established and described here so far, proposed to be suited for allowing to perform further *in vitro* studies to shed light on the effect of each hAgo on the maturation of shRNAs.

6.2.1 Survey of the maturation of shRNA 2672 upon recombinant hAgos over-expression

To investigate the effect of hAgos on the maturation of shRNAs, recombinant hAgos encoding plasmids were employed to allow their over-expression at the protein level. In this study, CLIP-hAgo 1-4 and a slicing deficient CLIP-hAgo2^{Mut}, described in 6.1.1. Before investigating the effect of CLIP-hAgos on the maturation of shRNAs the evaluation of their

expression via Western analysis was needed in order to test whether a similar expression level was achieved (Figure 6.15). In order to ensure shRNA transcription and maturation upon hAgo phenotypic over-expression, HeLa cells, 24h after seeding, were transfected with CLIP-hAgo1-4, CLIP-hAgo2^{Mut} or CLIP-tag encoding plasmids and 24 later with the shRNA-encoding plasmids. Non-treated cells were harvested as well to be loaded on 10%SDS-PAGE and served as additional control. Recombinant hAgos were detected as bands with an apparent mass of about 130 kDa. Their detection was performed by using mouse anti-CLIP-Tag antibody, while β -actin, which was used as loading control, was detected as 40 kDa band and its detection was achieved upon incubation of the membrane with polyclonal rabbit anti-human-actin antibody. Western analysis (Figure 6.15) showed

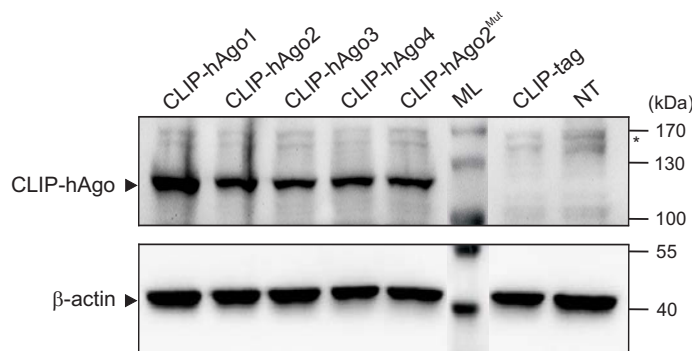


Figure 6.15: Western analysis showing the phenotypic expression of the CLIP-tagged hAgo1-4 and a slicing inactive CLIP-Ago2^{Mut} in HeLa cells. Twenty-four h after seeding, the cells were transfected with CLIP-tagged hAgo or CLIP-hAgo2^{Mut}-encoding plasmids by using Turbofect-mediated transfection method. Alternatively, the cells were transfected with a plasmid encoding CLIP-tag and used as negative control. The recombinant hAgos were detected as about 130 kDa bands by using mouse anti-CLIP-Tag antibody. β -actin detection was performed as well by incubating the membrane with polyclonal rabbit anti-human-actin antibody. It appeared as 40 kDa band and was used as loading control. ML: Mass ladder; NT: non-treated HeLa cells; * indicates unspecific signals. In both panels composed figures are shown.

a comparable expression among all the recombinant hAgos, therefore these constructs were used for further investigation. The interest about the observed effect of CLIP-hAgo2 or CLIP-hAgo2^{Mut} which resulted in the increase of the amount of shRNA-derived siRNAs (see 6.1.2.2), led to address the question of whether this influence could be exerted by hAgo1-3-4 as well and, more interestingly, what differences among the four hAgos could be highlighted, fulfilling the purpose of this study. Moreover, in a previous study it was hypothesized that, in addition to overlapping functions of mammalian Ago [154], hAgos could have different abilities and this could explain the existence of four different Ago proteins and their common capability to load ds siRNA or miRNA [186]. To test this hypothesis, the effect of all hAgos on the maturation of shRNA 2672 was investigated, which was chosen for this pilot study among the different sequences tested previously (Figure 6.16). In details, HeLa cells were transfected with CLIP-hAgo1-4, the slicing

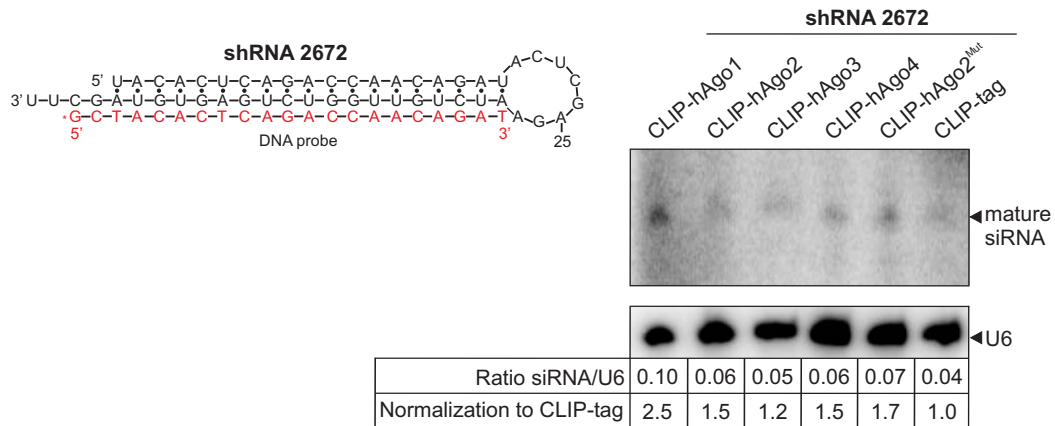


Figure 6.16: Northern analysis showing the maturation of shRNA 2672 upon expression of CLIP-tagged hAgo1-4 or the endonuclease inactive CLIP-Ago2^{Mut}. Otherwise, HeLa cells were transfected with CLIP-tag encoding plasmid that served as a negative control. Lipofectamine 2000 was used as transfecting reagent. The Sfold predicted structure of shRNA 2672 is shown on the left panel and the 5'-end radiolabeled DNA probe, which is specifically complementary to the antisense strand of shRNA 2672, is indicated in red. U6 small nuclear RNA (snRNA) was detected as a loading control. The ratio siRNA/U6 was normalized to the ratio siRNA/U6 relative to the expression of CLIP-tag which was set 1.

deficient CLIP-hAgo2^{Mut} or with CLIP-tag encoding plasmid used as negative control. Upon their over-expression, the introduction in the cells of shRNA 2672 encoding plasmid was carried out via transfection method and the cells were harvested after 48h to allow time for shRNA transcription and maturation. Northern analysis was performed to detect the antisense strand of the shRNA by using a perfect complementary DNA probe employed previously (see 6.1.2.2). U6 was detected as well to further normalize the ratio siRNA to the control which was set 1. The quantification corroborated the results obtained formerly: in fact, the up-regulation of CLIP-hAgo2 or CLIP-hAgo2^{Mut} increased the amount of shRNA-derived siRNA in comparison to the amount in CLIP-tag transfected cells: 1.5- or 1.7-fold, respectively (Figure 6.16). All hAgo proteins gave rise to an increased amount of shRNA-derived siRNA, confirming the initial hypothesis. Interestingly, the effect showed to be of different intensities among the four hAgos when compared to the control (Figure 6.16). Specifically, CLIP-hAgo1 over-expression determined an increase of the shRNA-derived siRNA by 2.5-fold while CLIP-hAgo3 or CLIP-hAgo4 induced an increment of 1.2- or 1.5-fold, respectively. The fact that the effect of hAgo3 is only marginal suggests a different behaviour of hAgo3 in comparison to other hAgos. Further experiments were needed to obtain more insight regarding different hAgo effects.

6.2.2 Investigation of the effect of hAgos on structurally different shRNAs

From the literature, an increasing effect of hAgo proteins was observed on the passenger strand of miRNA derived from transfected pre-miRNA and it was suggested that this effect was due to the binding of miRNA with Ago proteins that, consequently, increased

in the binding with PAZ domain of hAgo1 while it was demonstrated that a RNA substrate with 2nt overhang at the 3'-end was cleaved by Dicer more effectively than blunt ended molecule [111]. In the view of this, the influence of hAgos on the maturation of shRNA having different long 3'-overhang ends was investigated in order to clarify whether Ago effect was dependent on shRNA terminus structure and to carry out a structure-functional study that could permit to elucidate the differences among the four hAgo proteins.

6.2.2.1 Study of Ago effect on shRNA with different 3'-end length

With the purpose to elucidate hAgo influence on the maturation of shRNA, it was hypothesized a model to investigate (Figure 6.18). According to the model proposed by Park *et al.* [70] that described the RNA substrate positioned in Dicer domains, the question of whether Ago influence was due to the length of the 3'-end of shRNA was addressed: it may be to ensure its positioning in Dicer pockets. For this purpose, new shRNAs were designed by shortening or lengthening the 3'-overhang sequence of shRNA 2792 regarded as starting point. Actually, shRNA with 2 or 4 or 10 nt in the 3'-overhang were cloned and tested. HeLa cells were transfected with recombinant CLIP-hAgos or the slicing incompetent CLIP-hAgo2^{Mut}. After 24h they were transfected with a plasmid encoding shRNAs featured with 2, 4 or 10 nt overhang at the 3'-end and harvested after 48h to extract total cellular RNA in order to be examined via Northern analysis. The results for shRNA 2nt-3'-overhang are shown in Figure 6.19 A in which the shRNA-derived siRNA appeared as two different long siRNA products and the intermediate product was detected and visible under increased contrast. However, the sum of the two bands was considered for calcu-

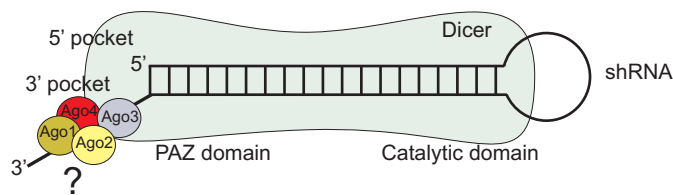


Figure 6.18: Model under investigation to clarify whether hAgo effect on the maturation of shRNA is dependent on its 3'-end length. This model was modified from Park *et al.* [70] that proposed a double anchor model in which the domains that hold the 3'- and 5'-end of the a substrate with 2 flanking nt are called 3'- and 5'-domains, respectively ensuring a fixed shRNA position.

lating the ratio mature siRNA/U6. The forthright observation was that only the cleavage competent hAgo2 gave rise to the enhancement of the amount of shRNA-derived siRNA which was detected as two bands, with a length of 22 and 21 nt, respectively (Figure 6.19 A). On the contrary, hAgo3 over-expression induced a reduction of 50% of shRNA-derived siRNA in comparison to the control which was set 1.

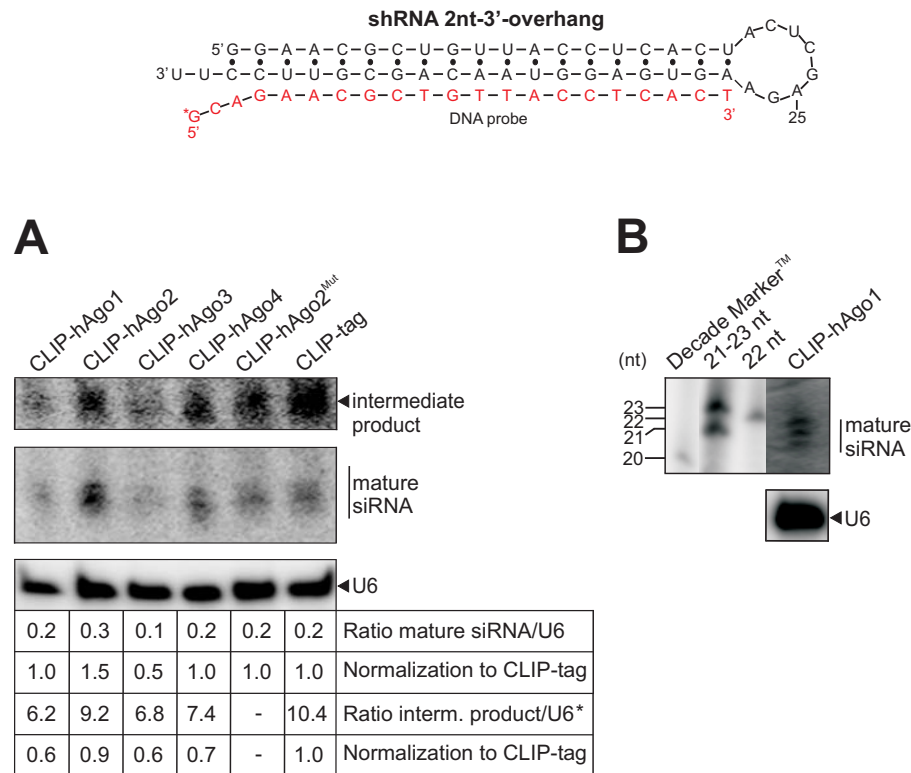


Figure 6.19: Northern analysis showing the maturation of a shRNA having 2 nt overhang at the 3'-end upon over-expression of CLIP-tagged hAgo1-4 or the slicing incompetent CLIP-hAgo2^{Mut}. On the top panel, Sfold predicted structure of shRNA-2nt-3'-overhang is shown and the DNA probe used for the detection of the antisense strand of the shRNA is in red. * Indicates the radiolabelled 5'-end of the probe. Twenty-four h after seeding, HeLa cells were transfected with each recombinant hAgo or with the mutant or with CLIP-tag used as control by using Turbofect as transfection method. Twenty-four h later, the transfection with the shRNA-2nt-3'-overhang encoding plasmid occurred. Northern analysis was performed after the harvest of cells which took place 48h after the second transfection. A) hAgo2 or hAgo3 influence the amount of shRNA-derived siRNA inducing increase or reduction, respectively. In all cases two shRNA-derived siRNA products were detected. The intermediate product is shown with increased contrast. B) High resolution Northern analysis showing the influence of hAgo1 on the siRNA derived from shRNA whose 3'-end was constituted by 2 nt overhang. Ago1 over-expression led to the formation of three different long fragments of which the longest was detected as 22 nt. RNA molecules of 21-22-23 nt in length were labelled at 5' end with [γ -³²P] and used as RNA markers. U6 detection was performed and used as loading control. The ratio mature siRNA/U6 was calculated and the control was set 1 for the normalization of the values. * Ratio values are expressed as 10⁻². In the panel B a composed figure is shown.

The amount of intermediate product of shRNA having 2 nt overhang at the 3'-end upon cleavage competent CLIP-hAgo2 was similar (ratio:0.9) to the control set 1 while the amount of shRNA-derived siRNA was increased by 1.5-fold. A possible explanation for these results could be that the endogenous hAgo2 may give rise to a minor pathway in which hAgo2 cleaves the shRNA inducing the formation of an intermediate product whose processing is not carried out completely. Conversely, the overexpressed recombinant hAgo2 may enhance a dominant pathway helping Dicer in shRNA processing and leading to an increased amount of shRNA-derived siRNA. On the contrary, hAgo3 over-

expression led to a strong decrease of the intermediate and mature products. It could be that hAgo3 may exert its effect in a step above the maturation process by binding the shRNA and leading to an inactive complex that is not able to interact with Dicer. As a consequence some shRNAs could be confiscated by hAgo3 and not available for further processing by Dicer. Surprisingly, different were the hAgo1 and hAgo4 effects since they did not have any influence on the amount of shRNA-derived siRNA but in both cases the quantity of the intermediate product was reduced (Figure 6.19 A). Also in this case, cleavage incompetent hAgos may bind to shRNAs favouring their processing by Dicer and thus competing with the activity of endogenous hAgo2 which leads to the formation of the pre-ac-shRNAs (intermediate products). By applying a high resolution Northern analysis (Figure 6.19 B) three different long shRNA-derived siRNA products (22, 21, 20.5 nt-long) were detected upon hAgo1 ectopic expression suggesting an Ago1-induced trimming effect. Further, the investigation of the maturation of shRNAs with 4 or 10 nt-long overhang at the 3'-end upon hAgo over-expression was also performed in order to get more insight in these phenomena. The results concerning shRNA with 4nt-overhang at the 3'-end (Figure 6.20) confirmed those obtained with shRNA 2672 (Figure 6.16) showing that not only hAgo2 but also Ago1-4-2^{Mut} induced an increase in the amount of shRNA-derived siRNA (detected as double bands) while hAgo3 had an inhibitory effect on the maturation of the shRNA. Over-expression of hAgo1 induced the production of three shRNA-derived siRNA sequences with different lengths, namely 21 nt and two smaller than 21 nt (Figure 6.20 B), further suggesting an hAgo1-induced trimming effect during the maturation of the shRNAs. These results gave rise to an intriguing question of why hAgo1,4 and hAgo2^{Mut} increased the amount of siRNA derived from shRNA with 4nt-overhang at the 3'-end (Figure 6.20) while they had no effect on the amount of siRNA derived from shRNA with 2 nt overhang at the 3'-end (Figure 6.19). This might find explanation in the fact that shRNAs with 2nt overhang at the 3'-end are canonical, therefore they are recognized and cleaved by Dicer, while a shRNA 4nt-3'-overhang may need the help of hAgo1-4 or hAgo2^{Mut} for its interaction with Dicer. Therefore, it could be hypothesized that hAgo over-expression may increase the formation of functional Dicer complexes carrying the RNA substrates and thus leading to the formation of a more stable RLC. Further, it was considered worthy to investigate the maturation of shRNA having a longer overhang at the 3'-end in order to check whether Ago effect is dependent on the 3'-end length. A shRNA sequence having 10 nt overhang at the 3'-end was tested (Figure 6.21) and also in this case, Ago3 induced a reduction in the amount of shRNA-derived siRNA (detected as double bands) suggesting that its effect was independent of the length of the overhanging sequence at the 3'-end. hAgo1 induced the production of the three shRNA-derived siRNA fragments with a length of 21-20 and <20 nt (Figure 6.21). The same result was seen by applying shRNA 4nt-3-overhang (Figure 6.20). Importantly, only hAgo1 showed to enhance the amount of siRNA derived from shRNA 10nt-3'-end-overhang supporting the hypothesis

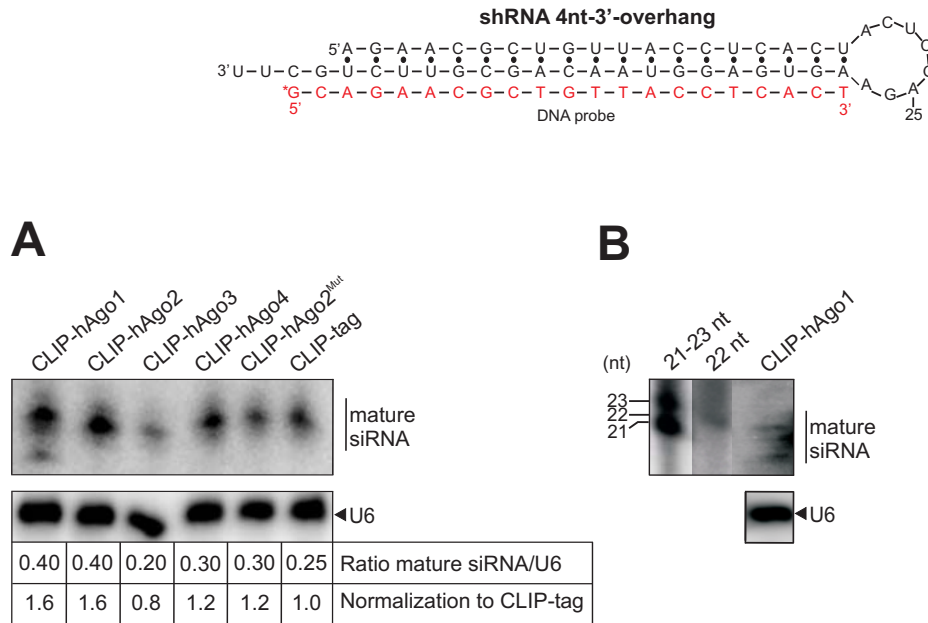


Figure 6.20: Differential effects of hAgos on the amount of siRNA derived from shRNA having 4nt overhang at the 3'-end via Northern analysis. The secondary structure of shRNA-4nt-3'-overhang structure which was predicted by using Sfold is shown in the top panel. The used DNA probe is indicated in red and the radiolabelled 5'-end is specified by *. A) CLIP-hAgo1-2-4 or the slicing incompetent CLIP-hAgo2^{Mut} effect led to enhanced amount of shRNA-derived siRNA which was detected as two different length fragments. An exception was represented by hAgo1 whose over-expression induced the formation of three shRNA-derived siRNA products. On the contrary, the over-expression of hAgo3 led to a reduced amount of the antisense strand of shRNA-derived siRNA. B) Assignment of the length of fragments upon CLIP-hAgo1 over-expression via High resolution Northern analysis and by loading RNA markers ranging between 21-23 nt in length and 5' radiolabelled. The transfection of HeLa cells with recombinant hAgos, with the mutant of hAgo2 or with CLIP-tag used as control and the transfection with the shRNA-4nt-3'-overhang encoding plasmids were performed by using Turbofect as transfecting reagent 24h and 48h after cell seeding, respectively. Cells were harvested 2 days after the second transfection to extract RNA in order to perform Northern analysis. DNA probe which recognized the antisense strand of shRNA-4nt-3'-overhang was 5' radiolabelled with [γ -³²P] and used. U6 was detected as loading control to allow the calculation of the ratio mature siRNA/U6 subsequently normalized to the control, that was set 1. The panel B shows a composed figure.

that only hAgo1 may induce the formation of a more stable RLC with shRNA having a long overhang at the 3'-end which results in an increased yield of derived siRNA. The detection of the intermediate products for shRNA 4nt and 10nt-3'-overhang was not possible due to the low signals (data not shown). Taken together, these results showed that the effect of hAgo1, 2, 4 and 2^{Mut} on the amount of shRNA-derived siRNA is dependent on the 3'-end length. shRNA-derived siRNA was detected as two bands with a size of 22 and 21 nt (shRNA 2nt-3'-overhang) (Figure 6.19) and 21 and <21 nt (shRNA 4 and 10nt-3'-overhang) (Figure 6.20 and Figure 6.21). The hAgo3 influence which resulted in decreasing the amount of shRNA-derived siRNA revealed to be independent on the 3'-end length. Ago1 behaviour differed from the other hAgos since it induced the production of three different shRNA-derived siRNA sequences and this effect showed to be independent from the length of the 3'-terminus suggesting that this is an hAgo1 intrinsic

6.2. Study of the effect of hAgo proteins on the maturation of shRNAs in HeLa cells 81

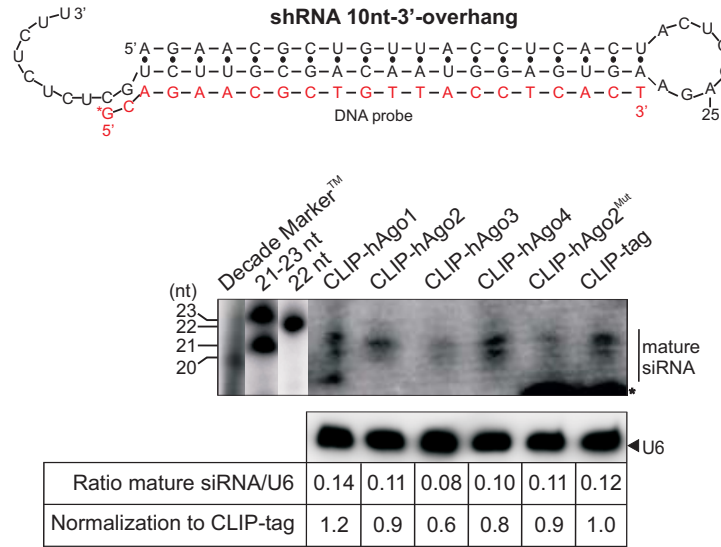


Figure 6.21: Effects of recombinant hAgos on the maturation of shRNA 10nt-3'-end-overhang. On the top panel, the Sfold predicted structure of shRNA-10nt-3'-overhang and base pairs between the antisense strand and the DNA probe, which was used for the detection and that is indicated in red. * Represents the [γ 32 P] at the 5'-end. The loading of RNA molecules of 21-22-23 nt in length which were labelled at 5'-end with [γ 32 P] allowed to determine the length of three siRNA products: 21, 20 and <20 nt. The transfection of HeLa cells with each recombinant hAgo or with the mutant hAgo2 or with CLIP-tag used as control and the transfection with the shRNA-4nt-3'-overhang encoding plasmids were performed via Turbofect-method 24h and 48h after cell seeding, respectively. U6 was detected as loading control and the ratio mature siRNA/U6 was subsequently calculated and normalized to the control that was set 1. The top panel shows a composed figure.

property. However, the resulting length of the fragments is dependent on the length of the overhang at the 3'-end. In order to characterize these hAgo proteins effects, further experiments were performed as described below.

6.2.2.2 shRNA 4nt 3'-overhang with inverted strands

The findings shown above indicate that the effect of hAgos on the amount of shRNA-derived siRNA, which is derived from structurally different shRNAs, was dependent on the overhang at the 3'-end, while the trimming effect mediated by Ago1 which resulted in the formation of three different long shRNA-derived siRNA products or the inhibiting Ago3 effect that led to the reduction of the amount of the antisense strand of shRNA-derived siRNA were not influenced by the length of the 3'-end. Considering that the loop sequence and the duplex length were not determining factors for Ago effect, as explained previously, the question of whether the different influence mediated by Ago proteins could be dependent on the shRNA sequence rather than the structure was addressed. Evidences indicated that shRNAs with ≤ 19 bp were too short to be cleaved by Dicer and that for such shRNAs the position of the loop was important in determining their processing [71]. Dallas *et al.* [71] investigated the processing of a shRNA that has the loop at the 3'- or 5'-end of the guide strand, called L or R respectively. They proposed that shRNA L or R were processed via a Dicer-independent mechanism in which L shRNA were deprived of a fragment of the passenger strand without loop cleavage, reminding the ac-precursor described by Diederick *et al.* [29]. On the contrary, R shRNA undergo loop cleavage via Dicer nuclease activity [71].

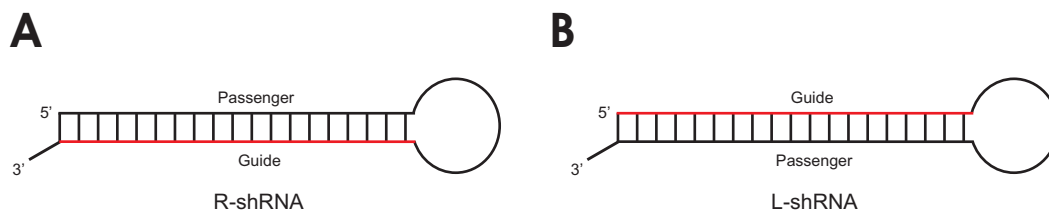


Figure 6.22: L and R shRNA structure depiction. A) Structure of shRNA tested in this study in which the loop is at the 5'-end of the guide strand and called R-shRNA. B) shRNA structure with inverted strands in which the loop is positioned at the 3'-end of the guide strand and named L-shRNA. The guide strand is color-coded in red.

In light of the role played by the loop position on shRNA processing, it was considered interesting to evaluate hAgo effect on the maturation of a shRNA having the same structure of shRNA 4-nt-3'-overhang (R shRNA in Figure 6.20) but with inverted strands (L-shRNA), as depicted in Figure 6.22, in order to obtain more insight about the different effect of hAgo proteins. The maturation of shRNA with inverted strands upon over-expression of recombinant hAgo1-4 or hAgo2^{Mut} was investigated via Northern analysis by employing a DNA probe able to recognize the antisense strand (Figure 6.23). These results showed that hAgo1 mediated a trimming effect also during the maturation of the shRNA with inverted strands. This suggested that it was an exclusive behaviour of hAgo1 unlike other hAgos and that it was independent both on the structure and on the sequence of the shRNA. The enhancing effect mediated by hAgo1-2-4 or the Ago2^{Mut} on the amount of siRNA

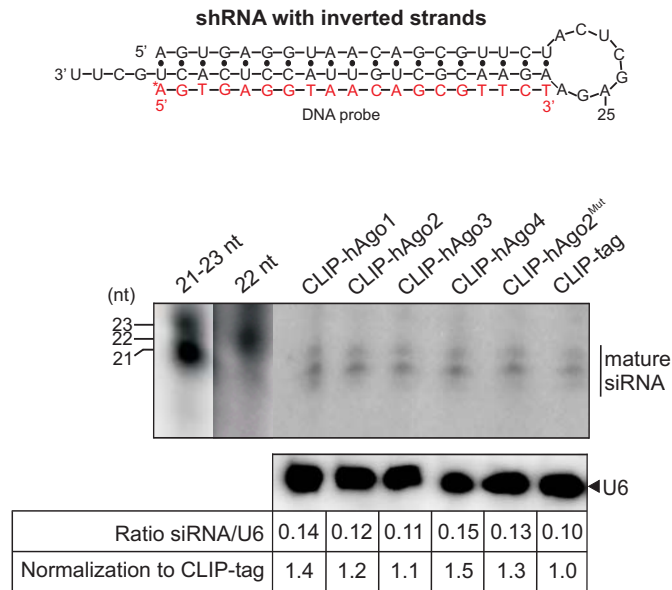


Figure 6.23: Northern analysis showing the maturation of shRNA with inverted strands upon the over-expression of recombinant hAgos. HeLa cells were seeded and 24h after they were transfected with plasmid encoding CLIP-tagged hAgo1-4 or the slicing incompetent CLIP-tagged hAgo2^{Mut}. CLIP-tag vector served as control. The day after the cells were transfected with plasmid encoding the shRNA with inverted strands. Turbofect reagent was used as transfectant. The cells were harvested 48h after the second transfection to extract RNA to examine via Northern analysis. In the top panel, the Sfold shRNA secondary structure is shown and the DNA probe used for the detection of the antisense strand is indicated in red. * indicates γ ³²P at the 5'-end. RNA molecules whose length ranges between 21-23 nt were 5'-end labeled and used as RNA markers. Reprobing of the blot for U6 snRNA served as loading control. The ratio mature siRNA/U6 was calculated and normalized to CLIP-tag which was set 1. In the top panel a composed figure is shown.

(detected as 21 and <21nt bands) derived from L-shRNA was comparable to what was observed for the R-shRNA 4nt 3'-overhang (Figure 6.20), confirming their dependence on the shRNA structure rather than the sequence. Surprisingly, hAgo3 up-regulation increased the amount of the antisense strand of siRNA derived from L-shRNA with inverted strands, although it was by a lesser amount when compared to other Agos. This observation led to speculate that Ago3 effect did not depend on the structure but on the sequence of the shRNA. This shows that it might play a role in determining the ratio antisense/sense strand of shRNA. This hypothesis found support in the recent literature which indicated Ago3 as able to enhance the *let-7a* passenger strand [82]. Additionally, also in the maturation of the shRNA with inverted strands the formation of three shRNA-derived siRNA products was evident upon over-expression of hAgo1 inducing, further supporting the hypothesis of a hAgo1-induced trimming effect. Taken together, these results allowed to underline different Ago effects on the maturation of shRNA having different structural characteristics which are summarized in Figure 6.24.

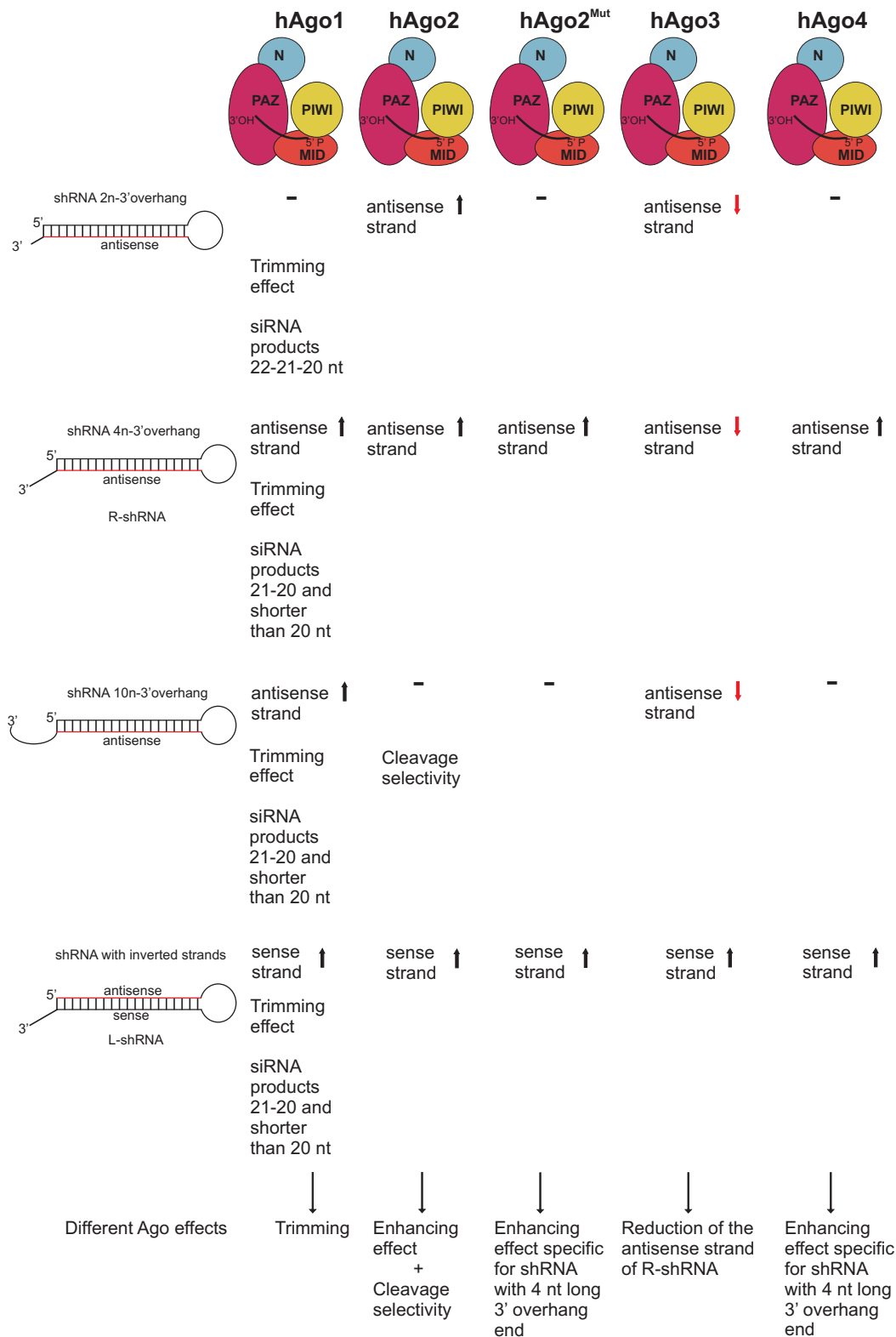


Figure 6.24: Effects of hAgo proteins on the maturation of shRNA having different structural features. On the top, a depiction of hAgo1-4 or hAgo2^{Mut} (cleavage incompetent) shows their N (blue), PAZ (purple) MID (orange) and PIWI (yellow) domains. On the left side, schematic structures of shRNA having 2,4 or 10 nt in the overhang at the 3'-end and shRNA with inverted strands are shown. The red line in each shRNA structure indicates the antisense strand. R-shRNA or L-shRNA mean shRNA in which the loop is at the 5'-end or at the 3'-end of the antisense strand, respectively. Black arrows facing upwards and the red arrows pointing downwards represent an increase or a reduction of the amount of the indicated strand of the shRNA-derived siRNA, respectively.

6.3 Analysis of the maturation of endogenous miRNAs in HeLa cells upon over-expression of recombinant hAgo

6.3.1 Identification of the most abundant miRNAs in HeLa cells

In light of the different influence of hAgo on the amount of shRNA-derived siRNA, the question of whether over-expressed hAgo exert a different effect also on the amount of the endogenous mature miRNA was addressed. To carry out this investigation, HeLa cells were chosen and a survey of the most abundant miRNAs was needed prior to the Northern analysis. For this purpose, the website microRNA.org [189] was consulted and the expression rate of some of the most expressed miRNAs which were object of this study is shown in Figure 6.25. Thus, miR-16, *let-7b*, miR-21 or miR-30a were considered for further investigation.

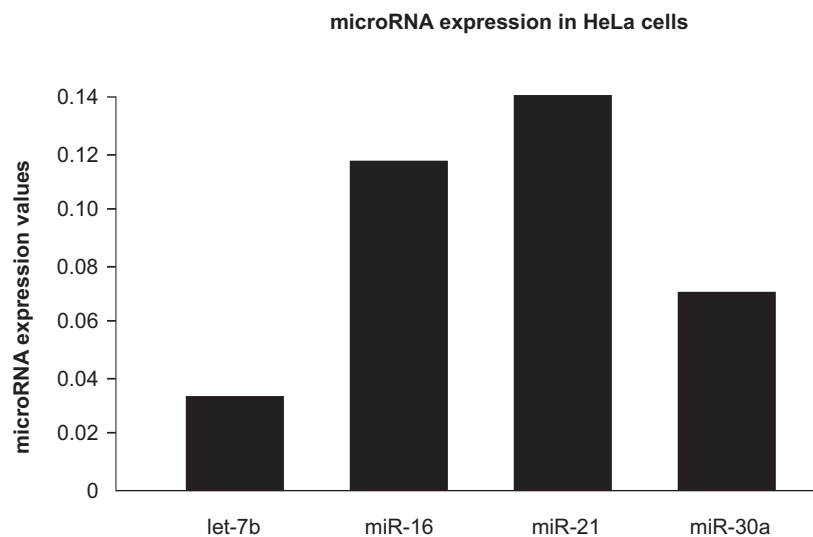


Figure 6.25: Graphic showing the expression levels of the miRNAs investigated in this study and which are mainly expressed in HeLa cells.

6.3.2 Investigation of hAgo effect on the maturation of endogenous miRNA

For studying the Ago effect on the maturation of endogenous miRNAs, the system established so far was applied. Actually, HeLa cells were transfected with a plasmid encoding CLIP-hAgo1-4 or CLIP-Ago2^{Mut} that was slicing inactive due to the mutation in the catalytic tetrad, or with CLIP-tag encoding vector that served as negative control. The cells were harvested after 48h to achieve the necessary hAgo over-expression at the protein level and to evaluate their effect on the amount of mature miRNA. Total cellular RNA was extracted to perform a Northern analysis. For the detection of the guide strand of each miRNA a specific DNA probe was used.

7. Discussion

7.1 A system to study the cellular role of hAgos

In the cell, ds RNAs undergo to processing by Dicer protein, followed by the unwinding of the two strands by the RISC [176]. HAgos, which are key components of RISC, play an important role in the RNAi [137, 190] and they are able to bind ds siRNAs or miRNAs [47, 186]. However, among the four hAgos only hAgo2 is cleavage competent [24, 25]. Despite several studies have been performed to elucidate the functions of hAgos in the cell, so far only little is known about these proteins. Therefore, in this study in order to shed light on the roles of the four hAgo proteins an experimental system was established and detailed *in vitro* studies were performed to study their effect on the maturation of exogenous shRNAs and endogenous pre-miRNAs. To carry out this investigation, the first necessary requirement was the downregulation of the endogenous Ago proteins from the cells. This was considered, at the beginning, to be a necessary condition to avoid background due to the endogenous proteins and to allow the expression of one recombinant hAgo at the time in order to evaluate the single Ago effect. Two strategies were identified in the literature for inhibiting the endogenous Ago expression [24, 154, 167, 191]. One was based on inactivation by knock-out of genes encoding for Ago proteins [154] while the other aimed to downregulate the protein level by acting on the corresponding mRNA [24, 167]. The first method is based on an inducible Ago1-4 knock-out system in mouse embryonic stem cells [154]. The second strategy involves the use of siRNAs [24] or asONs [167] that were tested in human cell lines and they are post-transcriptional gene silencing tools. The siRNAs recognize the mRNA target leading to its cleavage by exploiting the RNAi mechanism while asONs exert their effect via a RNase H-based activity. The goal of this study was to study the human Ago proteins therefore the second method was the most suited for this purpose. As first, a suitable human cell line needed to be identified for carrying out this study, therefore two cell lines were tested: the HeLa that are derived from cervical cancer of Henrietta Lacks [192] and they are widely used in the research field and the ECV304 cells that are derived from human urinary bladder carcinoma. Initially, a pilot study was performed in the use of siRNAs or asONs as tools to downregulate hAgo1 or hAgo2 (see 6.1.1.1 and 6.1.1.2).

7.1.0.1 Downregulation of endogenous Ago proteins

For achieving hAgo1 or hAgo2 downregulation, asONs or siRNAs or their combinations were tested in HeLa or ECV304 cells (see 6.1.1.1 and 6.1.1.2), on one hand, to check additional or synergic effect among those tools and on the other hand to find the most suitable cell line. Additionally, in order to compensate the decreasing level of the endogenous counterpart, recombinant hAgo1 or hAgo2 were transfected which did not carry any binding site for the investigated tools. Although siRNAs are reported to be suited tools for achieving downregulation [193, 194], in this study, they presented a limitation since they suppress a protein that is required to execute their function. To overcome this drawback of the siRNAs tools, asONs were also employed since they act with RNase-H mechanism (see 6.1.1). For the downregulation of hAgo1, two different asONs and one siRNA targeting hAgo1 were tested. Western analysis results showed that in ECV304 siAgo1, as well as asON1-A, led to 40% of Ago1 knock-down but their combination did not give rise to any additive effect (Figure 6.3). AsON1-B showed not only to be not ineffective, but when cotransfected with asON1-A and/or siAgo1, it reduced their effect of 20%. This could be due to the competition among the tools the binding to cellular proteins which participate in the suppression of hAgo1 expression, such as RNase H or RISC components, and thus hindering their activity (Figure 6.3 A). The endogenous level of hAgo1 in HeLa cells showed to be not affected by siAgo1 and it was increased upon asON1-A and/or asON1-B transfection (Figure 6.3 A). The combination of siAgo1 with asON1-A or asON1-B induced Ago1 knock-down of 30% or 50%, respectively. This could be due to the fact that the association of tools that hybridize with distant targeted regions of the transcript may lead to a higher protein suppression. This explanation could also justify the more efficient hAgo1 downregulation achieved upon the association of siAgo1 and asON-B in comparison to the association of siAgo1 and asON-A (Figure 6.2 and Figure 6.3). Additionally, the downregulating tools did not show any competitive effect in HeLa cells, maybe because this cell line provides an high number of proteins required for the interaction, therefore the tested tools did not compete with each other. Moreover, these data allowed to make an important observation concerning the expression of recombinant hAgo1 which was very abundant in ECV304 cells while it was very low in HeLa cells (Figure 6.3). A possible explanation could be that HeLa may not tolerate the effect caused by two Lipofectamine 2000-mediated transfections. For this reason, alternative methods which had low level of toxicity, like Lipofectamine LTX or Turbofect, were tested. Further, the knock-down of endogenous hAgo2 and the evaluation of the expression of recombinant hAgo2 were also performed for comparison and for choosing the cell line which was most suited for further investigations. For the knock-down of hAgo2 one asON and a siRNA were tested (see 6.1.1.2). In ECV304 cells the maximal Ago2 downregulation that was achieved was as 60% upon asON2 transfection, while asON2 induced a 80% of suppression of hAgo2 in HeLa cells (Figure 6.5). Thus it appeared that the siR-

NAs tested here and the asON1-A and asON1-B were not functional while the extent of inhibition by asON2 was considered not sufficient because no complete depletion of endogenous hAgo2 in the cells was achieved. Unlike the detection of recombinant hAgo1, HeLa cells showed a high expression of recombinant hAgo2 while only low expression of the recombinant was detected in ECV304 cells. For this reason, HeLa cells were chosen to perform further experiments. An additional approach to suppress endogenous level of hAgo1 or hAgo2 was represented by a shRNA-based method that overcomes a limitation of transfected asONs and siRNAs which is their transient effect. Therefore, shRNA sequences recognizing the mRNAs of hAgo1 or hAgo2 were designed and cloned into pSilencerTM 2.1 expression vector (see 6.1.2) which allowed the constitutive expression of the shRNAs in the cell. The shRNA-encoding vectors were then introduced into the cell upon the over-expression of hAgo2 or hAgo2^{Mut} cleavage incompetent to compensate the induced loss of the endogenous Ago. Western analysis was performed as well to evaluate whether hAgo1 or hAgo2 knock-down occurred (Figure 6.8 and Figure 6.9). However, also in the case of shRNA-based strategy, no protein suppression was achieved confirming the difficulty in downregulating proteins which are essential for biological processes. Further, a Northern analysis was performed in order to determine the extent of shRNA expression in transfected cells.

7.2 *Ago2* and *Ago2^{Mut}* over-expression leads to an increased amount of shRNA-derived mature siRNA

The expression level and the maturation of shRNAs (see 6.1.2.2) that were used to target hAgo1 or hAgo2 were evaluated via Northern analysis. Surprisingly, the amount of shRNA-derived siRNA was increased upon over-expression of hAgo2 or the cleavage incompetent of hAgo2^{Mut} (Figure 6.12 and 6.13). Moreover, bands ranging between 30-40 nt were detected as well and called intermediate products since they were supposed to derive from the cleavage of the sense strand that led to the removal of the fragment at the 5'-end resembling an ac-pre-miRNA described by Diederick and Haber [29]. The evidence that the phenomenon occurred also upon over-expression of non-cleaving *Ago2^{Mut}* and CLIP-tag may suggest that it could be due to the cleavage activity of the endogenous hAgo2 which is not suppressed by the shRNA investigated here as described in 6.1.2. Northern analysis of the maturation of shRNA 2792 (Figure 6.12) showed that CLIP-hAgo2 increased the amount of shRNA-derived siRNA of 5-fold in comparison to the control while it had no effect on the amount of intermediate product. This could find an explanation in the fact that the cleavage competent hAgo2 may help Dicer in the recognition of the cleavage position, increasing the abundance of shRNA-derived siRNA product in comparison to the control. Since the quantity of the intermediate product is similar to the one upon CLIP-tag, it could be that cleavage of the shRNAs into pre-ac-

RNA might be due to a minor and not favoured function of endogenous hAgo2. This hypothesis may explain why the amount of intermediate product does not change while the quantity of the shRNA-derived siRNA is enhanced. Concerning the effect exerted by the cleavage incompetent hAgo2^{Mut} it was possible to observe that, even though its inability of cleavage, the amount of shRNA-derived siRNA and of the intermediate product were increased suggesting that, CLIP-hAgo2^{Mut} may bind the shRNA making the conformation of the RLC more stable for the shRNA processing. This means that the endogenous hAgo2 still present in the cells may induce the cleavage of the sense strand more efficiently. The amount of siRNA derived from shRNA 2798 was enhanced of 2-fold upon the over-expression of CLIP-hAgo2 or CLIP-hAgo2^{Mut} (Figure 6.12). These results further confirmed that the observed phenomenon is independent of the cleavage activity of hAgo2. The detection of the intermediate products was not achieved maybe because the amount was under detection limit. The quantity of the shRNA 2672-derived siRNA was also affected by the upregulated level of recombinant hAgo proteins (Figure 6.13). However, the increasing effect mediated by CLIP-hAgo2 was only slightly evident when compared to the CLIP-tag. On the contrary, the over-expression of the slicing deficient CLIP-hAgo2^{Mut} gave rise to an increment of the amount of shRNA-derived siRNA of 1.5-fold (Figure 6.13). Unexpectedly, several intermediate products were detected upon CLIP-tag, CLIP-hAgo2 or CLIP-hAgo2^{Mut}. This could be probably due to different cleavages of the shRNA. However, the hAgo2 behavior was different on shRNA 3024 (Figure 6.13 B). In fact, CLIP-hAgo2 showed to decrease the amount of the intermediate product derived from shRNA 3024 (Figure 6.13 B) as well as the CLIP-hAgo2^{Mut} indicating that their over-expression enhance the conversion of the intermediate into the shRNA-derived siRNA product. hAgo2 did not influence the amount of intermediate of shRNA Grimm but it enhanced the yield of shRNA-derived siRNA suggesting that the sequence of the loop might also play a role in this recognition process by hAgo2. On the contrary, CLIP-hAgo2^{Mut} decreased the quantity of the intermediate. However in all cases, independently on the cleavage competence of hAgo2 and on their effect on the amount of intermediate products, the production of the shRNA-derived siRNA resulted increased. Taken together the results described above, showed that on one side the shRNA-based system designed here revealed to be not suited for the downregulation of hAgo1 or hAgo2, probably due to the absence of active shRNAs. Northern results concerning the maturation of shRNAs showed that over-expression of recombinant Ago2 and Ago2^{Mut} was sufficient to determine an effect on the amount of shRNA-derived siRNA. For this reason, it was possible to address an intriguing question of whether the investigation of the maturation of shRNA upon over-expression of the recombinant four hAgos could highlight any differences among these proteins. So far, none of published data allowed to understand the differences among the hAgo proteins, therefore, a more detailed investigation was needed. For this purpose, further experiments were performed in

HeLa cells which were transfected with shRNA encoding plasmids upon overexpressing recombinant hAgo1-4 or Ago2^{Mut}.

7.2.1 Human Ago1-4 proteins increase the quantity of shRNA 2672-derived siRNA to a different extent

The investigation of the effect of hAgo1-4 or Ago2^{Mut} on the maturation of shRNA 2672 was also performed (see 6.2.1). Interestingly, it pointed out a different hAgo influence on the amount of shRNA-derived siRNA. Specifically, the quantification showed that the over-expression of all hAgo proteins led to higher yield of siRNA derived from shRNA 2792 in comparison to the control with Ago1 leading to the highest amount of shRNA-derived siRNA. HAgo3 instead led to an increase of only 1.2-fold in the amount of shRNA-derived siRNA when compared to the CLIP-tag group. Although all four hAgos showed to lead to an increase in the amount of shRNA-derived siRNA, the extent of their effect was clearly different (Figure 6.16). In the light of recent published data, according to which hAgo proteins increase the stability of miRNAs [98], it can be assumed that hAgo proteins bind the shRNA making it more stable. Therefore, the over-expression of each hAgo might stabilize the RLC in a different way making the Dicer cleavage more efficient and leading to a higher production of shRNA-derived siRNA. The curiosity about this phenomenon brought to address the question of what is hAgo influence due to. Is the different hAgo behaviour an intrinsic characteristic of the protein or is it dependent on the structure or sequence of the shRNA? The established system that required the over-expression of each recombinant hAgo and the transfection of the cells with shRNA-encoding plasmids revealed to be an efficient system to study the influence of hAgo on the maturation of shRNA therefore it was used for further investigation. Moreover, the method was suited for performing a structure-effect based investigation to study a possible correlation between the effect of hAgos and the structure of shRNA as described in 6.2.2.

7.3 Human Agos show differential effects on the maturation of shRNAs carrying different 3' termini

In order to clarify whether the influence of hAgo proteins on the amount of shRNA-derived siRNA is due to a particular structural requirement of the shRNA or if it is a total independent effect, the design and testing of different structured shRNAs was required. Therefore, a survey of the shRNA structure was performed, allowing to identify three main domains: the loop, the central portion "stem" and the terminus (which is composed of the 5'-end and a single strand overhang at the 3'-end). In order to determine which domain was worthy to investigate, each portion needed to be considered in the light of the data obtained in this study and of the scientific evidences present in the literature concerning

the importance of the domains of shRNA, described as follows. Since shRNAs having different loop sequences have been tested (see 6.1.2.2) and since all of them were affected by Ago over-expression, the loop region was ruled out as possible discriminating factor for Ago influence. However, the loop is important for Dicer function and the loop size is known to affect the shRNA maturation, in fact loop sequences of about 4 nt are more prone to bypass Dicer processing [195]. Additionally, Gu *et al.* [141] suggested a loop counting rule adopted by Dicer in determining the cleavage position: Dicer considers the distance between the cleavage site and the loop sequence starting from the 5'-end [125]. Moreover, in the case of hAgos and their involvement in shRNA maturation, the effect did not seem to be related to the stem length because shRNA with different number of bps were tested and they showed the Ago-mediated effect (Figure 6.13 B). Conversely, it was found in the literature that the stem length influenced the processing of shRNA but not their silencing activity [196]. Sequences of shRNA with ≤ 19 bp are too short for the binding to Dicer therefore they do not undergo Dicer processing [72]. In the light of this, it was hypothesized that the hAgo-mediated effect was due to the length of the overhang at the 3'-end. This was also supported by many evidences that indicate the 3'-end is a determinant factor in several processes [124]. For example, the presence of 2 nt at the 3'-end makes dsRNA a suited substrate for Dicer while the blunt ended dsRNAs are not efficiently processed [124]. This is in perfect agreement with the finding that siRNAs with 2 nt overhang at the 3'-end can trigger RNAi more efficiently in *C. elegans*, in mice [197], in mammalian [20], as well as in *Drosophila* [19, 139, 142]. It was demonstrated in *Drosophila* that the 3'-end of the miRNA is responsible for its recognition by PAZ domain of Ago [139] such as in humans [144]. The length of the 3'-end was shown to be involved in determining Dicing polarity and selection of the strand which will be loaded by the RISC [188]. In order to investigate whether the 3'-terminus plays a role on the Ago-mediated effect, shRNAs with 2, 4 or 10 nt in the 3'-end-overhang were designed and tested (see 6.2.2). In the shRNA sequence the first base was chosen to be a purine since RNA polymerase III-mediated transcription was then more efficient. While the terminal UU was due to the insertion of a poly(T) tract in DNA sequence because this was recognized as terminator signal by RNA polymerase III. ShRNAs having 2nt in the 3'-end-overhang are considered canonical since they are the substrates preferred by Dicer [70]. In fact, it was shown that the canonical substrate for Dicer is a dsRNA with 2 nt overhang at the 3'-end since Dicer processing results more equable and effective in comparison to substrates with different long overhang at the 3'-end, whose cleavage leads to mature products having different lengths [70]. ShRNAs with 4 nt overhang at the 3'-end were the sequences tested at the beginning of this study (see 6.1.2.2). A shRNA having an extreme 3'-end-overhang was needed in this investigation for better highlighting eventual differences upon hAgo over-expression. The results in the use of these shRNAs (see 6.2.2) confirmed the different Ago-mediated effects that were previously described

for shRNA 2672 (see 6.2.1), strongly supporting a different Ago involvement in the maturation of shRNAs.

The results in 6.2.2.1 showed that in case of the shRNA with 2 nt overhang at the 3'-end only the over-expression of hAgo2 with cleavage activity gave rise to an increased of the total amount of shRNA-derived siRNA product leaving unchanged the amount of intermediate product. This could be due to the fact that shRNA having 2 nt overhang at the 3'-end is considered a canonical substrate for Dicer [70], and it may indicate that the RLC containing this shRNA is already maximally stabilized so that the over-expression of non-cleaving hAgos do not influence it. On the contrary, the over-expression of recombinant hAgo2 may lead to a more efficient cleavage performed by Dicer inducing the production preferentially of shRNA-derived siRNA products. This could explain the increase of the shRNA-derived siRNA and the unchanged amount of the intermediate product. Unlike the canonical, all hAgos had an increasing effect on the shRNA with 4 nt overhang at the 3'-end except hAgo3 which reduced it. These data endorsed the hypothesis that for shRNAs that are not canonical (4 nt overhang at the 3'-end) hAgo over-expression may induce a higher complex stability by binding the shRNA or by ensuring a better positioning of the shRNA in Dicer domains to lead to a more efficient cleavage. On the contrary, shRNA having a 10nt-long overhang at the 3'-end deviate highly from canonical feature so that the over-expression of hAgos may be not sufficient to guarantee a better positioning of the RNA in Dicer domains. Therefore, no increment of shRNA-derived siRNA was observed upon hAgo2-3-4 in comparison to the control. However, only hAgo1 seemed to have an enhancing effect may be due to the fact that hAgo1 might bind shRNA in a different way leading to the formation of a complex that interacts with Dicer in a more efficient way than the complexes formed by other hAgos. Additionally, more surprising findings were brought to light that allowed to distinguish among the different behaviors of hAgo1, hAgo2 and hAgo3. These results are discussed in detail below.

7.3.1 Human Ago1 protein shows two different effects on the maturation of shRNA with different termini

Northern analysis showed that hAgo1 exerts two different influences: one increases the amount of siRNA derived from shRNA sequences carrying 4 or 10 nt at the 3'-end and the other induces the formation of a third shorter siRNA product (see 6.2.2). The first effect revealed to be dependent on the 3'-end while the second effect which led to detect three shRNA-derived siRNA products having different length was independent of the length of the 3'-terminus. These are two possible models for Ago1-mediated effect (i) Ago1 forms with the shRNA a particular conformation that makes the shRNA more accessible to a trimming by a cellular nuclease; (ii) Ago1 may function by influencing the choice of the cleavage position by Dicer, as described for other Dicer partners like Ago2, TRBP and PACT [122]. Additionally, high resolution Northern analysis allowed to determine the size

of the shRNA-derived siRNA products (Figure 6.19, 6.20, 6.21). The data showed that shRNAs with 4 or 10 overhang at the 3'-end gave rise to a fragment of 21 nt and other two of <21 nt while shRNA with 2nt overhang at the 3'-end gave rise to 22, 21, 20 nt long fragments. In the light of the data described here and of *in vitro* studies, [124, 198] showing that Dicer specificity can be influenced by many factors (like the overhang at the 3'-end) it was conceivable that hAgo1 may be able to induce a shift of the cleavage site by Dicer which is responsible for the processing of the shRNAs.

7.3.2 Ago2 has an enhancing effect on the siRNA derived from shRNA with 2 or 4 nt overhang at the 3'-end

Upregulated level of cleavage active hAgo2 led to an enhanced amount of siRNA derived from shRNA with 2 or 4 nt overhang at the 3'-end in comparison to the amount upon expression of the CLIP-tag only which served as control (Figure 6.19 and Figure 6.20). Instead, Ago2 did not induce any increment of the yield of siRNA derived from the shRNA having 10 overhang nt at the 3'-end (Figure 6.21) but it seemed to induce preferentially the formation of the 21nt-long product in comparison to the control group and to the other Ago proteins. These results led to hypothesize that Ago2 could ensure the position for Dicer cleavage for those substrates which deviate too much from the canonical structure.

7.3.3 Over-expression of hAgo3 inhibits the maturation of shRNAs

The tested shRNAs showed that the amount of shRNA-derived siRNA is reduced by the over-expression of hAgo3 independently of the 3'-end length, suggesting a possible inhibitory role of hAgo3 in the maturation of shRNAs. This behaviour is different from the one of other Agos and it might be that hAgo3 exert its effect in a step above the maturation process by binding the shRNA and leading to a complex whose conformation is too bulky for the formation of the RLC. It could also be that Ago3 binds to shRNAs confiscating them and thus inhibiting their processing by Dicer. Further explanation could be that hAgo3 binds Dicer directly, but its binding destabilizes the complex with shRNA inducing a lower cleavage efficiency or occupying the binding sites of other hAgos and thus functioning as antagonist.

7.3.4 Ago4 leads to an increased amount of shRNA-derived siRNA having 4 nt overhang at the 3'-end

HAgo4 showed to enhance the amount of siRNA derived from the shRNAs having 4 nt overhang at the 3'-end (Figure 6.16, Figure 6.20). This hAgo4-mediated increasing effect was observed also on the amount of siRNA derived from shRNA with inverted strand sequences (Figure 6.23). On the contrary, hAgo4 effect was totally absent on shRNA having 2 nt overhang at the 3'-end while it decreased the amount of the intermediate

product (Figure 6.19). ShRNA 10nt-3'-overhang upon CLIP-hAgo4 gave rise to only a slightly lesser amount of shRNA-derived siRNA (Figure 6.21). Taken together, these results indicate that hAgo4 effect was dependent on the overhang length at the 3'-end rather than the shRNA sequence. HAgo4 may bind to the shRNA and, only in the case of shRNA having 4 nt overhang at the 3'-end, it may lead to a more stable shRNA-Dicer complex.

7.4 The Ago-enhancing effect is dependent on the 3'-terminus of shRNA while Ago3 inhibitory effect is influenced by the shRNA sequence

The results obtained so far showed that Ago1 or Ago2 or Ago4 increased the amount of shRNA-derived siRNA in a way dependent on the length of the overhang at the 3'-end (see 6.2.2), while the Ago1-induced trimming effect or the Ago3 inhibitory effect were not influenced by 3'-terminus. In the light of this and in order to have more insights in hAgo properties, the next step was to investigate whether the position of the loop and consequently the nt sequence of the shRNA also plays a role in determining hAgo effect. According to the literature, shRNAs with ≤ 19 bp undergo to Dicer processing depending on whether the guide strand is located at 5'- or 3'-end of the loop and are named L- or R shRNAs, respectively [71]. Dallas *et al.* [71] suggested that only R shRNAs undergo loop cleavage. On the contrary, L shRNAs require the cutting of the sense strand without loop removal leading to the formation of a ds structure with a long flanking 5'-end. In the case of L shRNAs, the target recognition can occur via base pairing with the overhang at the 5'-end or with the central portion of the shRNAs upon unwinding allowing the yield of a long ss molecule in which the antisense strand binds the target transcript. On the contrary, shRNAs with >19 bp do not present any difference in their activity when R and L shRNA were compared [199]. The choice to investigate, in this study, hAgo effect on shRNAs having the loop at different positions was based also on evidences that showed that the overhang at the 3'-end was a necessary requirement for R shRNAs activity but not for L shRNAs [200]. To test this idea, a shRNA with 4nt-3'-overhang structure having inverted strands was cloned and tested. Therefore, HeLa cells were transfected with a plasmid encoding shRNA with inverted strands upon over-expression of recombinant hAgo. Northern analysis was performed to investigate hAgo effect on the amount of the derived siRNA (see 6.2.2.2). The obtained results (Figure 6.20 and Figure 6.23) clearly showed that all hAgo increase the yield of the shRNA-derived siRNA independently of the position of the loop or of the sequence of the guide strand. Also in this case upon Ago1 over-expression, three siRNA products are clearly evident (Figure 6.20 and Figure 6.23). These findings further support the idea that the Ago1-induced trimming effect

may be an intrinsic property of hAgo1 since it does not depend neither on the shRNA structure nor on its sequence. Surprisingly, hAgo3 showed here a different behavior when compared to the results obtained in the use of R shRNAs. In fact, it lost the capability to decrease the yield of the shRNA-derived siRNA since its over-expression enhanced the amount of siRNA derived from L-shRNA of 1.8-fold in comparison to the control which was set 1. However, in comparison to the effect of the other hAgos, hAgo3 induced only a minor increase in the amount of shRNA-derived siRNA. These results implied that Ago3 behaves different from other hAgos and that its effect depends on the sequence of the shRNA.

7.5 Nuclear export of shRNA with blunt end or with 5'-overhang

In this study shRNAs having different long overhang at the 5'-end or blunt end were also tested, but no data are shown since no bands were detected by Northern analysis despite the several tested experimental conditions. This could be due to the experimental conditions applied here or to the fact that only few molecules of shRNA were exported from nucleus to the cytoplasm by Exp5 and therefore they could not be detected. Exp5 was identified as the pre-miRNA-specific export carrier [48]. Pre-miRNA binding by Exp5 is inhibited by a 5'-overhang [201]. This protein requires for the binding at least 2nt at the 3'-end of the shRNA [202, 203] and can be considered a regulating point for having an higher silencing activity mediated by shRNA [204].

7.6 Endogenous miRNAs are not affected by hAgo up-regulation

Because it was shown that miRNAs influence several biological mechanisms [205–207], their biogenesis and their regulation have been so far objects of deep investigation [208, 209]. In the light of this, it was interesting to study the effect of hAgos on the maturation of endogenous pre-miRNA. Northern analysis revealed that the guide strand of the investigated miRNAs was not affected by hAgo over-expression (see 6.3.2). Recent studies showed that hAgo proteins increase the amount of miRNA by enhancing their stability [98]. It is important to notice that, in those studies, the passenger strand of miRNAs derived from transfected pre-miRNAs or from plasmids encoding miRNA precursors was investigated while in this work the guide strand was detected. Most investigations concerning hAgo effect on miRNAs were carried out by introducing exogenous precursor [98]. For example, the study of hAgo effect in determining the length of miRNA was performed by co-expressing miR-124 with plasmid encoding recombinant hAgo [156]. Here, endogenous miRNA were investigated and no effect by recombinant hAgos was observed. This could be due to the fact that the miRNA biogenesis is regulated mostly at transcriptional level, although also their nuclear export, their loading by the RISC [210]

and the pri-miRNA processing mediated by Drosha seem to be involved in the regulation of miRNA activity and maturation [84, 106].

In conclusion, this work was helpful to shed light on some of the hAgo properties and on their differences and it can be used for future experiments in order to discover other still unknown hAgo characteristics.

8. Conclusions and Perspectives

The results elucidated in this work describe the establishment of a cell-based system to study the role of hAgo and its usefulness in the investigation of hAgo effect on the maturation of shRNAs and endogenous pre-miRNA. Further, the results observed for shRNAs with various 3'-ends shed light on the different properties existing among the four hAgos. Surprisingly, hAgo1 induced a trimming effect leading to the formation of a smaller shRNA-derived siRNA product and this effect was independent on the length of the overhang at the 3'-end. Instead, hAgo3 had an inhibitory effect on the amount of shRNA-derived siRNA being dependent on the sequence rather than the structure of the shRNA. Additionally, the experiments performed on endogenous miRNAs allowed to point out that the maturation of the guide strand step of miRNAs might be not regulated by hAgo proteins. However, the investigation of the effect of hAgo effect on shRNAs having a completed paired 3'-end and different long 5'-end remains an unresolved issue due to difficulties encountered in their detection via Northern analysis. This problem could be overcome by using another strategy based on shRNAs with different long 5'-end but having 2 flanking nt at the 3'-end in order to favour their Exp5-mediated export from the nucleus into the cytoplasm. This would probably lead to an increase in the amount of shRNA-derived siRNA making its detection possible. In conclusion, the established system shows to be useful to perform a systematic search of different hAgo roles which would be very helpful in providing clarification in the understanding of the RNAi process.

9. References

- [1] J. F. Curtin, M. Candolfi, W. Xiong, P. R. Lowenstein, and M. G. Castro. Turning the gene tap off; implications of regulating gene expression for cancer therapeutics. *Molecular cancer therapeutics*, 7(3):439–448, 2008.
- [2] A. Fire, D. Albertson, S. W. Harrison, and D Moerman. Production of antisense RNA leads to effective and specific inhibition of gene expression in *C. elegans* muscle. *Development*, 113(2):503–514, 1991.
- [3] J. G. Izant and H. Weintraub. Inhibition of thymidine kinase gene expression by anti-sense RNA : a molecular approach to genetic analysis. *Cell*, 36(4):1007–1015, 1984.
- [4] W. Nellen and C. Lichtenstein. What makes an mRNA anti-sense-itive? *Trends in Biochemical Sciences*, 18(11):419–423, 1993.
- [5] S. Guo and K.J. Kempfues. *par-1*, a gene required for establishing polarity in *C. elegans* embryos, encodes a putative Ser/Thr kinase that is asymmetrically distributed. *Cell*, 81(4):611–620, 1995.
- [6] A. Fire, S. Xu, M. K Montgomery, S. A. Kostas, S. E. Driver, and C. C. Mello. Potent and specific genetic interference by double-stranded RNA in *Caenorhabditis elegans*. *Nature*, 391(6669):806–811, 1998.
- [7] B. L. Bass. Double-stranded RNA as a template for gene silencing. *Cell*, 101(3):235–238, 2000.
- [8] M. K. Montgomery, S. Xu, and A. Fire. RNA as a target of double-stranded RNA-mediated genetic interference in *Caenorhabditis elegans*. *Proceedings of the National Academy of Sciences*, 95(26):15502–15507, 1998.
- [9] H. Vaucheret, C. Bclin, T. Elmayan, F. Feuerbach, C. Godon, J. Morel, P. Mourrain, J. Palauqui, and S. Vernhettes. Transgene-induced gene silencing in plants. *The Plant Journal*, 16(6):651–659, 1998.
- [10] C. Cogoni and G. Macino. Post-transcriptional gene silencing across kingdoms. *Current opinion in genetics & Development*, 10(6):638–643, 2000.

- [11] C. C. Mello and D. Conte. Revealing the world of RNA interference. *Nature*, 431(7006):338–342, 2004.
- [12] M. Wassenegger and T. Plissier. A model for RNA-mediated gene silencing in higher plants. *Plant molecular biology*, 37(2):349–362, 1998.
- [13] D. C. Baulcombe. RNA as a target and an initiator of post-transcriptional gene silencing in transgenic plants. *Plant molecular biology*, 32(1-2):79–88, 1996.
- [14] M. A. Matzke and A. J. M. Matzke. How and why do plants inactivate homologous (trans) genes? *Plant Physiology*, 107(3):679, 1995.
- [15] H. Vaucheret and M. Fagard. Transcriptional gene silencing in plants: targets, inducers and regulators. *Trends in Genetics*, 17(1):29–35, 2001.
- [16] T. Tuschl, P. D. Zamore, R. Lehmann, D. P. Bartel, and P. A. Sharp. Targeted mRNA degradation by double-stranded RNA in vitro. *Genes & Development*, 13(24):3191–3197, 1999.
- [17] P. D. Zamore, T. Tuschl, P. A. Sharp, and D. P. Bartel. RNAi: double-stranded RNA directs the ATP-dependent cleavage of mRNA at 21 to 23 nucleotide intervals. *Cell*, 101(1):25–33, 2000.
- [18] S. M. Hammond, E. Bernstein, D. Beach, and G. J. Hannon. An RNA-directed nuclease mediates post-transcriptional gene silencing in *Drosophila* cells. *Nature*, 404(6775):293–296, 2000.
- [19] S. M. Elbashir, W. Lendeckel, and T. Tuschl. RNA interference is mediated by 21- and 22-nucleotide RNAs. *Genes & Development*, 15(2):188–200, 2001.
- [20] S. M. Elbashir, J. Harborth, W. Lendeckel, A. Yalcin, K. Weber, and T. Tuschl. Duplexes of 21-nucleotide RNAs mediate RNA interference in cultured mammalian cells. *Nature*, 411(6836):494–498, 2001.
- [21] E. Bernstein, A. A. Caudy, S. M. Hammond, and G. J. Hannon. Role for a bidentate ribonuclease in the initiation step of RNA interference. *Nature*, 409(6818):363–366, 2001.
- [22] G. Hutvagner, J. McLachlan, A. E. Pasquinelli, É. Bálint, T. Tuschl, and P. D. Zamore. A cellular function for the RNA-interference enzyme Dicer in the maturation of the *let-7* small temporal RNA. *Science*, 293(5531):834–838, 2001.
- [23] S. M. Hammond, S. Boettcher, A. A. Caudy, R. Kobayashi, and G. J. Hannon. Argonaute2, a link between genetic and biochemical analyses of RNAi. *Science*, 293(5532):1146–1150, 2001.

- [24] G. Meister, M. Landthaler, A. Patkaniowska, Y. Dorsett, G. Teng, and T. Tuschl. Human Argonaute2 mediates RNA cleavage targeted by miRNAs and siRNAs. *Molecular cell*, 15(2):185–197, 2004.
- [25] J. Liu, M. A. Carmell, F. V. Rivas, C. G. Marsden, J. M. Thomson, J. Song, S. M. Hammond, L. Joshua-Tor, and G. J. Hannon. Argonaute2 is the catalytic engine of mammalian RNAi. *Science*, 305(5689):1437–1441, 2004.
- [26] N. T Schirle and I. J. MacRae. The crystal structure of human Argonaute2. *Science*, 336(6084):1037–1040, 2012.
- [27] E. Elkayam, C.-D. Kuhn, A. Tocilj, A. D. Haase, E. M. Greene, G. J. Hannon, and L. Joshua-Tor. The structure of human Argonaute-2 in complex with miR-20a. *Cell*, 150(1):100–110, 2012.
- [28] H. W. Wang, C. Noland, B. Siridechadilok, D. W. Taylor, E. Ma, K. Felderer, J. A. Doudna, and E. Nogales. Structural insights into RNA processing by the human RISC-loading complex. *Nature structural & molecular biology*, 16(11):1148–1153, 2009.
- [29] S. Diederichs and D. A. Haber. Dual role for Argonautes in microRNA processing and posttranscriptional regulation of microRNA expression. *Cell*, 131(6):1097–1108, 2007.
- [30] S. Cheloufi, C. O. Dos Santos, M. M. W. Chong, and G. J. Hannon. A Dicer-independent miRNA biogenesis pathway that requires Ago catalysis. *Nature*, 465(7298):584–589, 2010.
- [31] D. Cifuentes, H. Xue, D. W. Taylor, H. Heather Patnode, Y. Mishima, S. Cheloufi, E. Ma, S. Mane, G. J. Hannon, N. D. Lawson, and *et al.* A novel miRNA processing pathway independent of Dicer requires Argonaute2 catalytic activity. *Science*, 328(5986):1694–1698, 2010.
- [32] J. Hauptmann, A. Dueck, S. Harlander, J. Pfaff, R. Merkl, and G. Meister. Turning catalytically inactive human Argonaute proteins into active slicer enzymes. *Nature structural & molecular biology*, 20(7):814–817, 2013.
- [33] S. Das, A. Marwal, D. K. Choudhary, V. K. Gupta, and R. K. Gaur. Mechanism of RNA interference (RNAi): Current concept. In *Proceedings of International Conference on Food Engineering and Biotechnology (ICFEB 2011)*, 2011.
- [34] G. S. Mack. MicroRNA gets down to business. *Nature biotechnology*, 25(6):631–638, 2007.

- [35] P. J. Paddison, A. A. Caudy, E. Bernstein, G. J. Hannon, and D. S. Conklin. Short hairpin RNAs (shRNAs) induce sequence-specific silencing in mammalian cells. *Genes & Development*, 16(8):948–958, 2002.
- [36] R. I. Gregory, T. P. Chendrimada, N. Cooch, and R. Shiekhattar. Human RISC couples microRNA biogenesis and posttranscriptional gene silencing. *Cell*, 123(4):631–640, 2005.
- [37] T. A. Rand, S. Petersen, F. Du, and X. Wang. Argonaute2 cleaves the anti-guide strand of siRNA during RISC activation. *Cell*, 123(4):621–629, 2005.
- [38] J. Martinez, A. Patkaniowska, H. Urlaub, R. Lührmann, and T. Tuschl. Single-stranded antisense siRNAs guide target RNA cleavage in RNAi. *Cell*, 110(5):563–574, 2002.
- [39] T. P. Chendrimada, R. I. Gregory, E. Kumaraswamy, J. Norman, N. Cooch, K. Nishikura, and R. Shiekhattar. TRBP recruits the Dicer complex to Ago2 for microRNA processing and gene silencing. *Nature*, 436(7051):740–744, 2005.
- [40] A. D. Redfern, S. M. Colley, D. J. Beveridge, N. Ikeda, M. R. Epis, X. Li, C. E. Foulds, L. M. Stuart, A. Barker, V. J. Russell, and *et al.* RNA-induced silencing complex (RISC) proteins PACT, TRBP, and Dicer are SRA binding nuclear receptor coregulators. *Proceedings of the National Academy of Sciences*, 110(16):6536–6541, 2013.
- [41] C. Matranga, Y. Tomari, C. Shin, D. P. Bartel, and P. D. Zamore. Passenger-strand cleavage facilitates assembly of siRNA into Ago2-containing RNAi enzyme complexes. *Cell*, 123(4):607–620, 2005.
- [42] D. S. Schwarz, G. Hutvagner, T. Du, Z. Xu, N. I. Aronin, and P. D. Zamore. Asymmetry in the assembly of the RNAi enzyme complex. *Cell*, 115(2):199–208, 2003.
- [43] P. J. F. Leuschner, S. L. Ameres, S. Kueng, and J. Martinez. Cleavage of the siRNA passenger strand during RISC assembly in human cells. *EMBO reports*, 7(3):314–320, 2006.
- [44] J. M. Silva, R. Sachidanandam, and G. J. Hannon. Free energy lights the path toward more effective RNAi. *Nature genetics*, 35(4):303–306, 2003.
- [45] J. Martinez and T. Tuschl. RISC is a 5' phosphomonoester-producing RNA endonuclease. *Genes & Development*, 18(9):975–980, 2004.
- [46] I. J. MacRae, E. Ma, M. Zhou, C. V. Robinson, and J. A. Doudna. In vitro reconstitution of the human RISC-loading complex. *Proceedings of the National Academy of Sciences*, 105(2):512–517, 2008.

- [47] M. Yoda, T. Kawamata, Z. Paroo, X. Ye, S. Iwasaki, Q. Liu, and Y. Tomari. ATP-dependent human RISC assembly pathways. *Nature structural & molecular biology*, 17(1):17–23, 2010.
- [48] M. T. Bohnsack, K. Czaplinski, and D. Görlich. Exportin-5 is a RanGTP-dependent dsRNA-binding protein that mediates nuclear export of pre-miRNAs. *RNA*, 10(2):185–191, 2004.
- [49] A. de Fougerolles, H.-P. Vornlocher, J. Maraganore, and J. Lieberman. Interfering with disease: a progress report on siRNA-based therapeutics. *Nature reviews Drug discovery*, 6(6):443–453, 2007.
- [50] A. Nykänen, B. Haley, and P. D. Zamore. ATP requirements and small interfering RNA structure in the RNA interference pathway. *Cell*, 107(3):309–321, 2001.
- [51] J. W. Pham, J. L. Pellino, Y. S. Lee, R. W. Carthew, and E. J. Sontheimer. A Dicer-2-dependent 80S complex cleaves targeted mRNAs during RNAi in *Drosophila*. *Cell*, 117(1):83–94, 2004.
- [52] Q. Liu, T. A. Rand, S. Kalidas, F. Du, H.-E. Kim, D. P. Smith, and X. Wang. R2D2, a bridge between the initiation and effector steps of the *Drosophila* RNAi pathway. *Science*, 301(5641):1921–1925, 2003.
- [53] Y. Tomari, C. Matranga, B. Haley, N. Martinez, and P. D. Zamore. A protein sensor for siRNA asymmetry. *Science*, 306(5700):1377–1380, 2004.
- [54] K. Förstemann, M. D. Horwich, L. Wee, Y. Tomari, and P. D. Zamore. *Drosophila* microRNAs are sorted into functionally distinct Argonaute complexes after production by Dicer-1. *Cell*, 130(2):287–297, 2007.
- [55] Y. Tomari, T. Du, and P. D. Zamore. Sorting of *Drosophila* small silencing RNAs. *Cell*, 130(2):299–308, 2007.
- [56] D. S. Schwarz, Y. Tomari, and P. D. Zamore. The RNA-induced silencing complex is a Mg^{2+} -dependent endonuclease. *Current Biology*, 14(9):787–791, 2004.
- [57] B. Haley and P. D. Zamore. Kinetic analysis of the RNAi enzyme complex. *Nature structural & molecular biology*, 11(7):599–606, 2004.
- [58] A. Reynolds, D. Leake, Q. Boese, S. Scaringe, W. S. Marshall, and A. Khvorova. Rational siRNA design for RNA interference. *Nature biotechnology*, 22(3):326–330, 2004.
- [59] A. L. Jackson, S. R. Bartz, J. Schelter, S. V. Kobayashi, J. Burchard, M. Mao, B. Li, G. Cavet, and P. S. Linsley. Expression profiling reveals off-target gene regulation by RNAi. *Nature biotechnology*, 21(6):635–637, 2003.

- [60] A. Khvorova, A. Reynolds, and S. D. Jayasena. Functional siRNAs and miRNAs exhibit strand bias. *Cell*, 115(2):209–216, 2003.
- [61] F. V. Rivas, N. H. Tolia, J.-J. Song, J. P. Aragon, J. Liu, G. J. Hannon, and L. Joshua-Tor. Purified Argonaute2 and an siRNA form recombinant human RISC. *Nature structural & molecular biology*, 12(4):340–349, 2005.
- [62] S. Rüdell, Y. Wang, R. Lenobel, R. Körner, H.-H. Hsiao, H. Urlaub, D. Patel, and G. Meister. Phosphorylation of human Argonaute proteins affects small RNA binding. *Nucleic acids research*, 39(6):2330–2343, 2011.
- [63] P. C. Scacheri, O. Rozenblatt-Rosen, N. J. Caplen, T. G. Wolfsberg, L. Umayam, J. C. Lee, C. M. Hughes, K. S. Shanmugam, A. Bhattacharjee, and M. and *et al.* Meyerson. Short interfering RNAs can induce unexpected and divergent changes in the levels of untargeted proteins in mammalian cells. *Proceedings of the National Academy of Sciences of the United States of America*, 101(7):1892–1897, 2004.
- [64] C. A. Sledz, M. Holko, M. J. De Veer, R. H. Silverman, and B. R.G. Williams. Activation of the interferon system by short-interfering RNAs. *Nature cell biology*, 5(9):834–839, 2003.
- [65] A. Grishok, A. E. Pasquinelli, D. Conte, N. Li, S. Parrish, I. Ha, D. L. Baillie, A. Fire, G. Ruvkun, and C. C. Mello. Genes and mechanisms related to RNA interference regulate expression of the small temporal RNAs that control *C. elegans* developmental timing. *Cell*, 106(1):23–34, 2001.
- [66] S. Gu, L. Jin, F. Zhang, Y. Huang, D. Grimm, J. J. Rossi, and M. A. Kay. Thermodynamic stability of small hairpin RNAs highly influences the loading process of different mammalian Argonautes. *Proceedings of the National Academy of Sciences*, 108(22):9208–9213, 2011.
- [67] M. Miyagishi and K. Taira. U6 promoter-driven siRNAs with four uridine 3' overhangs efficiently suppress targeted gene expression in mammalian cells. *Nature biotechnology*, 20(5):497–500, 2002.
- [68] C. P. Paul, P. D. Good, I. Winer, and D. R. Engelke. Effective expression of small interfering RNA in human cells. *Nature biotechnology*, 20(5):505–508, 2002.
- [69] G. J. McIntyre and G. C. Fanning. Design and cloning strategies for constructing shRNA expression vectors. *BMC biotechnology*, 6(1):1, 2006.
- [70] J.-E. Park, I. Heo, Y. Tian, D. K. Simanshu, H. Chang, D. Jee, D. J. Patel, and V. N. Kim. Dicer recognizes the 5' end of RNA for efficient and accurate processing. *Nature*, 475(7355):201–205, 2011.

- [71] A. Dallas, H. Ilves, Q. Ge, P. Kumar, J. Shorestein, S. A. Kazakov, T. L. Cuelar, M. T. McManus, M. A. Behlke, and B. H. Johnston. Right-and left-loop short shRNAs have distinct and unusual mechanisms of gene silencing. *NAR*, 40(18):9255–9271, 2012.
- [72] D. Siolas, C. Lerner, J. Burchard, W. Ge, P. S. Linsley, P. J. Paddison, G. J. Hannon, and M. A. Cleary. Synthetic shRNAs as potent RNAi triggers. *Nature biotechnology*, 23(2):227–231, 2005.
- [73] M. R. Fabian and N. Sonenberg. The mechanics of miRNA-mediated gene silencing: a look under the hood of miRISC. *Nature structural & molecular biology*, 19(6):586–593, 2012.
- [74] Y. Lee, M. Kim, J. Han, K.-H. Yeom, S. Lee, S. H. Baek, and V. N. Kim. MicroRNA genes are transcribed by RNA polymerase II. *The EMBO journal*, 23(20):4051–4060, 2004.
- [75] Y. Lee, C. Ahn, J. Han, H. Choi, J. Kim, J. Yim, J. Lee, P. Provost, O. Rådmark, S. Kim, and *et al.* The nuclear RNase III Drosha initiates microRNA processing. *Nature*, 425(6956):415–419, 2003.
- [76] J. Han, Y. Lee, K.-H. Yeom, Y.-K. Kim, H. Jin, and V. N. Kim. The Drosha-DGCR8 complex in primary microRNA processing. *Genes & Development*, 18(24):3016–3027, 2004.
- [77] Y. Lee, K. Jeon, J.-T. Lee, S. Kim, and V. N. Kim. MicroRNA maturation: stepwise processing and subcellular localization. *The EMBO journal*, 21(17):4663–4670, 2002.
- [78] J. Han, Y. Lee, K.-H. Yeom, J.-W. Nam, I. Heo, J.-K. Rhee, S. Y. Sohn, Y. Cho, B.-T. Zhang, and V. N. Kim. Molecular basis for the recognition of primary microRNAs by the Drosha-DGCR8 complex. *Cell*, 125(5):887–901, 2006.
- [79] T. M. Rana. Illuminating the silence: understanding the structure and function of small RNAs. *Nature reviews Molecular cell biology*, 8(1):23–36, 2007.
- [80] P. Landgraf, M. Rusu, R. Sheridan, A. Sewer, N. Iovino, A. Aravin, S. Pfeffer, A. Rice, A. O. Kamphorst, M. Landthaler, and *et al.* A mammalian microRNA expression atlas based on small RNA library sequencing. *Cell*, 129(7):1401–1414, 2007.
- [81] W. P. Tsang and T. T. Kwok. The mir-18a* microRNA functions as a potential tumor suppressor by targeting on K-Ras. *Carcinogenesis*, 30(6):953–959, 2009.

- [82] J. Winter, S. Link, D. Witzigmann, C. Hildenbrand, C. Previti, and S. Diederichs. Loop-miRs: active microRNAs generated from single-stranded loop regions. *NAR*, 41(10):5503–5512, 2013.
- [83] G. D. Bossé and M. J. Simard. A new twist in the microRNA pathway: Not Dicer but Argonaute is required for a microRNA production. *Cell Research*, 20(7):735–737., 2010.
- [84] J. Winter, S. Jung, S. Keller, R. I. Gregory, and S. Diederichs. Many roads to maturity: microRNA biogenesis pathways and their regulation. *Nature cell biology*, 11(3):228–234, 2009.
- [85] J.-S. Yang, E. C. Lai, and *et al.* Dicer-independent, Ago2-mediated microRNA biogenesis in vertebrates. *Cell Cycle*, 9(22):4455–4460, 2010.
- [86] J.-S. Yang, T. Maurin, and E. C. Lai. Functional parameters of Dicer-independent microRNA biogenesis. *RNA*, 18(5):945–957, 2012.
- [87] R. J. Taft, E. A. Glazov, T. Lassmann, Y. Hayashizaki, P. Carninci, and J. S. Mattick. Small RNAs derived from snoRNAs. *RNA*, 15(7):1233–1240, 2009.
- [88] K. Okamura, J. W. Hagen, H. Duan, D. M. Tyler, and E. C. Lai. The mirtron pathway generates microRNA-class regulatory RNAs in *Drosophila*. *Cell*, 130(1):89–100, 2007.
- [89] J. G. Ruby, C. H. Jan, and D. P. Bartel. Intronic microRNA precursors that bypass Drosha processing. *Nature*, 448(7149):83–86, 2007.
- [90] M. A. Havens, A. A. Reich, D. M. Duelli, and M. L. Hastings. Biogenesis of mammalian microRNAs by a non-canonical processing pathway. *NAR*, 40(10):4626–4640, 2012.
- [91] K. Okamura, A. Ishizuka, H. Siomi, and M. C. Siomi. Distinct roles for Argonaute proteins in small RNA-directed RNA cleavage pathways. *Genes & Development*, 18(14):1655–1666, 2004.
- [92] A. Dueck, C. Ziegler, A. Eichner, E. Berezikov, and G. Meister. microRNAs associated with the different human Argonaute proteins. *NAR*, 40(19):9850–9862, 2012.
- [93] T. Kawamata, H. Seitz, and Y. Tomari. Structural determinants of miRNAs for RISC loading and slicer-independent unwinding. *Nature structural & molecular biology*, 16(9):953–960, 2009.

- [94] B. P. Lewis, I.-H. Shih, M. W. Jones-Rhoades, D. P. Bartel, C. B. Burge, and *et al.* Prediction of mammalian microRNA targets. *Cell*, 115(7):787–798, 2003.
- [95] U. Sheth and R. Parker. Decapping and decay of messenger RNA occur in cytoplasmic processing bodies. *Science*, 300(5620):805–808, 2003.
- [96] E. C. Lai, C. Wiel, and G. M. Rubin. Complementary miRNA pairs suggest a regulatory role for miRNA: miRNA duplexes. *RNA*, 10(2):171–175, 2004.
- [97] X. Liu, D.-Y. Jin, M. T. McManus, and Z. Mourelatos. Precursor microRNA-programmed silencing complex assembly pathways in mammals. *Molecular cell*, 46(4):507–517, 2012.
- [98] J. Winter and S. Diederichs. Argonaute proteins regulate microRNA stability. *RNA Biol*, 8:1149–1157, 2011.
- [99] J. Brennecke, A. Stark, R. B. Russell, and S. M. Cohen. Principles of microRNA-target recognition. *PLoS biology*, 3(3):e85, 2005.
- [100] J. G. Doench and P. A. Sharp. Specificity of microRNA target selection in translational repression. *Genes & Development*, 18(5):504–511, 2004.
- [101] A. Grimson, K. K.-H. Farh, W. K. Johnston, P. Garrett-Engele, L. P. Lim, and D. P. Bartel. MicroRNA targeting specificity in mammals: determinants beyond seed pairing. *Molecular cell*, 27(1):91–105, 2007.
- [102] S. Diederichs and D. A. Haber. Sequence variations of microRNAs in human cancer: alterations in predicted secondary structure do not affect processing. *Cancer research*, 66(12):6097–6104, 2006.
- [103] B. M. Roth, D. Ishimaru, and M. Hennig. The core microprocessor component DiGeorge syndrome critical region 8 (DGCR8) is a nonspecific RNA-binding protein. *Journal of Biological Chemistry*, 288(37):26785–26799, 2013.
- [104] A. M. Denli, B. B. J. Tops, R. H. A. Plasterk, R. F. Ketting, and G. J. Hannon. Processing of primary microRNAs by the Microprocessor complex. *Nature*, 432(7014):231–235, 2004.
- [105] M. Landthaler, A. Yalcin, and T. Tuschl. The human DiGeorge syndrome critical region gene 8 and its *D. melanogaster* homolog are required for miRNA biogenesis. *Current Biology*, 14(23):2162–2167, 2004.
- [106] R. I. Gregory, K.-P. Yan, G. Amuthan, T. Chendrimada, B. Doratotaj, N. Cooch, and R. Shiekhattar. The Microprocessor complex mediates the genesis of microRNAs. *Nature*, 432(7014):235–240, 2004.

- [107] Y. Tomari and P. D. Zamore. MicroRNA biogenesis: drosha can't cut it without a partner. *Current Biology*, 15(2):R61–R64, 2005.
- [108] Y. Zeng, R. Yi, and B. R. Cullen. Recognition and cleavage of primary microRNA precursors by the nuclear processing enzyme Drosha. *The EMBO journal*, 24(1):138–148, 2005.
- [109] Y. Zeng and B. R. Cullen. Efficient processing of primary microRNA hairpins by Drosha requires flanking nonstructured RNA sequences. *Journal of Biological Chemistry*, 280(30):27595–27603, 2005.
- [110] I. J. MacRae, K. Zhou, F. Li, A. Repic, A. N. Brooks, W. Z. Cande, P. D. Adams, and J. A. Doudna. Structural basis for double-stranded RNA processing by Dicer. *Science*, 311(5758):195–198, 2006.
- [111] H. Zhang, F. A. Kolb, L. Jaskiewicz, E. Westhof, and W. Filipowicz. Single processing center models for human Dicer and bacterial RNase III. *Cell*, 118(1):57–68, 2004.
- [112] C. Kanellopoulou, S. A. Muljo, A. L. Kung, S. Ganesan, R. Drapkin, T. Jenuwein, D. M. Livingston, and K. Rajewsky. Dicer-deficient mouse embryonic stem cells are defective in differentiation and centromeric silencing. *Genes & Development*, 19(4):489–501, 2005.
- [113] E. P. Murchison, J. F. Partridge, O. H. Tam, S. Cheloufi, and G. J. Hannon. Characterization of Dicer-deficient murine embryonic stem cells. *Proceedings of the National Academy of Sciences of the United States of America*, 102(34):12135–12140, 2005.
- [114] E. Bernstein, S. Y. Kim, M. A. Carmell, E. P. Murchison, H. Alcorn, M. Z. Li, A. A. Mills, S. J. Elledge, K. V. Anderson, and G. J. Hannon. Dicer is essential for mouse development. *Nature genetics*, 35(3):215–217, 2003.
- [115] J. G. Betancur and Y. Tomari. Dicer is dispensable for asymmetric RISC loading in mammals. *RNA*, 18(1):24–30, 2012.
- [116] Y. S. Lee, K. Nakahara, J. W. Pham, K. Kim, Z. He, E. J. Sontheimer, and R. W. Carthew. Distinct roles for *Drosophila* Dicer-1 and Dicer-2 in the siRNA/miRNA silencing pathways. *Cell*, 117(1):69–81, 2004.
- [117] A. Tsutsumi, T. Kawamata, N. Izumi, H. Seitz, and Y. Tomari. Recognition of the pre-miRNA structure by *Drosophila* Dicer-1. *Nature structural & molecular biology*, 18(10):1153–1158, 2011.

- [118] C. Wostenberg, J. W. Lary, D. Sahu, R. Acevedo, K. A. Quarles, J. L. Cole, and S. A. Showalter. The role of human Dicer-dsRBD in processing small regulatory RNAs. *PLoS one*, 7(12):e51829, 2012.
- [119] P. Provost, D. Dishart, J. Doucet, D. Frendewey, B. Samuelsson, and O. Rådmark. Ribonuclease activity and RNA binding of recombinant human Dicer. *The EMBO Journal*, 21(21):5864–5874, 2002.
- [120] H. Zhang, F. A. Kolb, V. Brondani, E. Billy, and W. Filipowicz. Human Dicer preferentially cleaves dsRNAs at their termini without a requirement for ATP. *The EMBO journal*, 21(21):5875–5885, 2002.
- [121] R. Fukunaga, B. W. Han, J.-H. Hung, J. Xu, Z. Weng, and P. D. Zamore. Dicer partner proteins tune the length of mature miRNAs in flies and mammals. *Cell*, 151(3):533–546, 2012.
- [122] E. Koscianska, J. Starega-Roslan, and W. J. Krzyzosiak. The role of Dicer protein partners in the processing of microRNA precursors. *PLoS one*, 6(12):e28548, 2011.
- [123] E. Ma, K. Zhou, M. A. Kidwell, and J. A. Doudna. Coordinated activities of human Dicer domains in regulatory RNA processing. *Journal of molecular biology*, 422(4):466–476, 2012.
- [124] A. Vermeulen, L. Behlen, A. Reynolds, A. Wolfson, W. S. Marshall, J. Karpilow, and A. Khvorova. The contributions of dsRNA structure to Dicer specificity and efficiency. *RNA*, 11(5):674–682, 2005.
- [125] S. Gu, L. Jin, Y. Zhang, Y. Huang, F. Zhang, P. N. Valdmann, and M. A. Kay. The loop position of shRNAs and pre-miRNAs is critical for the accuracy of Dicer processing in vivo. *Cell*, 151(4):900–911, 2012.
- [126] K. Sakurai, M. Amarzguioui, D.-H. Kim, J. Alluin, B. Heale, M.-S. Song, A. Gagnon, M. A. Behlke, and J. J. Rossi. A role for human Dicer in pre-RISC loading of siRNAs. *NAR*, 39(4):1510–1525, 2011.
- [127] K.-F. Wei, L.-J. Wu, J. Chen, Y.-F. Chen, and D.-X. Xie. Structural evolution and functional diversification analyses of Argonaute protein. *Journal of cellular biochemistry*, 113(8):2576–2585, 2012.
- [128] N. H. Tolia and L. Joshua-Tor. Slicer and the Argonautes. *Nature chemical biology*, 3(1):36–43, 2007.
- [129] B. Czech and G. J. Hannon. Small RNA sorting: matchmaking for Argonautes. *Nature Reviews Genetics*, 12(1):19–31, 2011.

- [130] M. Jinek and J. A. Doudna. A three-dimensional view of the molecular machinery of RNA interference. *Nature*, 457(7228):405–412, 2009.
- [131] J. Pak and A. Fire. Distinct populations of primary and secondary effectors during RNAi in *C. elegans*. *Science*, 315(5809):241–244, 2007.
- [132] T. Sijen, F. A. Steiner, K. L. Thijssen, and R. H. A. Plasterk. Secondary siRNAs result from unprimed RNA synthesis and form a distinct class. *Science*, 315(5809):244–247, 2007.
- [133] D. Grimm, L. Wang, J. S. Lee, N. Schürmann, S. Gu, K. Börner, T. A. Storm, and M. A. Kay. Argonaute proteins are key determinants of RNAi efficacy, toxicity, and persistence in the adult mouse liver. *The Journal of clinical investigation*, 120(9):3106, 2010.
- [134] J. Höck and G. Meister. The Argonaute protein family. *Genome Biol*, 9(2):210, 2008.
- [135] G. Hutvagner and M. J. Simard. Argonaute proteins: key players in RNA silencing. *Nature reviews Molecular cell biology*, 9(1):22–32, 2008.
- [136] <http://www.uniprot.org/>.
- [137] G. Meister. Argonaute proteins: functional insights and emerging roles. *Nature Reviews Genetics*, 14(7):447–459, 2013.
- [138] P. B. Kwak and Y. Tomari. The N domain of Argonaute drives duplex unwinding during RISC assembly. *Nature structural & molecular biology*, 19(2):145–151, 2012.
- [139] A. Lingel, B. Simon, E. Izaurralde, and M. Sattler. Nucleic acid 3'-end recognition by the Argonaute2 PAZ domain. *Nature structural & molecular biology*, 11(6), 2004.
- [140] J.-J. Song, S. K. Smith, G. J. Hannon, and L. Joshua-Tor. Crystal structure of Argonaute and its implications for RISC slicer activity. *Science*, 305(5689):1434–1437, 2004.
- [141] S. Gu, L. Jin, Y. Huang, F. Zhang, and M. A. Kay. Slicing-independent RISC activation requires the argonaute PAZ domain. *Current Biology*, 22(16):1536–1542, 2012.
- [142] J.-J. Song, J. Liu, N. H. Tolia, J. Schneiderman, S. K. Smith, R. A. Martienssen, G. J. Hannon, and L. Joshua-Tor. The crystal structure of the Argonaute2 PAZ domain reveals an RNA binding motif in RNAi effector complexes. *Nature Structural & Molecular Biology*, 10(12):1026–1032, 2003.

- [143] K. S. Yan, S. Yan, A. Farooq, A. Han, L. Zeng, and M.-M. Zhou. Structure and conserved RNA binding of the PAZ domain. *Nature*, 426(6965):469–474, 2003.
- [144] J.-B. Ma, K. Ye, and D. J. Patel. Structural basis for overhang-specific small interfering RNA recognition by the PAZ domain. *Nature*, 429(6989):318–322, 2004.
- [145] F. Frank, N. Sonenberg, and B. Nagar. Structural basis for 5'-nucleotide base-specific recognition of guide RNA by human AGO2. *Nature*, 465(7299):818–822, 2010.
- [146] C. R. Faehnle, E. Elkayam, A. D. Haase, G. J. Hannon, and L. Joshua-Tor. The making of a slicer: activation of human Argonaute-1. *Cell reports*, 3(6):1901–1909, 2013.
- [147] N. Schürmann, L. G. Trabuco, C. Bender, R. B. Russell, and D. Grimm. Molecular dissection of human Argonaute proteins by DNA shuffling. *Nature structural & molecular biology*, 20(7):818–826, 2013.
- [148] A. Verdel, S. Jia, S. Gerber, T. Sugiyama, S. Gygi, S. I. S. Grewal, and D. Moazed. RNAi-mediated targeting of heterochromatin by the RITS complex. *Science*, 303(5658):672–676, 2004.
- [149] T. A. Volpe, C. Kidner, I. M. Hall, G. Teng, S. I. S. Grewal, and R. A. Martienssen. Regulation of heterochromatic silencing and Histone H3 lysine-9 methylation by RNAi. *Science*, 297(5588):1833–1837, 2002.
- [150] I. M. Hall, G. D. Shankaranarayana, K.-I. Noma, N. Ayoub, A. Cohen, and S. I. S. Grewal. Establishment and maintenance of a heterochromatin domain. *Science*, 297(5590):2232–2237, 2002.
- [151] G. J. Hannon. RNA interference. *Nature*, 418(6894):244–251, 2002.
- [152] K. Miyoshi, H. Tsukumo, T. Nagami, H. Siomi, and M. C. Siomi. Slicer function of *Drosophila* Argonautes and its involvement in RISC formation. *Genes & Development*, 19(23):2837–2848, 2005.
- [153] J. A. Broderick, W. E. Salomon, S. P. Ryder, N. Aronin, and P. D. Zamore. Argonaute protein identity and pairing geometry determine cooperativity in mammalian RNA silencing. *RNA*, 17(10):1858–1869, 2011.
- [154] H. Su, M. I. Trombly, J. Chen, and X. Wang. Essential and overlapping functions for mammalian Argonautes in microRNA silencing. *Genes & Development*, 23(3):304–317, 2009.

- [155] W. F. Lima, H. Wu, J. G. Nichols, H. Sun, H. M. Murray, and S. T. Crooke. Binding and cleavage specificities of human Argonaute2. *Journal of biological chemistry*, 284(38):26017–26028, 2009.
- [156] P. K. Juvvuna, P. Khandelvia, L. M. Lee, and E. V. Makeyev. Argonaute identity defines the length of mature mammalian microRNAs. *NAR*, 40(14):6808–6820, 2012.
- [157] D. O’Carroll, I. Mecklenbrauker, P. P. Das, A. Santana, U. Koenig, A. J. Enright, E. A. Miska, and A. Tarakhovsky. A slicer-independent role for Argonaute 2 in hematopoiesis and the microRNA pathway. *Genes & Development*, 21(16):1999–2004, 2007.
- [158] N. J. Martinez and R. I. Gregory. Argonaute2 expression is post-transcriptionally coupled to microRNA abundance. *RNA*, 19(5):605–612, 2013.
- [159] P. Smibert, J.-S. Yang, G. Azzam, J.-L. Liu, and E. C. Lai. Homeostatic control of Argonaute stability by microRNA availability. *Nature structural & molecular biology*, 20(7):789–795, 2013.
- [160] N. De, L. Young, P.-W. Lau, N.-C. Meisner, D. V. Morrissey, and I. J. MacRae. Highly complementary target RNAs promote release of guide RNAs from human Argonaute2. *Molecular cell*, 50(3):344–355, 2013.
- [161] A. Azuma-Mukai, H. Oguri, T. Mituyama, Z. R. Qian, K. Asai, H. Siomi, and M. C. Siomi. Characterization of endogenous human Argonautes and their miRNA partners in RNA silencing. *Proceedings of the National Academy of Sciences*, 105(23):7964–7969, 2008.
- [162] K. Nishi, A. Nishi, T. Nagasawa, and K. Ui-Tei. Human TNRC6A is an Argonaute-navigator protein for microRNA-mediated gene silencing in the nucleus. *RNA*, 19(1):17–35, 2013.
- [163] A. Eulalio, F. Tritschler, and E. Izaurralde. The GW182 protein family in animal cells: new insights into domains required for miRNA-mediated gene silencing. *RNA*, 15(8):1433–1442, 2009.
- [164] G. S. Tan, B. G. Garchow, X. Liu, J. Yeung, J. P. Morris, T. L. Cuellar, M. T. McManus, and M. Kiriakidou. Expanded RNA-binding activities of mammalian Argonaute2. *NAR*, 37(22):7533–7545, 2009.
- [165] B. P. Lucey, W. A. Nelson-Rees, and G. M. Hutchins. Henrietta Lacks, HeLa cells, and cell culture contamination. *Archives of pathology & laboratory medicine*, 133(9):1463–1467, 2009.

- [166] W. G. Dirks, R. A. F. MacLeod, and H. G. Drexler. ECV304 (endothelial) is really T24 (bladder carcinoma): cell line cross-contamination at source. *In Vitro Cellular & Developmental Biology-Animal*, 35(10):558–559, 1999.
- [167] A. Mescalchin, A. Detzer, U. Weirauch, M. J. Hahnel, C. Engel, and G. Sczakiel. Antisense tools for functional studies of human Argonaute proteins. *RNA*, 16(12):2529–2536, 2010.
- [168] R. Kretschmer-Kazemi Far and G. Sczakiel. The activity of siRNA in mammalian cells is related to structural target accessibility: a comparison with antisense oligonucleotides. *NAR*, 31(15):4417–4424, 2003.
- [169] <http://www.ambion.com/techlib/>.
- [170] D. Grimm, K. L. Streetz, C. L. Jopling, T. A. Storm, K. Pandey, C. R. Davis, P. Marion, F. Salazar, and M. A. Kay. Fatality in mice due to oversaturation of cellular microRNA/short hairpin RNA pathways. *Nature*, 441(7092):537–541, 2006.
- [171] T. Holen, M. Amarzguoui, M. T. Wiiger, E. Babaie, and H. Prydz. Positional effects of short interfering RNAs targeting the human coagulation trigger tissue factor. *NAR*, 30(8):1757–1766, 2002.
- [172] E. A. Bohula, A. J. Salisbury, M. Sohail, M. P. Playford, J. Riedemann, E. M. Southern, and V. M. Macaulay. The efficacy of small interfering RNAs targeted to the type 1 insulin-like growth factor receptor (IGF1R) is influenced by secondary structure in the IGF1R transcript. *Journal of Biological Chemistry*, 278(18):15991–15997, 2003.
- [173] T. A. Vickers, S. Koo, C. F. Bennett, S. T. Crooke, N. M. Dean, and B. F. Baker. Efficient reduction of target RNAs by small interfering RNA and RNase H-dependent antisense agents a comparative analysis. *Journal of Biological Chemistry*, 278(9):7108–7118, 2003.
- [174] N. Dias and C. A. Stein. Antisense oligonucleotides: basic concepts and mechanisms. *Molecular cancer therapeutics*, 1(5):347–355, 2002.
- [175] V. Patzel, U. Steidl, R. Kronenwett, R. Haas, and G. Sczakiel. A theoretical approach to select effective antisense oligodeoxyribonucleotides at high statistical probability. *NAR*, 27(22):4328–4334, 1999.
- [176] C. Ender and G. Meister. Argonaute proteins at a glance. *Journal of cell science*, 123(11):1819–1823, 2010.

- [177] R. Kretschmer-Kazemi Far, W. Nedbal, and G. Sczakiel. Concepts to automate the theoretical design of effective antisense oligonucleotides. *Bioinformatics*, 17(11):1058–1061, 2001.
- [178] M. Hemmings-Mieszczak, G. Dorn, F. J. Natt, J. Hall, and W. L. Wishart. Independent combinatorial effect of antisense oligonucleotides and RNAi-mediated specific inhibition of the recombinant Rat P2X3 receptor. *Nucleic Acids Research*, 31(8):2117–2126, 2003.
- [179] G. Sui, C. Soohoo, E. B. Affar, F. Gay, Y. Shi, W. C. Forrester, and Y. Shi. A DNA vector-based RNAi technology to suppress gene expression in mammalian cells. *Proceedings of the National Academy of Sciences*, 99(8):5515–5520, 2002.
- [180] J.-Y. Yu, S. L. DeRuiter, and D. L. Turner. RNA interference by expression of short-interfering RNAs and hairpin RNAs in mammalian cells. *Proceedings of the National Academy of Sciences*, 99(9):6047–6052, 2002.
- [181] K. Suzuki, S. Hattori, K. Marks, C. Ahlenstiel, Y. Maeda, T. Ishida, M. Millington, M. Boyd, G. Symonds, D. A. Cooper, and *et al.* Promoter targeting shRNA suppresses HIV-1 infection *in vivo* through transcriptional gene silencing. *Molecular TherapyNucleic Acids*, 2(12):e137, 2013.
- [182] Q. Jiang, H. Zhang, P. Zhang, and *et al.* ShRNA-mediated gene silencing of MTA1 influenced on protein expression of ER alpha, MMP-9, cyclinD1 and invasiveness, proliferation in breast cancer cell lines MTA-MB-231 and MCF-7 *in vitro*. *J Exp Clin Cancer Res*, 30(1):60, 2011.
- [183] M. Hayafune, N. Miyano-Kurosaki, W. Park, Y. Mouri, and H. Takaku. Silencing of HIV-1 gene expression by two types of siRNA expression systems. *Antiviral Chemistry and Chemotherapy-Institutional Subscription*, 17(5):241–250, 2006.
- [184] <http://sfold.wadsworth.org/cgi-bin/srna.pl>.
- [185] G. Meister and T. Tuschl. Mechanisms of gene silencing by double-stranded RNA. *Nature*, 431(7006):343–349, 2004.
- [186] T. Kawamata and Y. Tomari. Making RISC. *Trends in biochemical sciences*, 35(7):368–376, 2010.
- [187] A. Ambesajir, A. Kaushik, J. J. Kaushik, and S. T. Petros. RNA interference: A futuristic tool and its therapeutic applications. *Saudi journal of biological sciences*, 19(4):395–403, 2012.
- [188] J. Zhou, M.-S. Song, A. M. Jacobi, M. A. Behlke, X. Wu, and J. J. Rossi. Deep sequencing analyses of dsiRNAs reveal the influence of 3' terminal overhangs on

- dicing polarity, strand selectivity, and RNA editing of siRNAs. *Molecular Therapy-Nucleic Acids*, 1(4):e17, 2012.
- [189] <http://www.microrna.org/microrna/home.do>.
- [190] L. Peters and G. Meister. Argonaute proteins: mediators of RNA silencing. *Molecular cell*, 26(5):611–623, 2007.
- [191] N.J. Caplen. Gene therapy progress and prospects. Downregulating gene expression: the impact of RNA interference. *Gene therapy*, 11(16):1241–1248, 2004.
- [192] W. F. Scherer, J. T. Syverton, and G. O. Gey. Studies on the propagation in vitro of poliomyelitis viruses IV. Viral multiplication in a stable strain of human malignant epithelial cells (strain HeLa) derived from an epidermoid carcinoma of the cervix. *The Journal of experimental medicine*, 97(5):695–710, 1953.
- [193] D. Semizarov, P. Kroeger, and S. Fesik. siRNA-mediated gene silencing: a global genome view. *NAR*, 32(13):3836–3845, 2004.
- [194] W. Filipowicz, L. Jaskiewicz, F. A. Kolb, and R. S. Pillai. Post-transcriptional gene silencing by siRNAs and miRNAs. *Current opinion in structural biology*, 15(3):331–341, 2005.
- [195] L. Li, X. Lin, A. Khvorova, S. W. Fesik, and Y. Shen. Defining the optimal parameters for hairpin-based knockdown constructs. *RNA*, 13(10):1765–1774, 2007.
- [196] G. J. McIntyre, Y.-H. Yu, M. Lomas, and G. C. Fanning. The effects of stem length and core placement on shRNA activity. *BMC molecular biology*, 12(1):34, 2011.
- [197] N. J. Caplen, S. Parrish, F. Imani, A. Fire, and R. A. Morgan. Specific inhibition of gene expression by small double-stranded RNAs in invertebrate and vertebrate systems. *Proceedings of the National Academy of Sciences*, 98(17):9742–9747, 2001.
- [198] S. D. Rose, D.-H. Kim, M. Amarzguioui, J. D. Heidel, M. A. Collingwood, M. E. Davis, J. J. Rossi, and M. A. Behlke. Functional polarity is introduced by Dicer processing of short substrate RNAs. *NAR*, 33(13):4140–4156, 2005.
- [199] M. T. McManus, C. P. Petersen, B. B. Haines, J. Chen, and P. A. Sharp. Gene silencing using micro-RNA designed hairpins. *RNA*, 8(6):842–850, 2002.
- [200] Q. Ge, H. Ilves, A. Dallas, P. Kumar, J. Shorenstein, S. A. Kazakov, and B. H. Johnston. Minimal-length short hairpin RNAs: the relationship of structure and RNAi activity. *RNA*, 16(1):106–117, 2010.

- [201] Y. Zeng and B. R. Cullen. Structural requirements for pre-microRNA binding and nuclear export by Exportin-5. *NAR*, 32(16):4776–4785, 2004.
- [202] R. Yi, Y. Qin, I. G. Macara, and B. R. Cullen. Exportin-5 mediates the nuclear export of pre-microRNAs and short hairpin RNAs. *Genes & Development*, 17(24):3011–3016, 2003.
- [203] C. Gwizdek, B. Ossareh-Nazari, A. M. Brownawell, A. Doglio, E. Bertrand, I. G. Macara, and C. Dargemont. Exportin-5 mediates nuclear export of minihelix-containing RNAs. *Journal of Biological Chemistry*, 278(8):5505–5508, 2003.
- [204] R. Yi, B. P. Doehle, Y. Qin, I. G. Macara, and B. R. Cullen. Overexpression of exportin 5 enhances RNA interference mediated by short hairpin RNAs and microRNAs. *RNA*, 11(2):220–226, 2005.
- [205] W. P. Kloosterman and R. H. A. Plasterk. The diverse functions of microRNAs in animal development and disease. *Developmental cell*, 11(4):441–450, 2006.
- [206] V. K. Gangaraju and H. Lin. MicroRNAs: key regulators of stem cells. *Nature Reviews Molecular Cell Biology*, 10(2):116–125, 2009.
- [207] R. S. Pillai. MicroRNA function: multiple mechanisms for a tiny RNA? *RNA*, 11(12):1753–1761, 2005.
- [208] K. A. O’Donnell, E. A. Wentzel, K. I. Zeller, C. V. Dang, and J. T. Mendell. c-Myc-regulated microRNAs modulate E2F1 expression. *Nature*, 435(7043):839–843, 2005.
- [209] T.-C. Chang, D. Yu, Y.-S. Lee, E. A. Wentzel, D. E. Arking, K. M. West, C. V. Dang, A. Thomas-Tikhonenko, and J. T. Mendell. Widespread microRNA repression by Myc contributes to tumorigenesis. *Nature genetics*, 40(1):43–50, 2008.
- [210] B. N. Davis and A. Hata. Regulation of microRNA biogenesis: A miRiad of mechanisms. *Cell Commun Signal*, 7(18):10–1186, 2009.

10. Acknowledgements

I thank the Graduate School of Lübeck for giving me the opportunity to carry out this Ph.D. project and for contributing, through a structured doctoral program which included also workshops and exams, to enrich my scientific background. My special thanks go to:

- **Prof. Dr. rer. nat. Georg Sczakiel** - for his important support, teachings and all the time that he has provided for the scientific discussions and for the realization of this thesis.
- **PD Dr. rer. nat. Sven Müller-Loennies** - for the second supervision of this project and his willingness to have scientific meetings.
- **Dr. rer. nat. Alessandra Mescalchin** - for being my mentor and guide. I extend to her my personal thanks for all the teachings that she gave me in the scientific field and in the daily life. Moreover, I am very grateful to her for having confidence in me and for the time that she has provided in every phase of this project and this thesis.
- **Dr. rer. nat. Rosel Kretschmer-Kazemi Far** - for the suggestions in many scientific issues addressed in this thesis. Thank you very much for all the meetings, which have always been for me opportunities to learn.
- **Prof. Dr. rer. nat. Tobias Restle** - for his participation in the weekly seminars and his scientific observations.
- **Dr. rer. nat. Tillman Vollbrandt** - for his work in "Isotopen Labor" which allowed me to perform the experiments required for this project.
- **Petra Höltig** for the bureaucratic support, **Kirsten Frank** for her technical help in the lab, **Michael Schütt** for the computer assistance.
- All my **colleagues** - for sharing with me this great experience inside and outside the lab.
- My **family** - that is always supportive and patient with me in every moment of my life.